UNIVERSIDAD AUTÓNOMA DE MADRID

FACULTAD DE CIENCIAS

DEPARTAMENTO DE BIOLOGÍA MOLECULAR

THE MESOTHELIAL ORIGIN OF CARCINOMA-ASSOCIATED FIBROBLASTS IN PERITONEAL METASTASIS. THE MESOTHELIAL-TO-MESENCHYMAL TRANSITION AS A POSSIBLE THERAPEUTIC TARGET

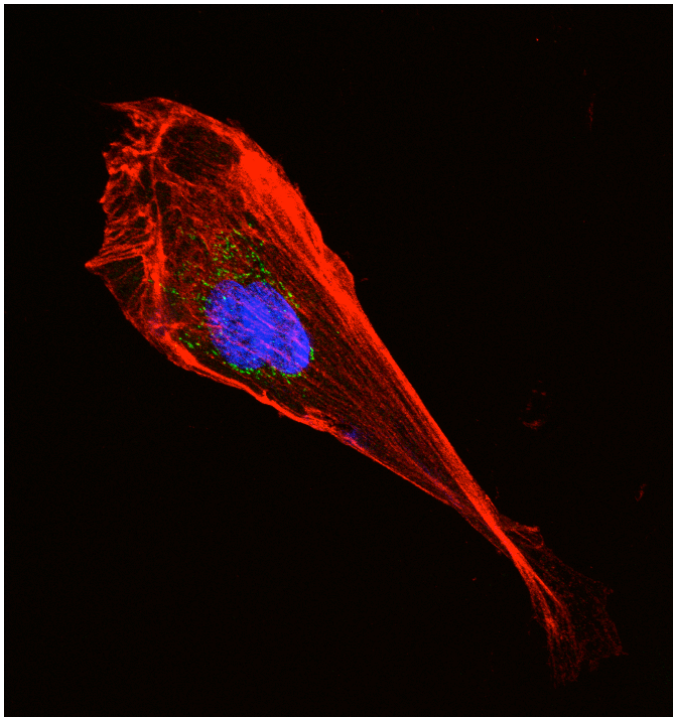

DOCTORAL THESIS

Ángela Rynne Vidal

Madrid, 2016

UNIVERSIDAD AUTÓNOMA DE MADRID
FACULTAD DE CIENCIAS

DEPARTAMENTO DE BIOLOGÍA MOLECULAR

THE MESOTHELIAL ORIGIN OF CARCINOMA-ASSOCIATED FIBROBLASTS IN PERITONEAL METASTASIS. THE MESOTHELIAL-TO-MESENCHYMAL TRANSITION AS A POSSIBLE THERAPEUTIC TARGET

ÁNGELA RYNNE VIDAL

Centro de Biología Molecular
"Severo Ochoa"

MD Anderson Cancer Center

Thesis directors

Dr. Manuel López Cabrera **Dr. Pilar Sandoval Correa**

Thesis tutor

Dr. Pedro Bonay Miarons

For my parents.

Acknowledgments

Firstly, I would like to thank both my thesis directors, Dr. Manuel López Cabrera and Dr. Pilar Sandoval Correa. To Manuel I am thankful for entrusting me with this work and allowing me to discover such a beautiful subject, to which I have dedicated the past four and a half years. I will be always grateful to you for giving me the liberty to explore things I was interested in, for taking into consideration my suggestions and always being available to talk when I needed it. I want to thank Pilar for teaching me so much over these years, for guiding me and advising me along the way, and for helping this work be what it is today; I would not have been able to do it without you.

I thank all my lab colleagues in the CBM and in the La Princesa and La Paz hospitals, and all the doctors and surgeons that have supplied us with samples and biopsies over the years, making every experiment possible. I thank all the patients who disinterestedly donated their samples for research. I especially want to thank María Luisa, for tutoring me and giving me advice when I most needed it, for setting an example of persistence and hard work, and for showing me that it's worth it to keep trying even when you're not sure any more.

I want to thank the students I've had the pleasure to work with: Adrián, Diego and Lucía. Thank you for being so enthusiastic and motivated, for listening, for always wanting to learn and improve yourselves, and for helping us in the lab with different experiments. I wish you all the best with your future in science.

I am very grateful to Dr. José Fernández Piqueras and Dr. Javier Santos Hernández for giving me my first opportunity in research when I was still a student. Those two years working with you convinced me about continuing in research. I thank all the lab members in your group for their help, particularly Laura, for having the patience to teach me how to do my first Western blots, PCRs and flow cytometry assays, and for inspiring in me a love for research that continues to this day.

I thank Dr. Samuel Mok for allowing me to work with his group in the MD Anderson Cancer Center. The months I worked under your supervision were some of the most successful of my thesis and inspired ideas for new experiments when I came back to Spain. I thank all the lab members, especially Chi Lam, who always had a smile and made my days much better.

Other people in the MD Anderson: Daisy, Suety, Suetyan and John, for the talks we had inside and outside of the hospital and for making my stay there much more fun.

Christine, JP, Joe and Juha from the Karolinska Institutet, for letting me work with them in such an interesting project, for being stimulating and motivated; it has been a great experience to spend my last weeks in the lab with you.

I thank all people who have helped me and made my life much easier in the departments of IT, confocal microscopy, flow cytometry, and the animal facility.

Heni, for everything: helping me preserve my sanity, talking about experiments and frustrations relentlessly, and for being such a great friend inside and outside of the CBM. It's going to be weird not eating with you every day; thankfully, we're still neighbours ;)

Miguel and Antonio, thanks for our great conversations and those constant emails that brighten my day.

I thank all of my other friends inside and outside the CBM: Alba, Sandra, Blanca, Laura, Berta (both of them) Sara and Javi. Marta, thanks for your helping me out lentivirus and other experiments and random talks. Kostas, thanks for showing me how to use the IVIS and help me out in my first days there. Javi and Curro, thanks for all the breakfasts we've had, for telling me the gossip in the CBM and the bizarre nicknames you come up with, for the help in the lab and for making my days here always fun. all the others I have surely forgotten to include here..

Che, thank you for always listening, being thoughtful, giving me good advice till the end, and for supporting me and being as great as you are.

All my friends from Aranjuez: Aurora, Inés, Anabel, María and Belén, for their support and help, and for listening to my scientific rants even though they didn't understand what I was talking about.

Finally, I want to thank my grandparents May Anne and David, my brother, my parents and the rest of my family for always being there for me, supporting me, believing in me and making me who I am today.

CONTENTS

SUMMARY **1**

RESUMEN **5**

ABBREVIATIONS **9**

INTRODUCTION **13**

1. PERITONEAL METASTASIS 15

1.1. Ovarian cancer *16*

2. THE SEED AND SOIL THEORY IN PERITONEAL METASTASIS 16

3. CARCINOMA-ASSOCIATED FIBROBLASTS IN THE PERITONEUM 17

3.1. Mesothelial cells as a possible source of carcinoma-associated fibroblasts *18*

4. MESOTHELIAL-TO-MESENCHYMAL TRANSITION AND PROMOTING STIMULI IN PERITONEAL METASTASIS 20

4.1. TGF-β signalling pathway *25*

5. IMPLICATION OF MESOTHELIAL CELLS IN ADHESION, INVASION AND PROGRESSION OF PERITONEAL METASTASIS 27

OBJECTIVES **31**

MATERIAL AND METHODS **35**

1. HUMAN SAMPLES 37

1.1. Biopsies from patients with peritoneal metastasis *37*

1.2. Primary mesothelial cells *37*

2. CELL CULTURE AND IN VITRO ASSAYS 38

2.1. Cell lines *38*

2.2. Induction of MMT in vitro *38*

2.3. Adhesion assays *39*

2.4. Invasion assays *39*

2.5. Treatment of mesothelial and cancer cells with TGF-β1 ..... *40*

3. ADENOVIRAL PRODUCTION 40

4. BACTERIAL TRANSFORMATION, LENTIVIRAL VECTOR PRODUCTION AND TITRATION 40

5. MICE 41

5.1. Mouse model of carcinoma peritoneal dissemination *42*

5.2. Subcutaneous xenografts *42*

5.3. Peritoneum pre-conditioning *42*

5.3.1. Adenoviral delivery of TGF-β1 42

5.3.2. Conditioned medium from cancer cells 43

5.3.3. Smad3 knockdown with lentiviral delivery 43

6. IMMUNOHISTOCHEMICAL ANALYSIS 43
6.1. Human samples *43*
6.2. Mouse samples *44*
7. IMMUNOFLUORESCENCE ANALYSIS 44
7.1. Peritoneal tissues from mice *44*
7.2. Mesothelial and SKOV-3 cells *45*
8. FLOW CYTOMETRY 45
9. WESTERN BLOT 45
10. QUANTITATIVE REAL-TIME PCR (QRT-PCR) 46
11. SCANNING ELECTRON MICROSCOPY 46
12. STATISTICAL ANALYSIS 47
13. RNA-SEQUENCING AND FUNCTIONAL ANNOTATION 47
13.1. RNA extraction *47*
13.2. RNA sequencing *48*
13.3. Data analysis *48*
13.4. Analysis of differential expression genes by IPA software *48*

RESULTS 51

1. HUMAN BIOPSIES ANALYSIS SHOWS THAT CAFS ORIGINATE FROM MCS AND COLLABORATE IN TUMOUR ANGIOGENESIS 53
2. CAFS ORIGINATE FROM MCS IN A MOUSE MODEL OF PERITONEAL DISSEMINATION 57
3. CONDITIONED MEDIUM FROM CARCINOMA CELLS INDUCES MMT IN VITRO 63
4. MESENCHYMAL CONVERSION OF MCS ENHANCES THE ADHESION OF TUMOUR CELLS 67
5. MCS AND TUMOUR CELLS MUTUALLY STIMULATE THEIR INVASIVE CAPACITY 69
6. ASCITIC FLUID-DERIVED MESOTHELIAL CELLS UNDERGO A MESOTHELIAL-TO-MESENCHYMAL TRANSITION 72
7. ASCITIC FLUID-DERIVED MESOTHELIAL CELLS PROMOTE TUMOUR GROWTH OF OVARIAN CANCER CELLS IN A SUBCUTANEOUS XENOGRAFT MOUSE MODEL 74
8. IDENTIFICATION OF A MESOTHELIAL-TO-MESENCHYMAL GENE SIGNATURE IN ASCITIC FLUID-DERIVED MESOTHELIAL CELLS 74
9. MESOTHELIAL-TO-MESENCHYMAL TRANSITION VIA TGF-B1 IN THE PERITONEUM RENDERS PERITONEUM MORE SUSCEPTIBLE TO METASTASIS 77
10. CROSSTALK BETWEEN MESOTHELIAL-DERIVED CARCINOMA-ASSOCIATED FIBROBLASTS AND CANCER CELLS TAKES PLACE VIA TGF-B1/PSMAD3 PATHWAY 78
11. LENTIVIRAL KNOCKDOWN OF SMAD3 IN THE PERITONEUM REDUCES METASTASIS 83

DISCUSSION 87

CONCLUSIONS **101**

CONCLUSIONES **105**

REFERENCES **109**

ANNEX I **127**

Figure 1. Multiple origins of CAFs. 20
Figure 2. Schematic illustration of the key events during MMT. 21
Figure 3. Malignant ascites and modification of the peritoneal membrane. 23
Figure 4. Smad-dependent signalling pathways of TGF-β and BMP-7 in the MMT context. 26
Figure 5. Analysis of human peritoneal carcinoma implants reveals the mesothelial origin for CAFs. 54
Figure 6. Analysis of human lung cancer-derived metastasis in the pleura. 55
Figure 8. Vessel number increases in areas adjacent to micrometastases. 56
Figure 9. MC-derived CAFs accumulate close to micrometastases and express large amounts of VEGF. 57
Figure 10. CAFs originate from MCs in a mouse model of peritoneal dissemination. 59
Figure 11. Mesothelial-derived CAFs co-express WT1 and α-SMA in the mouse model of peritoneal dissemination. 60
Figure 12. Expression pattern of mesothelial markers in primary HPMCs, either treated or not with TGF-β 1 plus IL-1β, and in SKOV-3 cells 61
Figure 13. Increased angiogenesis is found in sites where MC-derived CAFs expressing high amounts of VEGF accumulate 61
Figure 14. Large tumour implants coexist with fibrotic areas where CAFs express mesothelial markers. 62
Figure 15. Analysis of omental metastasis in the mouse model of peritoneal dissemination. 63
Figure 16. Conditioned medium from SKOV-3 cells induces MMT in vitro. 65
Figure 17. Conditioned medium from HT29 cells induces a MMT *in vitro*. 66
Figure 18. Blockade of TGF-β receptor I inhibitor interferes with the MMT. 66
Figure 19. Tumour cells adhere mainly to the transdifferentiated MC monolayer through cell–cell interactions. 68
Figure 20. Mesenchymal-like HPMCs strongly stimulate the invasive capacity of carcinoma cells. 70

Figure 21. Tumour cells embedded in the matrix induce MC invasion. 71
Figure 22. AFMCs undergo a MMT.....73
Figure 23. AFMCs favour tumour progression in a subcutaneous xenograft mouse model. 75
Figure 24. RNA-seq analysis of AFMCs. 76
Figure 25. Overexpression of TGF-β in the peritoneum supports tumour progression. 77
Figure 26. Blockade of TGF-β receptor I blocks the tumour growth induced by cancer cell media....79
Figure 28. TGF-β1/Smad3 pathway is truncated in SKOV-3 cells. 81
Figure 29. Immunohistochemical analysis of mouse peritoneal tissues.....82
Figure 30. Immunohistochemical analysis of human peritoneal implants of ovarian cancer. 84
Figure 32. Model for transformation of the pre-metastatic niche by mesothelial-to-mesenchymal transition in the peritoneum.....94
Figure 33. Targets for therapeutic strategies in the treatment of peritoneal metastasis.....95

Table 1. Top 100 downregulated genes in AFMCs compared to HPMCs. 129
Table 2. Top 100 upregulated genes in AFMCs compared to HPMCs.....134

SUMMARY

Peritoneal dissemination is the primary metastatic route for ovarian cancer, which is generally diagnosed at advanced stages and has a high mortality rate. Ovarian cancer is often accompanied by the accumulation of ascitic fluid, which contains a high concentration of cytokines, chemokines, exosomes and suspended cells. During peritoneal metastasis, cancer cells detach from the primary tumour, disseminate through the peritoneal fluid and attach to the mesothelial cell (MC) monolayer that lines the peritoneal cavity. Then, they invade the submesothelial compact zone where carcinoma-associated fibroblasts (CAFs) accumulate. CAFs represent an important population in the tumour microenvironment, may derive from different sources, and participate in several stages of tumour progression, including cancer cell migration/invasion and metastasis. This work shows that in peritoneal metastasis, a sizeable subpopulation of CAFs originates from MCs through a mesothelial-to-mesenchymal transition (MMT) induced by cancer cells. Additionally, immunofluorescence staining and RT-PCR analysis indicated that MCs in malignant ascitic fluid (AFMCs) are undergoing MMT; and RNA-seq analysis confirmed a large proportion of the differentially regulated pathways were associated primarily with MMT. The MMT in AFMCs is shown to be taking place via a TGF-β1 Smad-dependent pathway, and the mesenchymal conversion in these cells favoured tumour growth in a subcutaneous xenograft mouse model. In peritoneal biopsies of ovarian cancer patients, nuclear pSmad3-positive MC-derived CAFs surrounded the micrometastases. Surprisingly, in cancer cells, pSmad3 expression remained cytoplasmic. This differential localization was confirmed *in vitro* upon TGF-β1 stimulation, suggesting that, despite producing large amounts of TGF-β1, the Smad-dependent pathway is truncated in ovarian cancer cells, requiring MCs for environment transformation. Consequently, the impact of MMT in tumour progression was studied using an *in vivo* bioluminescence imaging mouse model for peritoneal dissemination. By overexpressing or blocking TGF-β1 in the peritoneum, tumour growth was favoured or reduced, respectively. Also, knockdown of Smad3 in the peritoneum resulted in reduced tumour progression, confirming the Smad-dependent pathway is relevant in peritoneal metastasis. These results suggest that CAFs derived from MCs through a MMT create a suitable metastatic niche for ovarian cancer progression. This work suggests the peritoneal environment could constitute an alternative target in the treatment of ovarian cancer metastasis, by strategically modulating the MMT with known pharmacological agents.

RESUMEN

El cáncer de ovario se detecta generalmente en estadios avanzados, tiene una alta tasa de mortalidad, y metastatiza principalmente por la ruta peritoneal. Suele ir acompañado de la acumulación de líquido ascítico, que contiene una alta concentración de citoquinas, quimioquinas, exosomas y células en suspensión. Durante la metástasis peritoneal, las células cancerosas se desprenden del tumor primario, diseminan a través del líquido peritoneal y se adhieren a la monocapa de células mesoteliales (MCs) que recubre la cavidad peritoneal. A continuación, invaden la zona submesotelial, donde se acumulan los fibroblastos asociados a cáncer (CAFs). Los CAFs son una población celular importante en el microambiente tumoral, derivan de varios tipos celulares, y participan en varias etapas de la progresión tumoral, como la migración/invasión y metástasis. Este trabajo muestra que, en la metástasis peritoneal, una parte considerable de los CAFs proviene de las MCs mediante una transición mesotelio-mesénquima (MMT) inducida por las células cancerosas. Se observó mediante inmunofluorescencia, RT-PCR y RNA-seq que las MCs del líquido ascítico maligno (AFMCs) han sufrido una MMT. Esta MMT en AFMCs se lleva a cabo mediante la ruta Smad-dependiente de TGF-β1, y la conversión mesenquimal de estas células favoreció el crecimiento tumoral en un modelo de xenoinjerto subcutáneo en ratón. En biopsias peritoneales de cáncer de ovario, los CAFs derivados de MCs rodeaban las micrometástasis y expresaban pSmad3 nuclear. Sorprendentemente, en las células cancerosas, la expresión de pSmad3 se limitaba al citpolasma. Esta localización diferencial se confirmó in vitro tras estimular con TGF-β1 y sugiere que, a pesar de producir grandes cantidades de TGF-β1, la ruta Smad-dependiente está truncada en las células de cáncer de ovario, que requieren a las MCs para transformar el ambiente. Por ello, se estudió el impacto de la MMT en la progresión tumoral intraperitoneal. La sobreexpresión o el bloqueo de TGF-β1 en el peritoneo favoreció o disminuyó el crecimiento tumoral, respectivamente. El knockdown de Smad3 en el peritoneo resultó en una progresión tumoral reducida, confirmando el papel de la vía Smad-dependiente en la metástasis peritoneal. Esto sugiere que los CAFs derivados de MCs mediante una MMT crean un nicho metastático favorable para la progresión del cáncer de ovario. El presente trabajo sugiere que el ambiente peritoneal podría representar una diana terapéutica alternativa en el tratamiento de la metástasis del cáncer de ovario, modulando estratégicamente la MMT.

ABBREVIATIONS

AFMCs	Ascitic Fluid-derived Mesothelial Cells
α-SMA	α -smooth muscle actin
BCEF-AM	2',7'-bis(2-carboxyethyl)-5(6)-carboxyfluorescein acetoxymethyl
BMP-7	Bone morphogenetic protein 7
CA125/MUC16	Cancer antigen 125/mucin 16
CAFs	Carcinoma-associated fibroblasts
CAV-1	Caveolin 1
DAB	3,3′-diaminobenzidine
DAPI	4,6-diamidino-2-phenylindole
DMEM	Dulbecco's modified eagle medium
DMSO	Dimethyl sulfoxide
ECL	Enhanced chemiluminiscence
ECM	Extracellular matrix
EDTA	Ethylenediaminetetraacetic acid
EGFR	Epidermal growth factor receptor
ELISA	Enzyme-linked immunosorbent assay
EMT	Epithelial-to-Mesenchymal Transition
EndMT	Endothelial-to-Mesenchymal Transition
ERK	Extracellular signal-Regulated Kinase
ET-1	Endothelin 1
FAP	Fibroblast activation protein
FGF-2	Fibroblast growth factor 2
FBS	Fetal bovine serum
FSP1	Fibroblast specific protein 1
FSP1	Fibroblast-specific protein 1
H&E	Haematoxilyn and Eosin
HGF	Hepatocyte growth factor
HGFR	Hepatocyte growth factor receptor
HIPEC	Hyperthermic intraperitoneal chemotheraphy
HPMCs	Human peritoneal mesothelial cells
ICAM-1	Intercellular adhesion molecule 1
IL-10	Interleukin 10
IL-1β	Interleukin 1 beta
IL-6	Interleukin 6
IL-8	Interleukin 8
ILK	Integrin-linked kinase
JNK	C-Jun N-terminal Kinase

LB	Lysogeny broth
MAPK	Mitogen-activated protein kinase
MCs	Mesothelial cells
miRNA	Micro RNA
MMP-2	Matrix metalloprotease 2
MMP-9	Matrix metalloprotease 9
MMT	Mesothelial-to-Mesenchymal Transition
NF-κB	Nuclear Factor-kappa B
NRP1	Neuropilin 1
PAI-1	Plasminogen activator inhibitor 1
PBN	A-phenyl-N-tert-butyl-nitrone
PBS	Phosphate buffered saline
PCR	Polymerase chain reaction
PDGF	Plateled-derived growth factor
PI3K/Akt	Phosphoinositide 3-kinase/protein kinase b
PPAR	Peroxisome proliferator-activated receptor
qRT-PCR	Quantitative real time polymerase chain reaction
RIPA	Radioimmunoprecipitation assay
rMMT	Reverse MMT
RPMI	Roswell Park Memorial Institute medium
RXR	Retinoid X receptor
shRNA	Small hairpin RNA
SOC	Super Optimal Broth with Catabolite repression
T+I	Transforming Growth Factor beta 1 + Interleukin-1 beta
TAK-1	Transforming Growth Factor beta-Activated Kinase 1
TBS	Tris-buffered saline
TGF-β1	Transforming Growth Factor beta 1
TNF-α	Tumour Necrosis Factor α
TSP1	Thrombospondin 1
uPA	Urokinase-type Plasminogen Activator
VCAM-1	Vascular cell adhesion molecule 1
VDR	Vitamin D receptor
VEGF	Vascular endothelial growth factor
VEGFR2	Vascular endothelial growth factor receptor 2
WT1	Wilm's tumour 1
ZO-1	Zona occludens 1

INTRODUCTION

1. Peritoneal metastasis

The majority of tumours are confined to the organ where they first originated and are usually treatable and curable with local therapy. However, several neoplasias are incurable due to processes that govern the ability of cells to disseminate and implant in distant locations. Although hematogenous and lymphatic dissemination are the most common routes for metastasis, tumours originating adjacent to the peritoneal cavity, such as ovarian or colorectal cancer, frequently disseminate via transcoelomic route to develop peritoneal metastases. Cancer cells detached from the primary tumour are transported by peritoneal fluid to subsequently spread locally, colonizing the peritoneum (Tan et al. 2006; de Cuba et al. 2012). This process is known as peritoneal metastasis and signifies that the disease is at advanced stage, is difficult to treat and, often, there is no prospect of cure. A common characteristic of abdominal cancers that progress with peritoneal metastasis is that they generally evolve very rapidly and correlate with poor prognosis. The peritoneal cavity is the site of metastases in up to 28% of recurrent endometrial cancers (Sohaib et al. 2007), 42% of colorectal cancers (Koppe et al. 2006), 40% of gastric cancers (Montori et al. 2014) and 70% of ovarian advanced cancers (Tan et al. 2006). Surgery is inefficient to render patients free of disease, resulting in low survival rates. This is in part due to the diffuse nature of peritoneal metastases, making them generally intractable to surgical resection. Nowadays, aggressive surgical tumour removal (tumour cytoreduction) coupled with hyperthermic intraperitoneal chemotherapy (HIPEC) represents the cornerstone of advanced abdominal oncologic surgery. The combination of both treatments seems to be encouraging and, in colorectal and gynecological cancers, provides 5-year survival rates of over 40% and 45%, respectively (Glehen et al. 2006; Bakrin et al. 2014). However, these are complex therapies that require specialized technological facilities with highly qualified human resources, and the possibility of curing advanced stage intraperitoneal tumours still remains limited (Glockzin et al. 2009). Part of this problem derives from the fact that the pathogenesis of peritoneal carcinomatosis is not well understood. Therefore, to design new therapeutic

approaches it is necessary to improve our knowledge of the mechanisms implicated in tumour progression in the peritoneum.

1.1. Ovarian cancer

Ovarian cancer is the fifth leading cause of cancer-related deaths in women (Siegel et al. 2016). The epithelial type is the most frequent (90% of cases) and, based on histopathology, can be divided into serous (most common), mucinous, endometrioid and other less common types, such as clear cell (Hennessy et al. 2009). Ovarian cancers are classified in 4 stages, I and II being early-stage, and III and IV advanced-stage. The high mortality rates are explained by the fact that, at diagnosis, 70% of women present an advanced stage, meaning that cancer cells have reached the peritoneal cavity (Tan et al. 2006; Hennessy et al. 2009; Lengyel 2010; Thibault et al. 2014). Long-term survival rates (>10 years) are dramatically different between early-stage (80-95%) and advanced-stage (10-30%) (Hennessy et al. 2009). In contrast to other types of cancer, ovarian preferentially metastasizes through the peritoneal cavity, and not hematogenously (Tan et al. 2006).

2. The seed and soil theory in peritoneal metastasis

Metastasis remains the major cause of death for cancer patients. Cancers that metastasize are generally more difficult to treat and have a worse prognosis than those that remain at the site of origin (Chambers et al. 2002). During peritoneal metastasis, cancer cells leave the primary tumour to colonize the secondary organ (peritoneum), where they develop into metastatic lesions. The peritoneum is a well-known metastatic site for several intra-abdominal malignancies, such as ovarian, colon, gastric, pancreatic, endometrial and rectal cancer. However, the specific site of distant metastasis is not simply due to the intrinsic features of the primary tumour, its anatomic location or proximity to secondary sites but, rather, it involves interactions between tumour cells and the local microenvironment at the secondary site. Therefore, in the establishment of metastasis, the properties of the tumour are as important as the metastatic niche. In 1899, Stephen Paget suggested the “seed and soil” hypothesis to

explain how sites where metastases occur are defined not only by the tumour cell ("seed") but also the microenvironment of the secondary metastatic site ("soil"). Accordingly, metastases are influenced by innumerable factors and complex cellular interactions between the seed and the soil (Mendoza and Khanna 2009; Mathot and Stenninger 2012). In the case of peritoneal carcinomatosis, the metastatic niche is composed of the surface of the peritoneum overlying the abdominal cavity. The organization of the peritoneum is simple: a single layer of mesothelial cells (MCs) lines a compact region that is composed of connective tissue with a few fibroblasts, mast cells, macrophages and blood vessels (Di Paolo and Sacchi 2000). The "seed and soil" mechanism could be especially relevant in peritoneal metastasis, since modification of the surrounding metastatic stroma may facilitate the processes of attaching to and invading through the peritoneal membrane.

3. Carcinoma-associated fibroblasts in the peritoneum

Currently, there is an increased understanding of the processes that govern the malignant transformation of cells. It is known that tumour development is mainly associated with the accumulation of multiple genetic and epigenetic alterations in cancer cells which pave the way for the transformation of a normal cell into a malignant cell (Hanahan and Weinberg 2011). However, tumours are highly complex organs composed of different cell types. Cancer tissue consists of both tumour cells and stromal cells surrounded by an extensive extracellular matrix (ECM). The stromal component constitutes a large part of most solid tumours and includes multiple cell types like mesenchymal, vascular and immune cells that converge to support a tumourigenic niche. The development of the tumour microenvironment is triggered by stimulating molecules secreted by cancer cells that corrupt the adjacent normal tissue to create an "activated" stroma (Bhome et al. 2015).

The peritoneal pre-metastatic niche is basically composed of MCs, fibroblasts, endothelial cells, adipocytes and immune cells, including macrophages. However, during peritoneal metastasis normal mesothelium is replaced by a strong stromal reaction

(desmoplasia) characterized by the accumulation of activated fibroblasts (myofibroblasts) (Kojima et al. 2014). The exacerbated accumulation of activated fibroblasts in the peritoneum has been previously described in other fibrotic disorders including peritoneal dialysis-induced fibrosis (Jimenez-Heffernan et al. 2004) and abdominal adhesions (Chegini 2008; Sandoval et al. 2016). In cancer stroma, carcinoma-associated fibroblasts (CAFs)—also called activated or reactive stromal fibroblasts—are prominent modifiers of tumour progression towards advanced stages, favouring proliferation, survival and invasion of cancer cells, and their presence is often associated with poor clinical prognosis for oncology patients (Shimoda et al. 2010; Polanska and Orimo 2013). CAFs share characteristics with myofibroblasts like the expression of alpha-smooth muscle actin (α-SMA) (Desmoulière et al. 1993; Lazard et al. 1993; Desmoulière and Gabbiani 1994), fibroblast activation protein-alpha (FAP-α) (Calon et al. 2012; Wikberg et al. 2013) and fibroblast-specific protein 1 (FSP1) (Strutz et al. 1995; Polanska and Orimo 2013). CAFs are capable of producing a wide array of cytokines, growth factors, proteases, and ECM components, thereby promoting inflammation, immunosuppression and ECM remodelling (Polanska and Orimo 2013). Additionally, CAFs have been widely implicated in promoting tumour angiogenesis, which is necessary for cancer survival and metastasis towards secondary organs (Bhowmick et al. 2004; Wels et al. 2008).

3.1. Mesothelial cells as a possible source of carcinoma-associated fibroblasts

An important effect of the tumour nesting into the peritoneal membrane is the exacerbated accumulation of CAFs (Kojima et al. 2014). However, the multiple origins of peritoneal CAFs are still debated today. It has been proposed that CAFs may derive from different sources depending on the surrounding tumour metastatic niche (Figure 1). Additionally, there is emerging evidence that the origin of CAFs may vary between cancer types and within different areas of individual tumours (Cirri and Chiarugi 2012). The activation of resident fibroblasts was considered the main origin of CAFs in the tumour microenvironment (Desmoulière et al. 2004). However, recent studies have revealed that bone marrow-derived

stem cells (fibrocytes) (Ishii et al. 2003; Direkze et al. 2004; Kidd et al. 2012) and adipocytes (Jotzu et al. 2010; Bochet et al. 2013) differentiate into CAFs and are integrated into the tumour stroma. Pericytes have also been described to convert into myofibroblasts at injury sites, representing another possible source of CAFs (Göritz et al. 2011; Dulauroy et al. 2012). Cancer cells of epithelial origin can undergo an epithelial-to-mesenchymal transition to acquire myofibroblast properties, although their contribution to the CAF population is considered to be small (Kalluri and Zeisberg 2006; Radisky et al. 2007; Cirri and Chiarugi 2012). In addition, it has been shown that endothelial cells, through an endothelial-to-mesenchymal transition, may also be a source of CAFs (Potenta et al. 2008; Zeisberg et al. 2008). Moreover, MCs are considered an important source of activated fibroblasts in pathologies that present fibrosis. The presence of MCs converted into myofibroblasts through mesothelial-to-mesenchymal transition (MMT) was first described in the peritoneum of peritoneal dialysis patients (Yanez-Mo et al. 2003), and has recently been implicated in the formation of post-surgical adhesions (Sandoval et al. 2016). Emerging evidence has subsequently revealed that MMT is an important event in numerous fibrogenic disorders such as idiopathic lung fibrosis (Karki et al. 2014), liver fibrogenesis (Li et al. 2013) and myocardial infarction scars (Deb and Ubil 2014; Ruiz-Villalba et al. 2015). Interestingly, FAP-positive mesothelium in gastric cancer patients has been associated with advanced stage disease, peritoneal dissemination and poor survival (Miao et al. 2014). However, the possible conversion of MCs into CAFs during peritoneal carcinomatosis via a MMT has not yet been studied.

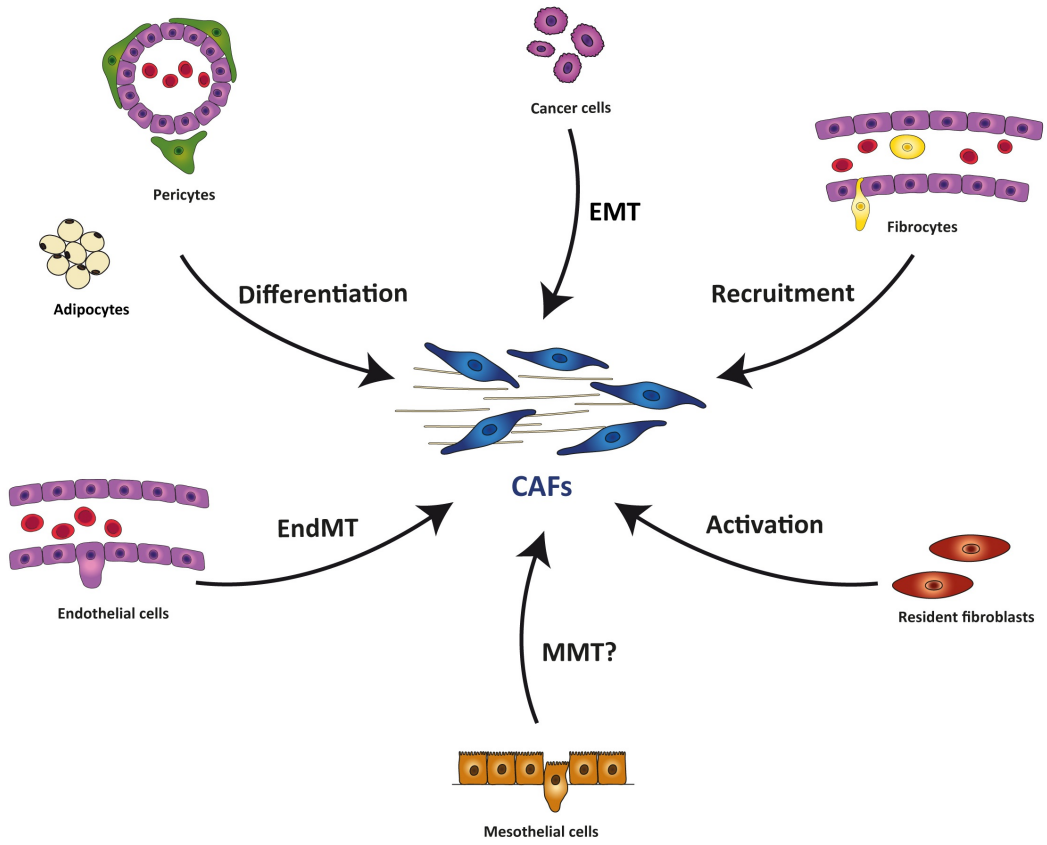

Figure 1. Multiple origins of CAFs.
CAFs may derive from at least six different sources through various mechanisms: phenotypic activation from interstitial fibroblasts; differentiation from adipocytes and vascular pericytes; recruitment from circulating fibrocytes; capillary endothelial-mesenchymal transition (EndMT); and epithelial-mesenchymal transition (EMT). The relative contribution of each source to the CAF pool in peritoneal metastasis has not yet been elucidated. In this context, the possible conversion of MCs into CAFs via a MMT has not yet been studied. *Modified from M López-Cabrera, Advances in Medicine 2014.*

4. Mesothelial-to-mesenchymal transition and promoting stimuli in peritoneal metastasis

The MMT is a complex and stepwise epithelial-to-mesenchymal transition (EMT)-like process that involves alterations in the cellular architecture and a deep molecular reprogramming (Figure 2), where MCs lose their epithelial characteristics and acquire a myofibroblastic phenotype (Yanez-Mo et al. 2003; López-Cabrera 2014). The process starts with the dissociation of intercellular junctions, due to downregulation of intercellular adhesion molecules, and with the loss of microvilli and apico-basal polarity. Then, cells adopt a front-

back polarity, acquire α-SMA expression and increase their migratory capacity. In the last stages of the MMT, the cells acquire the capacity to degrade the basement membrane and to invade the fibrotic compact zone (Kalluri and Weinberg 2009). During the end stages of myofibroblast conversion, MCs are able to produce a large amount of extracellular matrix components and synthesize a wide range of inflammatory, profibrotic and angiogenic factors that may contribute to structural and functional changes in the peritoneal membrane (Margetts and Bonniaud 2003; Yanez-Mo et al. 2003; Aguilera et al. 2005; Aroeira et al. 2007; Devuyst et al. 2010; López-Cabrera 2014).

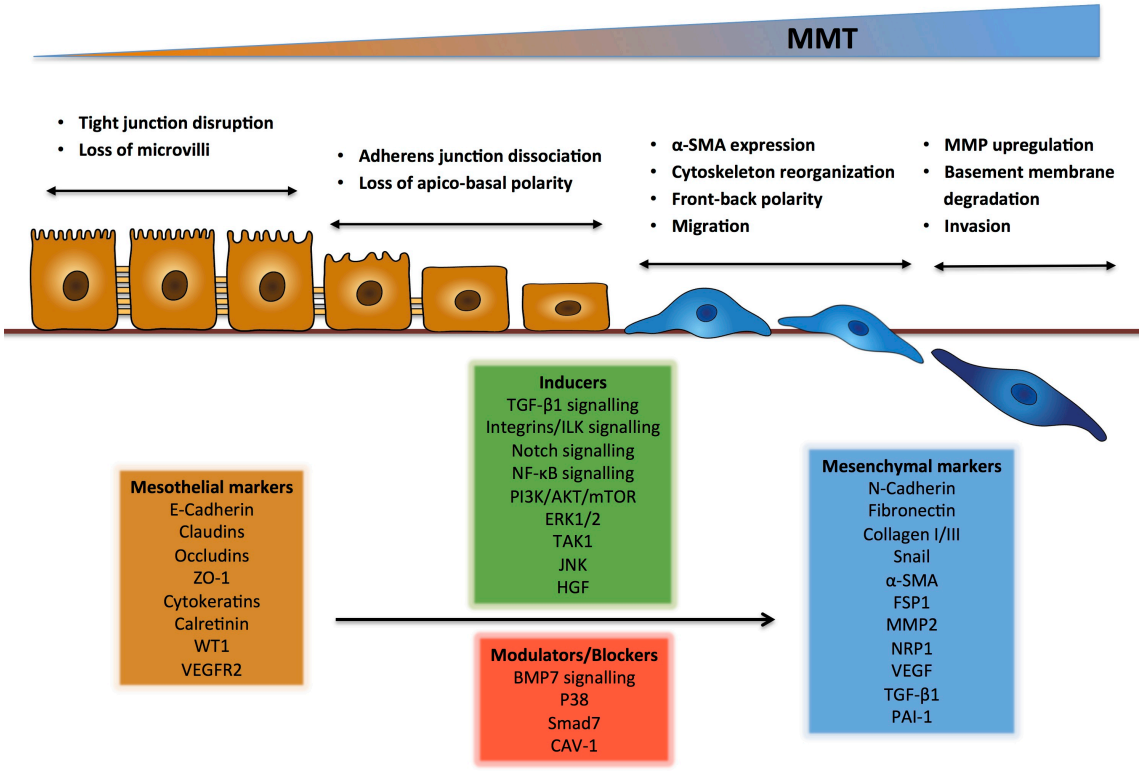

Figure 2. Schematic illustration of the key events during MMT.
Mesothelial to mesenchymal transition (MMT) occurs when mesothelial cells lose their epithelial-like characteristics, including dissolution of cell-cell junctions (tight junctions, adherens junctions and desmosomes) and loss of apico-basal polarity. Then, cells acquire a mesenchymal phenotype, characterized by actin reorganization and stress fiber formation, and the ability to migrate and invade the stroma. The diagram shows four essential key steps for the completion of an entire MMT, the most commonly used mesothelial and mesenchymal markers, and the molecules and signal transduction pathways that act either as inducers or modulators of the MMT process. *Modified from M López-Cabrera, Advances in Medicine 2014.*

In the context of peritoneal metastasis, the promoting stimuli able to induce the mesenchymal conversion of MCs are not still completely characterized. On this note, an important characteristic of patients that develop peritoneal carcinomatosis is the presence of ascites, the pathological accumulation of fluid in the peritoneal cavity (Figure 3). Ascites is the combined result of lymphatic obstruction, the effect of soluble factors, and an increase in peritoneal fluid production and in vascular permeability (Adam and Adam 2004). In this context, ovarian cancer can account for up to 47% of malignant ascites, followed by other gastrointestinal cancers; all of them correlate with poor survival, gastrointestinal tumours being the most severe (Parsons et al. 1996; Ayantunde and Parsons 2007; Ayhan et al. 2007). Malignant ascitic fluid is composed of cytokines, chemokines, growth factors, exosomes and suspended cells that vary in proportion between patients: leukocytes, MCs, macrophages, tumour cells and plasma cells (Sheid 1992; Milliken et al. 2002; Graves et al. 2004; Choi et al. 2011; Matte et al. 2012).

Exosomes are vesicular portions of membrane material, which were initially described by Thery et al. (Théry et al. 2002) and serve as vehicles that transfer proteins, as well as RNA (mRNA and miRNA), between cells. Tumours are able to release exosomes, and these have been found in malignant ascites from patients with ovarian and gastrointestinal cancers (Choi et al. 2011; Peng et al. 2011; Cappellesso et al. 2014; Tokuhisa et al. 2015). While the precise mechanism of communication between cancer and MCs in the peritoneum remains unclear, there is growing evidence that exosomes may serve as prognostic/diagnostic indicators of peritoneal dissemination. Regarding this idea, exosomes derived from colorectal cancer ascites contain proteins that may promote tumour progression via angiogenesis, disruption of epithelial cell polarity, immune modulation, tumour growth and invasion (Choi et al. 2011).

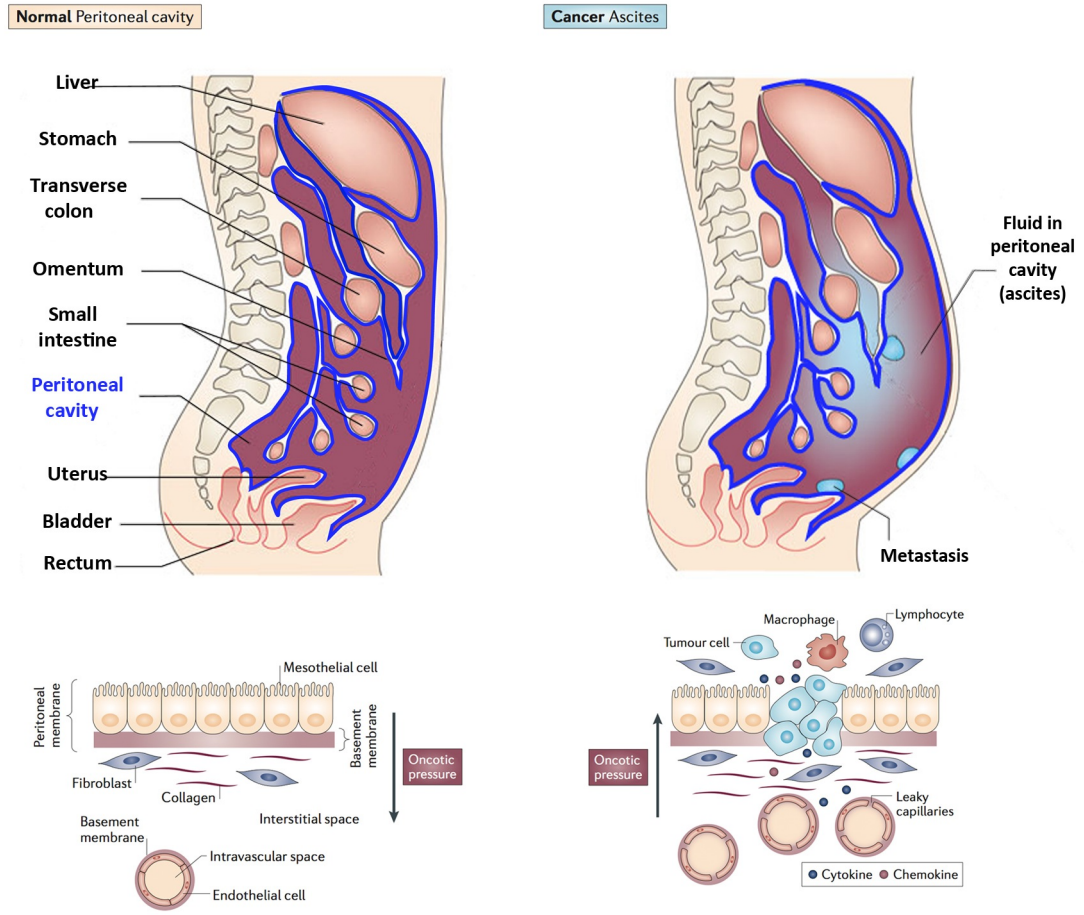

Figure 3. Malignant ascites and modification of the peritoneal membrane.
The peritoneal membrane (outlined in blue) lines the abdominal wall and visceral organs. The structure of a normal peritoneal membrane (left) consists of a monolayer of mesothelial cells, bound by tight junctions, that line the stroma, containing extracellular matrix, fibroblasts and capillaries. In normal conditions, the oncotic pressure is high at the endothelial layer and low at the mesothelial layer, limiting capillary fluid filtration and allowing the reabsorption of water into the capillaries. Patients with tumours in the abdominal cavity (right) have an increased number of permeable vessels and filtration surface for fluid. Malignant ascites contains a high protein concentration, accumulates cytokines and chemokines, and has a reduced lymphatic flow. This translates into a lower peritoneal oncotic pressure, and a flow of fluid into the peritoneal cavity, leading to ascites. *Modified from E. Kipps et al., Nat Rev Cancer 2013.*

On this note, ovarian cancer exosomes administered to mice prior to tumour cell injection have been shown to induce a more aggressive disease and to increase tumour growth (Vaksman et al. 2014). Of the miRNAs contained in exosomes, miR-21, known for its pro-oncogenic activity (Selcuklu et al. 2009), is present in both ovarian (Cappellesso et al. 2014) and gastric (Tokuhisa et al. 2015) cancer ascites. Expression of miR-21 in exosomes is associated with pathways related to transforming growth factor β (TGF-β) signalling, ECM-

receptor interaction, mesothelial clearance and worse prognosis/diagnostic value; thus, it may provide a novel approach for early diagnosis of peritoneal dissemination (Vaksman et al. 2014; Tokuhisa et al. 2015). Also, Vaksman et al. concluded that the effect of exosomes is mainly exerted on MCs, rather than on tumour cells, and higher miRNA levels are associated with poor survival (Vaksman et al. 2014). These data suggest that exosomes may play a role in modifying the metastatic niche to favour peritoneal dissemination.

Also present in the malignant ascitic fluid is a high concentration of cytokines and growth factors, including TGF-β1, tumour necrosis factor-alpha (TNF-α), vascular endothelial growth factor (VEGF), hepatocyte growth factor (HGF), interleukin-1 beta (IL-1β), interleukin-6 (IL-6), interleukin-8 (IL-8) and interleukin-10 (IL-10) (Moradi et al. 1993; Nash et al. 1998; Sowter et al. 1999; Santin et al. 2001; Manenti et al. 2003; Stadlmann et al. 2005; Mustea et al. 2006; Giuntoli et al. 2009; Matte et al. 2014a). Interestingly, many of these soluble mediators, such as TNF-α, IL-6, TGF-β1 and IL-1β, have important pro-inflammatory roles in the peritoneal environment and, as a consequence, have been widely implicated in fibrosis by stimulating fibroblast proliferation (Masunaga et al. 2003; Fredj et al. 2005), ECM component deposition, and MMT induction (Demir et al. 2005; López-Cabrera 2014). Therefore, it is tempting to speculate that, in peritoneal metastasis, diverse cytokines could be contributing to the modification of the mesothelial surface in order to initiate tumour implantation (Freedman et al. 2004; Matte et al. 2014a; Kolomeyevskaya et al. 2015). To this effect, elevated IL-6 and TNF-α in ascites of patients in late stages of ovarian cancer are considered independent predictors of poor survival (Lane et al. 2011; Kolomeyevskaya et al. 2015).

Among the growth factors accumulated in ascites, HGF has recently been implicated in the implantation of endometrial cells (Ono et al. 2015) and ovarian cancer cells (Nakamura et al. 2015) in the peritoneum via a MMT.

4.1. TGF-β signalling pathway

The TGF-β superfamily of proteins includes, among others, TGF-βs, activins, and bone morphogenic proteins (BMPs), and is implicated in a wide range of cellular processes, such as proliferation, differentiation and apoptosis (Shi and Massagué 2003; Feng and Derynck 2005). TGF-β is a master molecule produced by many cell types, presents both anti- and pro-tumoural effects, and is found in high concentration in malignant ascitic fluid (Santin et al. 2001; Wakefield and Roberts 2002; Massagué and Gomis 2006). Tumour cells may evade the tumour suppressor activity of TGF-β while, at the same time, while responding to the tumour-promoting signals. TGF-β also has a effect on the stroma, and has been reported to increase the efficiency of organ colonization by tumour cells (Calon et al. 2012). A large proportion of tumours, including colorectal and ovarian cancer, display mutational inactivation of the TGF-β pathway yet some, paradoxically, are also characterized by elevated TGF-β production (Wakefield and Roberts 2002; Massagué and Gomis 2006; Yamamura et al. 2011; Calon et al. 2014). Moreover, TGF-β1 is a prototypical inducer of the myofibroblast conversion of MCs via MMT (Yanez-Mo et al. 2003; Loureiro et al. 2011). Additionally, the myofibroblast conversion of fibroblasts via TGF-β1 has been shown to take place in a Smad-dependent manner (Evans et al. 2003). On this note, in the EMT induced by TGF-β, Smad3 plays a key role in fibrosis, pro- and anti-tumoural effects and β1 integrin expression (Roberts et al. 2006; Yeh et al. 2010). Miao *et al.* demonstrated that gastric cancer cells expressing high levels of TGF-β1 promote both downregulation of E-cadherin and upregulation of α-SMA in the mesothelium (Miao et al. 2013). Thus, it can be speculated that targeting the TGF-β1 pathway could interfere with the accumulation of peritoneal CAFs.

TGF-β signalling can also take place via Smad-independent pathways, which may or not converge with the Smad-dependent ones, involving the mitogen-activated protein kinases (MAPKs) extracellular signal-regulated kinase (ERK), c-Jun N-terminal kinase (JNK) or p38, as well as nuclear factor-kappa B (NF-κB) and transforming growth factor beta-activated kinase 1 (TAK-1) and phosphoinositide 3-kinase/protein kinase B (PI3K/Akt) (Derynck and Zhang

2003; Massagué and Gomis 2006; López-Cabrera 2014). However, Smad signalling has been reported to play a central role in the regulation of EMT (Valcourt et al. 2005). The Smad-dependent activation or repression of gene transcription relies on the combination of Smads and co-activators or co-repressors in the nucleus, forming complexes that will selectively bind to the DNA (Figure 4) (Shi and Massagué 2003; de Caestecker 2004; Feng and Derynck 2005; Massagué and Gomis 2006; Derynck and Akhurst 2007).

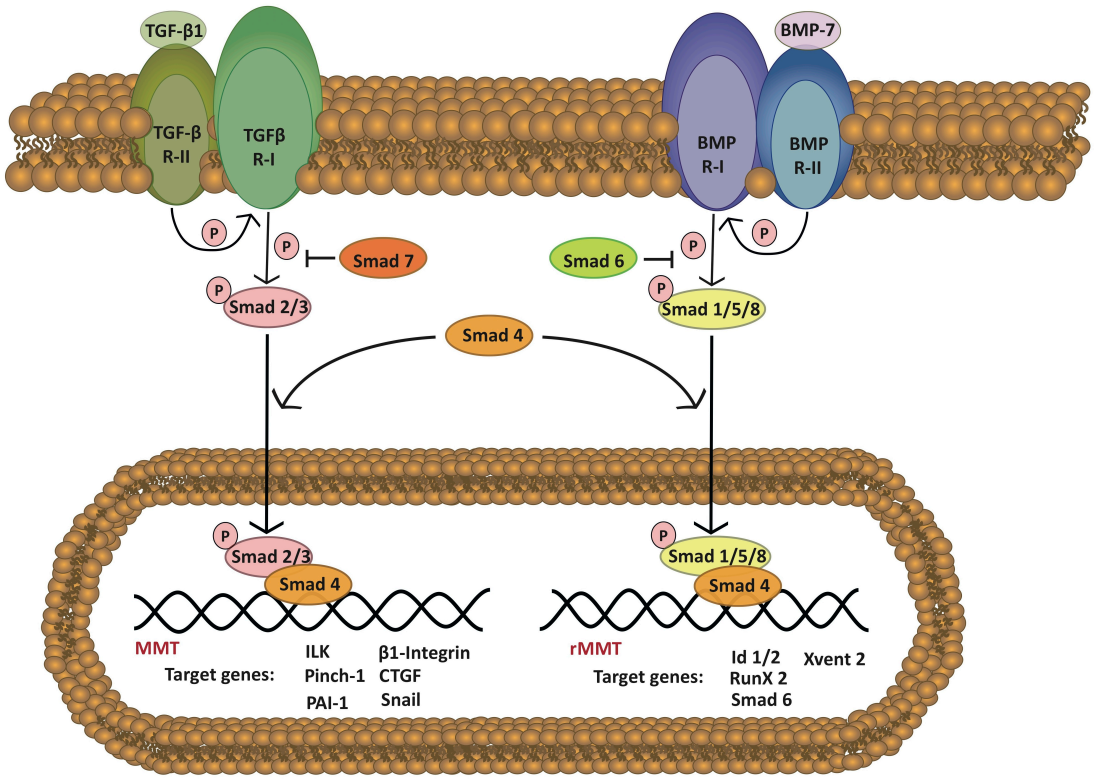

Figure 4. Smad-dependent signalling pathways of TGF-β and BMP-7 in the MMT context. TGF-β is secreted in its latent form and, once activated, binds to the constitutively active TGF-β type II receptor (TGF-β R-II), which then phosphorylates the TGF-β type I receptor (TGF-β R-I), activating it. BMP-7 has no latent form and binds its receptors in the same way. These receptors are transmembrane serine-threonine kinases. Once the receptors are activated, Smads 2 and 3 (in the case of TGF-β1), and Smads 1, 5 and 8 (in the case of BMP-7) are phosphorylated and form a trimeric complex with Smad4 to translocate into the nucleus. In the nucleus, these complexes activate or repress target genes involved in either the mesenchymal conversion of MCs (MMT), in the case of Smads2/3, or in the blocking/reversion of the mesenchymal transition (rMMT), in the case of Smads1/5/8. Smad6 and Smad7 block the phosphorylation and/or nuclear translocation of Smads and induce receptor complex degradation by recruiting ubiquitin ligases. *Modified from López-Cabrera, Advances in Medicine 2014.*

5. Implication of mesothelial cells in adhesion, invasion and progression of peritoneal metastasis

Independently of the MMT-promoting factors that could favour peritoneal metastasis, different hypotheses have tried to explain how malignant cells attach to the peritoneal membrane during the earliest stages. Initially, it was believed that MCs were simply victims of tumour aggression to the peritoneum (Heath et al. 2004; Na et al. 2010). Some experimental models proposed that intraperitoneal cancer spheroids gain access to the submesothelium by exerting force to clear MCs (Burleson et al. 2004; Iwanicki et al. 2011; Davidowitz et al. 2014). Subsequently, there was speculation that cancer cells do not adhere to the MCs but, rather, to the connective tissue under the MCs. The ECM is exposed in areas in the omentum (a fold of peritoneum containing fat tissue) called "milky spots" that have been identified as the preferred sites for peritoneal colonization (Hagiwara et al. 1993; Tsujimoto et al. 1995; Clark et al. 2013). However, "milky spots" are structures essentially comprised of an accumulation of immune cells and capillaries where the triggering of an inflammatory response can influence peritoneal metastasis, transforming the initial pattern of the "milky spot" attachment into a widespread pattern of dissemination (Sodek et al. 2012). In this context, De Vlieghere *et al.* have recently shown that microparticles coated with CAF-derived ECM proteins are able to selectively capture floating cancer cells, delaying tumour adhesion to the natural mesothelial niche (De Vlieghere et al. 2015). In the binding of cancer cells to the mesothelium, a wide range of adhesion molecules are reportedly involved, including CD44, CA125/MUC16, intercellular adhesion molecule-1 (ICAM-1) and vascular cell adhesion molecule 1 (VCAM-1) (Casey and Skubitz 2000; Ziprin et al. 2003; Rump et al. 2004; Alkhamesi et al. 2005; Ksiazek et al. 2010; Yu et al. 2010; Wagner et al. 2011). However, a growing body of experimental evidence on adhesion concurs that, at initial stages of peritoneal metastasis, cancer cells adhere to the peritoneum in a β1-integrin-dependent manner (Takatsuki et al. 2004; Watanabe et al. 2012;

Chen et al. 2015), which could indicate the adhesion is associated to the ECM. In agreement with this notion, it has been reported that cleavage of MC-associated matrix proteins fibronectin and vitronectin by MMP-2 enhances integrin-mediated carcinoma–mesothelium attachment (Kenny et al. 2008; Kenny and Lengyel 2009).

After attaching to the mesothelial monolayer, tumour cells reach the submesothelial compact zone. MCs increase their migration/invasion capacity during the MMT (Strippoli et al. 2012). Accordingly, MCs have been considered as the advancing front of the tumour in the processes of peritoneal carcinomatosis (Satoyoshi et al. 2015a; 2015b). MCs behave in a similar fashion to resident fibroblasts, in terms of the induction of carcinoma cell invasion *in vitro*. It has been shown that normal omentum fibroblasts induce the adhesion and invasion of carcinoma cells in 3D culture models (Kenny et al. 2007; 2008). On the other hand, Cai *et al.* reported that activated fibroblasts (either CAFs isolated from omentum from patients with ovarian cancer metastasis or normal omentum fibroblasts stimulated with TGF-β1) have stronger effects on carcinoma cell attachment and invasion than normal fibroblasts (Cai et al. 2011). Furthermore, the growth dynamics of cancer xenografts produced in response to intraperitoneal co-injection of omental MCs with either ovarian (Mikula-Pietrasik et al. 2014) or gastric (Tsukada et al. 2012) cancer cells was remarkably greater than for implantation of cancer cells alone. Therefore, in stark contrast to initial impressions, it is now accepted that MCs are not a passive barrier that prevents the progression of the tumour into the peritoneum, but are able to actively promote the process of adhesion to and invasion through the peritoneum.

In order for tumour cells to migrate and/or invade through the colonized organs, ECM disruption is crucial (Schropfer et al. 2010). Matrix metalloproteinases (MMP) are known to be important molecular players in the physiological processes of cancer progression by facilitating angiogenesis and tumour invasion through matrix degradation (John and Tuszynski 2001; Kessenbrock et al. 2010; Al-Alem and Curry 2015). In this context, CAFs have been widely

implicated in the remodeling of the ECM components through MMPs to consequently favour cancer invasion (Taddei et al. 2013; Paulsson and Micke 2014). It is well known that, at an intermediate stage of EMT, cells acquire the capacity to degrade the basement membrane and to invade the fibrotic stroma by upregulating the expression of MMPs (Kalluri and Weinberg 2009). In MCs, the expression of MMP-2 and MMP-9 increases in response to MMT-inducing stimuli such as TGF-β (Margetts et al. 2005) or TNF-α (Zhu et al. 2002). Interestingly, both of these MMPs can activate the latent form of TGF-β (Yu and Stamenkovic 2000). In addition, fibroblasts in omentum that have been activated by tumour cells have shown to promote ovarian invasiveness via MMP-2 overexpression (Cai et al. 2011). Similarly, exosomes of ovarian cancer ascites contain MMP-2, MMP-9 and urokinase-type plasminogen activator (uPa), all of them able to degrade the ECM, facilitating invasion and dissemination of tumour cells (Graves et al. 2004). Additionally, expression of VEGF by ovarian cancer cells is involved in transforming the ECM by stimulating MMP-9 expression at the tumour site (Belotti et al. 2008). With regard to the peritoneal environment, it could be speculated that, by increasing ECM deposition and MMP expression, mesothelial-derived CAFs regulate their own invasive capacity while helping to provide the appropriate ECM scaffold for cancer cells to survive in the metastatic niche (Birkedal-Hansen et al. 1993; Liotta and Kohn 2001; Lee et al. 2013; 2014).

CAFs in the tumour compartment have been implicated in promoting the growth and/or proliferation of cancer cells, ensuring their survival at the colonized organ. Although, mesothelial-derived CAFs have not yet been implicated in directly augmenting tumour growth, some authors have suggested that MCs establish communication with the tumour by secreting proliferating stimuli or by direct cell-cell contact which, in turn, stimulate proliferation of cancer cells and drive peritoneal dissemination (Tsukada et al. 2012; Mikula-Pietrasik et al. 2014).

At advanced stages of peritoneal metastasis, vascularization is necessary for tumour progression. Angiogenesis is also influenced by the organ microenvironment and is the result of an imbalance between positive and negative angiogenic factors released by tumour and host cells into the microenvironment of the neoplastic tissue (Kitadai 2010). In ovarian cancer progression in particular, the key role of VEGF has been well established and is correlated with decreased overall survival (Winiarski et al. 2014). Interestingly, vascular endothelial growth factor (VEGF) appears as one of the most induced factors in MCs transformed into myofibroblasts (Aroeira et al. 2005; Pérez-Lozano et al. 2013). The fact that the MCs that have undergone MMT express high amounts of VEGF suggests that peritoneal CAFs may play an important role in tumour vascularization (Sako et al. 2003).

OBJECTIVES

The general objective of this doctoral thesis is to study the role of the mesothelial-to-mesenchymal transition (MMT) in peritoneal metastasis. This objective can be divided into the following:

1. Identify and characterise the mesothelial (MC)-derived carcinoma-associated fibroblasts (CAFs) in the metastatic peritoneum.

2. Develop a mouse model to study peritoneal metastasis.

3. Study the effect on the peritoneum of a pre-conditioning that will induce or block the MMT in the mouse model.

4. Investigate the molecular mechanisms involved in the cancer cell-mesothelial cell interaction.

5. Obtain a gene profile for MC-derived CAFs to identify new possible therapeutic targets.

MATERIAL AND METHODS

1. Human samples

1.1. Biopsies from patients with peritoneal metastasis

Parietal peritoneum biopsies obtained from patients diagnosed with peritoneal carcinomatosis were considered in this study. Peritoneal metastases from eight serous ovarian carcinomas, four colonic adenocarcinomas, three pancreatic adenocarcinomas, one endometrial adenocarcinoma and pleural metastases from three pulmonary adenocarcinomas were considered in this study. Informed written consent to use surgical samples was obtained from the patients with the approval of the Ethics Committee of the Hospital Universitario de la Princesa (Madrid, Spain) and MD Anderson Cancer Center (Houston, USA). Tissue samples were fixed in neutral-buffered 3.7% formalin during 12-24 hours and embedded in paraffin to obtain serial sections 3-4 μm thick for histopathological analysis.

1.2. Primary mesothelial cells

Human peritoneal mesothelial cells (HPMCs) were obtained by trypsinization of omentum samples of patients undergoing unrelated abdominal surgery, as previously described (Yanez-Mo et al. 2003). Cells were cultured in Earle's M199 medium supplemented with 20% fetal bovine serum (FCS), 50 U/ml penicillin, 50 mg/ml streptomycin and 2% Biogro-2 (containing insulin, transferrin, ethanolamine and putrescine; Biological Industries, Beit Haemek, Israel).

MCs were also obtained from the ascitic fluid of eight ovarian cancer patients with peritoneal dissemination. The ascitic fluid was centrifuged and subsequently cultivated in Earle's 199 Medium. The purity of MC cultures was determined in both cases after 2-4 passages by the analysis of standard mesothelial markers (ICAM-1 and calretinin). The mesothelial cell type was confirmed by immunofluorescence staining using an antibody against calretinin (BioGenex, Fremont, CA, USA). Cell type was also confirmed by flow cytometry with antibodies against ICAM-1 (kindly provided by Dr. F. Sánchez-Madrid, Hospital Universitario de La Princesa, Madrid) using a BD FACSCalibur™ II flow cytometer (BD Biosciences, San

Jose, CA, USA). Cultures were negative for CD45, ruling out any contamination with macrophages.

Informed written consent to use omentum samples and ascitic fluid was obtained from the patients with the approval of the Ethics Committee of the Hospital Universitario de la Princesa (Madrid, Spain) and MD Anderson Cancer Center (Houston, USA). These studies adjust to the Declaration of Helsinki and were approved by the Ethics Committee of Centro de Biología Molecular "Severo Ochoa" (Madrid, Spain).

2. Cell culture and in vitro assays

2.1. Cell lines

The cell lines SKOV-3 and HT29, derived from human ovarian carcinoma and colorectal adenocarcinoma, respectively, were cultured in McCoy's 5A medium supplemented with 10% fetal bovine serum (FBS) at 37 ºC, 5% CO_2 atmosphere. HEK-293 cells were cultured in DMEM medium supplemented with 10% FBS at 37 ºC, 5% CO_2 atmosphere.

2.2. Induction of MMT *in vitro*

Induction of MMT *in vitro* is performed by treatment of MCs with 0.5 ng/mL of transforming growth factor-β1 (TGF-β1) (R&D Systems, Minneapolis, MN) plus 2.5 ng/mL of interleukin-1β (IL-1β) (R&D Systems) (T+I) for 72 hours or 6 days, which has been proven to be a suitable MMT model (Yanez-Mo et al. 2003; Strippoli et al. 2008; Aroeira et al. 2009; Sandoval et al. 2010; Loureiro et al. 2011; Strippoli et al. 2012; Pérez-Lozano et al. 2013).

To induce MMT with conditioned medium, sub-confluent omentum MCs, grown in 12-well plates, were treated with 75% of carcinoma cells supernatants supplemented with 2% FBS during 72 hours or 6 days. Untreated MCs were maintained in fresh medium supplemented with 2% FBS. At least 5 experiments were performed and each one was carried out in duplicate.

To obtain conditioned medium, confluent SKOV-3 and HT29 cells cultures were maintained in serum-free medium for 24 hours. Supernatants were then collected, centrifuged and stored at -80 ºC until used. Analysis of TGF-β1 in collected supernatants was achieved by

standard enzyme-linked immunoassay (ELISA) according to the manufacturer's instructions (R&D Systems).

2.3. Adhesion assays

To analyse the adhesion molecules involved in cell-cell interaction, MCs treated or not with T+I were plated in 96-microwell plates until confluence. SKOV-3 cells were loaded with the fluorescent probe BCECF-AM (Sigma-Aldrich), following manufacturer instructions, and subsequently added ($1x10^5$ cells/well) to the MC monolayers in presence or absence of the indicated monoclonal antibodies (20 µg/mL) in RPMI 1640 medium. Cells were maintained at 4 ºC for 10 min to allow antibody recognition and then allowed to adhere for 20 min at 37 ºC. Non adhered cells were washed with warm medium. Cells were measured by fluorescence of BCECF-AM with a fluorescence bottom reader (Tecan GENios). The percentage of adhesion was calculated considering the number of cells prior to wash as 100% of adhesion. The following monoclonal antibodies were applied in at least 3 experiments: Lia1/2 (blocking CD29); TS2/16 (activating CD29); 5E8D9 (blocking VLA-1); Lia 3/2 (blocking CD18) (Arroyo et al. 1992; Campanero et al. 1992).

2.4. Invasion assays

Invasion assays were performed in 12-mm diameter transwell units (3.0 µm pore size; Corning, MA, USA). First, the effect of carcinoma cells embedded in the matrix on MCs invasion capacity was analysed. Inserts were pre-coated with 300 µL of 1.5 mg/mL of rat-tail collagen I (BD Biosciences, San Jose, CA, USA) containing or not $2x10^5$ CFSE-labelled SKOV-3 cells. After gelling overnight at 37 ºC, $2x10^5$ MCs, resuspended in 200 µL of serum-free M199 medium, were added into the upper chamber. Assay medium supplemented with 5% FBS was added to the lower chamber. MCs were allowed to invade for 5 days at 37 ºC, 5% CO_2 atmosphere. To analyse the effect of MCs on carcinoma cell invasion, the inserts were collagen I pre-coated containing or not $2x10^5$ CFSE-labelled MCs with either epithelial-like or mesenchymal-like phenotype. After gelling, $2x10^5$ SKOV-3 cells, resuspended in 200 µL of

serum-free McCoy's 5A medium were added into the upper chamber, and medium supplemented with 5% FBS was added to the lower chamber. Tumour cells were allowed to invade for 5 days at 37 ºC, 5% CO_2 atmosphere. In all the cases, the transwells were then fixed in 10% formaldehyde and stained with propidium iodide (Sigma-Aldrich).

Images were captured by using a confocal laser-scanning microscope (LSM 710; Carl Zeiss MicroImaging), equipped with acquisition software (Zeiss Zen 2008), and using 10x objective. 3D double-color imaging was performed using the program ImageJ 1.46f (National Institutes of Health).

Parallel experiments were subjected following the same procedure to obtain 3-4 μm transversal sections of paraffin embedded gels. Images of H&E stained sections were acquired by optical microscope. Each experiment was carried out in duplicate and at least 3 experiments were performed.

2.5. Treatment of mesothelial and cancer cells with TGF-β1

HPMCs and SKOV-3 cells were plated at confluence on 22 mm^2 coverslips placed in 24-well tissue culture plates. Where indicated, cells where stimulated with TGF-β1 (4 ng/ml) for 1 and 6 hours. Coverslips were fixed in 4% paraformaldehyde and stained by immunofluorescence for phosphorylated Smad3 (pSmad3) (Cell Signaling).

3. Adenoviral production

HEK 293 A cells were infected with a control adenovirus or with an adenovirus encoding active TGF-β1, kindly provided by Fernando Rodríguez-Pascual (Otsuka et al. 2006). 4 days post-infection, adenoviral particles were recollected and purified with Adeno-X™ Maxi Purification Kit (Clonetch Laboratories, Mountain View, CA, USA) and later titrated with Adeno-X™ Rapid Titer Kit (Clontech).

4. Bacterial transformation, lentiviral vector production and titration

Plasmids containing the shRNA sequence targeting Smad3, and control plasmids (SHC003) were purchased from Sigma-Aldrich (St. Louis, MI, USA) in the pLKO.1-puro-

CMV-TurboGFP™ backbone. The MISSION® shRNA used was TRCN0000089026:5'CCGGCTGTCCAATGTCAACCGGAATCTCGAGATTCCGGTTGAC ATTGGACAGTTTTTG-3'. 100 µl of competent bacteria were mixed with 10 ng of each plasmid and incubated on ice for 30 min. A 42 °C heat-shock of 30 s was performed, followed by immediate placement on ice for 5 min. 200 µl of SOC medium were added to the bacterial suspensions before incubating at 37 °C for 1 h. Half of each the aliquot was plated out on 1.5% (w/v) LB agar plates with 100 µg/ml ampicillin at 37 °C overnight. The following day, single colonies were incubated in 200 ml of LB at 37 °C for 24 h. The LB medium was recollected and centrifuged at 4 ºC and 6,000 g for 20 min. The pellets obtained were used to purify the plasmid DNA with the QIAGEN Plasmid Maxi Kit (QIAGEN, Hilden, Germany) following manufacturer's instructions. Pseudoviral particles were prepared using the pPACK-F1 Lentivector packaging system (SBI System Biosciences, Mountain View, CA, USA) and HEK 293T producer cell line were used as described (Ding and Kilpatrick 2013). The titration of pseudoviral particles generated with the lentiviral vectors was determined by calculating the percentage of positive GFP expression cells by flow cytometry in a BD FACSCalibur™ II flow cytometer (BD Biosciences, San Jose, CA, USA) 72 h after infection. The lentivirus titers were calculated as described (Ding and Kilpatrick 2013) and expressed in infection forming units (ifu)/ml.

5. Mice

Swiss nu/nu 2-month-old mice were used in all studies (Charles River Laboratories, Barcelona, Spain). Food and water were provided *ad libitum* to the animals. The experimental protocols followed were in accordance with the National Institutes of Health Guide for Care and Use of Laboratory Animals and were approved by the Animal Ethics Committee of the "Unidad de Experimentación Animal" del Centro de Biología Molecular "Severo Ochoa" (Madrid, Spain).

5.1. Mouse model of carcinoma peritoneal dissemination

A total of $5x10^6$ SKOV-3 cells resuspended in 1000 μL of phosphate buffered saline (PBS) were inoculated into the peritoneal cavity of mice (n=10). Mice were sacrificed at different time points (four to eight weeks) and parietal peritoneum samples were collected for immunohistochemical analysis.

5.2. Subcutaneous xenografts

A preliminary assay with mice (n=2) co-inoculated in the left flank with $1x10^6$ SKOV3-luc-D3 Bioware® cells alone, and in the right flank with $1x10^6$ SKOV3-luc-D3 Bioware® cells plus and $0.5x10^6$ ascitic fluid-derived MCs (AFMCs). Mice were co-inoculated in the left flank with a combination of $1x10^6$ SKOV3-luc-D3 Bioware® cells and $0.5x10^6$ HPMCs resuspended in 100 μL of PBS. One the right flank, mice were co-inoculated with $1x10^6$ SKOV3-luc-D3 Bioware® and either $0.5x10^6$ HPMCs T+I in one group (n=8), or $0.5x10^6$ AFMCs (n=6), all resuspended in 100 μL of PBS. Upon injection of D-luciferin (Perkin-Elmer, Hopkinton, MA, USA), luciferase signal was detected and tumour growth was monitored weekly for 5 weeks with IVIS Lumina II (Perkin-Elmer).

5.3. Peritoneum pre-conditioning

5.3.1. Adenoviral delivery of TGF-β1

In order to induce a mesothelial-to-mesenchymal transition and pre-condition the peritoneum, the TGF-β1 gene was transduced into the peritoneal cavity with adenoviral vectors. Mice were infected with control adenovirus $1x10^7$ (n=6) or adenovirus encoding active TGF-β1 (n=6). 7 days post-infection, mice were inoculated i.p. with $5x10^6$ SKOV3-luc-D3 Bioware® resuspended in 1000 μL of PBS. Upon injection of D-luciferin (Perkin-Elmer), luciferase signal was detected and mice were monitored twice weekly with IVIS Lumina II (Perkin-Elmer, Hopkinton, MA, USA). Mice were sacrificed 41 days post-inoculation and parietal peritoneum samples were collected for immunohistochemical analysis.

5.3.2. Conditioned medium from cancer cells

In order to induce a mesothelial-to-mesenchymal transition, conditioned medium from SKOV-3 cells (maintained in McCoy's 5A medium supplemented with 1% serum for 48 hours) was administered intraperitoneally (i.p.) to mice 2 days prior to the inoculation in the peritoneal cavity of $5x10^6$ SKOV3-luc-D3 Bioware® cells (Perkin-Elmer, Hopkinton, MA, USA) resuspended in 1000 μL of PBS. The conditioned medium had been previously centrifuged and stored at -80 ºC until use. MMT was blocked with a TGF-β receptor I inhibitor, GW788388 (3 mg/kg/day, Tocris Bioscience, UK), and the vehicle DMSO was used as a control. GW788388 was administered into the peritoneal cavity 4 and 2 days prior to mice being inoculated with $5x10^6$ SKOV3-luc-D3 Bioware® cells. 4 groups of 6 mice each were used. Mice and tumour growth were monitored by *in vivo* bioluminiscence imaging twice weekly with IVIS Lumina II (Perkin-Elmer, Hopkinton, MA, USA). Mice were sacrificed 41 days post-inoculation and parietal peritoneum samples were collected for immunohistochemical analysis.

5.3.3. Smad3 knockdown with lentiviral delivery

18 mice were randomly grouped to be infected with $1x10^9$ ifu of either control or Smad3 shRNA-producing lentiviral particles (obtained as described later). 4 days post-infection, mice were inoculated i.p. with $5x10^6$ SKOV3-luc-D3 Bioware® resuspended in 1000 μL of PBS. Upon injection of D-luciferin (Perkin-Elmer), luciferase signal was detected and mice monitored twice weekly with IVIS Lumina II (Perkin-Elmer, Hopkinton, MA, USA). Mice were sacrificed 41 days post-inoculation and parietal peritoneum samples were collected for immunohistochemical analysis.

6. Immunohistochemical analysis

6.1. Human samples

Deparaffinized tissues were heated to expose the hidden antigens using Real Target Retrieval Solution containing citrate buffer, pH 6.0 (Dako, Glostrup, Denmark). Endogenous peroxidase was blocked with Real Peroxidase-Blocking Solution (Dako). Samples were stained

using primary antibodies to detect pan-cytokeratin (Dako); α-SMA (Dako); Calretinin (Novocastra Laboratories, Newcastle Upon Tyne, UK); Mesothelin (Roche Diagnostics); Cytokeratin-20 (Dako); Cytokeratin-7 (Dako); Cytokeratin AE1/AE3 (Roche Diagnostics), CD34 (Dako), pSmad3 (Cell Signaling), VEGF (Abcam, Cambridge, UK) and WT1 (Roche Diagnostics). Antibodies were visualized by means of a dextran–polymer conjugate technique (EnVision+, Dako) using 3,3′-diaminobenzidine (DAB) (Dako) as chromogen. Tissue sections were counterstained with haematoxylin.

6.2. Mouse samples

Similarly, mouse deparaffinized peritoneal samples were incubated with the following primary antibodies: α-SMA (Sigma-Aldrich, St Louis, MO, USA); pan-cytokeratin (Sigma-Aldrich); CD31 (Abcam, Cambridge, UK); pSmad3 (Cell Signaling), and WT1 (Santa Cruz Biotechnology, INC). Non-specific binding of secondary antibodies was blocked by pre-treating slides with goat serum. A Biotinylated goat anti-rabbit IgG (H+L) was applied to detect rabbit primary antibodies and complexes were visualized using the R.T.U Vectastain Elite ABC Kit (Vector Laboratories, Burlingame, CA, USA). Mouse primary antibodies were visualized applying the Vector M.O.M. Immunodetection Kit (Vector Laboratories) according to the manufacturer's instructions. Tissue sections were revealed using DAB (Dako) as chromogen and finally counterstained with haematoxylin.

7. Immunofluorescence analysis

7.1. Peritoneal tissues from mice

Deparaffinized tissues were stained for immunofluorescence with antibodies to visualize WT1 (Santa Cruz Biotechnology) and α-SMA (Sigma-Aldrich). Sections were heated to expose the hidden antigens using Real Target Retrieval Solution containing citrate buffer, pH 6.0 (Dako). Non-specific binding of secondary antibodies was blocked by pretreating slides with donkey serum (Abcam). Secondary antibodies Alexa Fluor 647 and Alexa Fluor 555 were incubated (Molecular Probes) at room temperature. Finally, the slides were mounted with a 4',6-

diamidino-2-phenylindole (DAPI) nuclear stain (Pierce; Thermo Fisher Scientific). The preparations were analysed with a Leica TCS-SP5 (Leica Microsystems) confocal microscope.

7.2. Mesothelial and SKOV-3 cells

Cells were fixed for 10 minutes in 4% paraformaldehyde and permeabilized 10 minutes in 0.1% NP-40. In all cases, 5% goat serum was applied for 20 minutes to block non-specific unions. Cells were stained for calretinin (labeled with Alexa Fluor 488), α-SMA (labeled for Alexa Fluor 555) and pSmad3 (labeled with Alexa Fluor 488) and mounted with fluorescent mounting medium (Dako). Confocal images were acquired with a LSM710 Zeiss Confocal Microscope, equipped with acquisition software (Zeiss Zen 2008) and using 40X or 60X objectives.

8. Flow cytometry

Confluent cultures of ascitic fluid-derived MCs were trypsinized, washed and resuspended in PBS supplemented with 0.5% BSA and 2 mM EDTA. A total of $1x10^5$ cells were incubated with 100 µl of polyclonal antibody against ICAM-1 washed with PBS and then incubated with 100 µl of a 1:50 dilution of an Alexa Fluor 488 anti–mouse Ig. Finally, fluorescence was measured using a BD FACSCalibur™ II flow cytometer (BD Biosciences, San Jose, CA, USA).

9. Western blot

MC and SKOV-3 cultures were lysed in RIPA buffer (1% sodium deoxycholate, 0.1% sodium dodecyl sulphate) plus a phosphatase and protease inhibitor cocktail (Pierce) and total protein was quantified by protein assays kit (Pierce). Equal amounts of denatured proteins (20 µg) from each sample were resolved by 8–10% sodium dodecyl sulphate–polyacrylamide gel electrophoresis under reducing conditions. Proteins were transferred on nitrocellulose membranes, which were then blocked with 5% non-fat milk in TBS–Tween buffer for 1 h and incubated with specific antibodies against WT1 (Santa Cruz Biotechnology), α-SMA (Sigma-Aldrich), pan-cytokeratin (Sigma-Aldrich), calretinin (Biogenex, CA, USA) and β-actin

(Sigma-Aldrich) in 0.5% milk in TBS-Tween overnight at 4 °C. These antibodies were detected with a peroxidase-conjugated goat anti-mouse and donkey anti-rabbit antibodies (Pierce), and then were visualized with enhanced chemiluminescence (ECL) detection kit (Pierce). Blot images were acquired using a GS-710 Imaging Densitometer (Bio-Rad, Hercules, CA, USA).

10. Quantitative real-time PCR (qRT-PCR)

The analysis of MMT-related molecules was achieved by real time qRT-PCR. Briefly, MCs were lysed in TRI Reagent (Ambion, Inc., Austin, TX) and total RNA was extracted according to the manufacturer's recommendation. Complementary DNA was obtained from 2 μg of RNA by reverse transcription (Applied Biosystems, Cheshire, UK). Quantitative PCR was carried out in a LightCycler 2.0 using a SYBR Green kit (Roche Diagnostics, Mannheim, Germany) and specific primers for Snail, E-cadherin, fibronectin, collagen I, vascular endothelial growth factor (VEGF), TGF-β1, and histone H3 (**Table 1**). Samples were normalized with respect to the value obtained for H3.

Table 1. Specific primers for real-time PCR

Gene	Forward primer	Reverse primer	T_m (ºC)
Snail	5′-GCAAATACTGCAACAAGG-3′	5′-GCACTGGTACTTCTTGACA-3′	55
E-cadherin	5′-TGAAGGTGACAGAGCCTCTG-3′	5′-TGGGTGAATTCGGGCTTGTT-3′	62
Fibronectin	5′-CCTGAAGCTGAAGAGACTTGC-3′	5′-CGTTTCTCCGACCACATAGGA-3′	66
Collagen I	5′-GCTATGATGAGAAATCAACCG-3′	5′-GCTTCCCCATCATCTCCATTC-3′	64
VEGF-A	5′-GCAGAAGGAGGAGGGCAGAAT-3′	5′-TATGTGCTGGCCTTGGTGAGG-3′	60
TGF-β1	5′-TGAACCGGCCTTTCCTGCTTCTCATG-3′	5′-CGGAAGTCAATGTACAGCTGCCGC-3′	70
H3 histone	5′-AAAGCCGCTCGCAAGAGTGCG-3′	5′-ACTTGCCTCCTGCAAAGCAC-3′	62

11. Scanning electron microscopy

MCs were plated at confluence on 22 mm^2 coverslips placed in 24-well tissue culture plates. Where indicated, cells where stimulated with T+I for 72 hours, and then washed twice. SKOV-3 cells labeled with Carboxyfluorescein diacetate Succinimidyl Ester (CFSE; Molecular Probes, Invitrogen) were added at a density of 1 x 10^5 cells per well. After 30 minutes, the wells

were gently washed to eliminate non-attached cells. Coverslips were then fixed in 4% paraformaldehyde and nuclei were stained with DAPI. Adherent SKOV-3 cells were evaluated in ten fields per sample. Representative images were captured with a digital camera coupled to a vertical fluorescence microscope (Axioskop2 plus, Carl Zeiss, INC). At least 5 experiments were performed in duplicate.

For scanning electron microscopy analysis, a parallel experimental procedure was carried out in which coverslips were fixed in 3% glutaraldehyde. Post-fixation was performed in 1% OsO_4 and after dehydration through graded series of ethanol, samples were dried in a critical-point drying system using liquid carbon dioxide. Finally, coverslips were mounted on aluminum stubs, sputter coated with gold, and examined using a scanning electron microscope (JEOL Scanning T-300). Images were interpreted using the image-processing program ImageJ 1.46f (National Institutes of Health, Bethesda, Maryland, USA).

12. Statistical analysis

Results are presented as 25th and 75th percentiles, median, minimum and maximum values in box plots graphics; and as mean ± SEM in bar graphics. Statistical analysis was performed using GraphPad Prism version 5.0 (La Jolla, CA, USA). Data groups of Figures 8, 16, 17, 18, 19, 20, 21, 22 and 27 were compared with the non-parametric Mann–Whitney rank sum U-test. Multiple t-test analysis was performed in Figures 23, 25, 26 and 31. $p < 0.05$ was considered statistically significant in all cases.

13. RNA-sequencing and functional annotation

13.1. RNA extraction

Total RNA was extracted from HPMCs and AFMCs by lysing in TRI Reagent (Ambion, Inc., Austin, TX) following manufacturer's recommendation. Before performing the RNA sequencing, RNA integrity was checked using the Agilent Bioanalyzer 2100® (Agilent Technologies, Santa Clara, CA, USA).

13.2. RNA sequencing

Samples were depleted of rRNA, then the RNA was sheared into smaller fragments with Covaris S220 (Covaris, Woburn, MA, USA). The cDNA library was prepared using the Beckman SPRIworks system (Beckman Coulter Inc., Fullerton, CA, USA). Library fragments hybridize to complementary oligonucleotides, and clusters of clones are generated in the Illumina cBOT instrument (Illumina, Inc., San Diego, CA, USA). The XX libraries were sequenced onto an Illumina HiSeq 2000 (Illumina, Inc., San Diego, CA, USA) and subjected to 100 cycles of paired-end (200 bp insert size) sequencing, generating 412 million reads.

13.3. Data analysis

Raw sequences obtained from the Illumina platform in FASTQ format were analyzed using publicly available tools. Quality reads were analyzed using FastQC. Due to the high quality of reads there was no need to trim of filter them. The sequences were mapped to the GRCh38.p2 human reference genome sequence using a series of programs, including Bowtie2 for short-read mapping, and TopHat for defining exon–intron junctions. The expression level of each transcript was expressed as the fragments per transcript kilobase per million fragments mapped (FPKM) value, which was calculated based on the number of mapped reads using Cufflinks. Cuffdiff was used to detect differentially expressed genes using three replicates. Heatmaps were generated using heatmap.2 in the R package gplots (ver. 2.11.0) with the Z-scores of RPKM values.

13.4. Analysis of differential expression genes by IPA software

Genes that were differentially regulated were uploaded to the Igenuity Pathway Analysis (IPA) tool (Ingenuity® Systems, www.ingenuity.com) to perform analysis of canonical pathways and upstream regulators. Fisher's exact test was used to measure the significance of the association between the list of genes and a canonical pathway. Pathways with a p-value < 0.05 (Benjamini-Hochberg method) were considered to be statistically significant. When analysing the resulting pathways in order to study their relevance in the

context of ovarian cancer patients, canonical pathways that are specific to other cells types or unrelated pathologies have been excluded, e.g. “airway inflammation in asthma”, “axonal guidance signalling”. The upstream regulator analysis function was used to identify potential transcriptional regulators; and only the regulators that are also differentially expressed in our data set have been considered. Upstream regulator analysis takes into account two measures: the statistical significance of genes in the dataset to overlap with the list of downstream targets of a given regulator (p-value of overlap; $p < 0.05$ was considered significant), and the prediction of activation or inhibition of a putative regulator based on published findings included in the Ingenuity Knowledge Base (activation z-score; a z-score of $\geq|2|$ was considered significant).

RESULTS

1. Human biopsies analysis shows that CAFs originate from MCs and collaborate in tumour angiogenesis.

Histological observation of peritoneal biopsies from human ovarian carcinoma implants showed the localization of metastatic foci in the submesothelial area surrounded by spindle-like cells. Immunostaining of serial sections showed overlapped expression of α-smooth muscle actin (α-SMA) and mesothelial markers, such as cytokeratins and calretinin, in the stromal tissue surrounding the tumour implants. As expected, cytokeratin staining also revealed the epithelial nature of metastasizing cells (Figure 5A). Additional mesothelial markers, such as Wilm's tumour protein-1 (WT1) and mesothelin, were also expressed in fibroblast-like cells proximal to peritoneal micrometastases derived from an endometrial adenocarcinoma (Figure 5B). The co-expression of mesothelial and mesenchymal markers suggested that in peritoneal metastases CAFs may derive from MCs via MMT.

Using the differential expression of cytokeratins, the mesothelial origin of CAFs was confirmed; e.g. colon carcinoma cells express cytokeratin-20 but not cytokeratin-7 and, conversely, MCs express cytokeratin-7 but not cytokeratin-20. The analysis of peritoneal metastases of colon carcinoma in humans demonstrated that the expression of cytokeratin-20 was confined to tumour implants, whereas the expression of cytokeratin-7 was observed in the preserved mesothelium of tumour-free regions and in fibroblast-like cells located in the close proximity of tumour micrometastases (Figure 5C). To further verify that CAFs may originate from MCs, metastatic implants of lung cancers in the pleura (another anatomical cavity lined by mesothelium) were analysed. Here, CAFs expressing calretinin close to cancer implants can be observed (Figure 6). In addition, there was no expression of mesothelial makers in CAFs of tumours located outside the coelomic cavities (Figure 7).

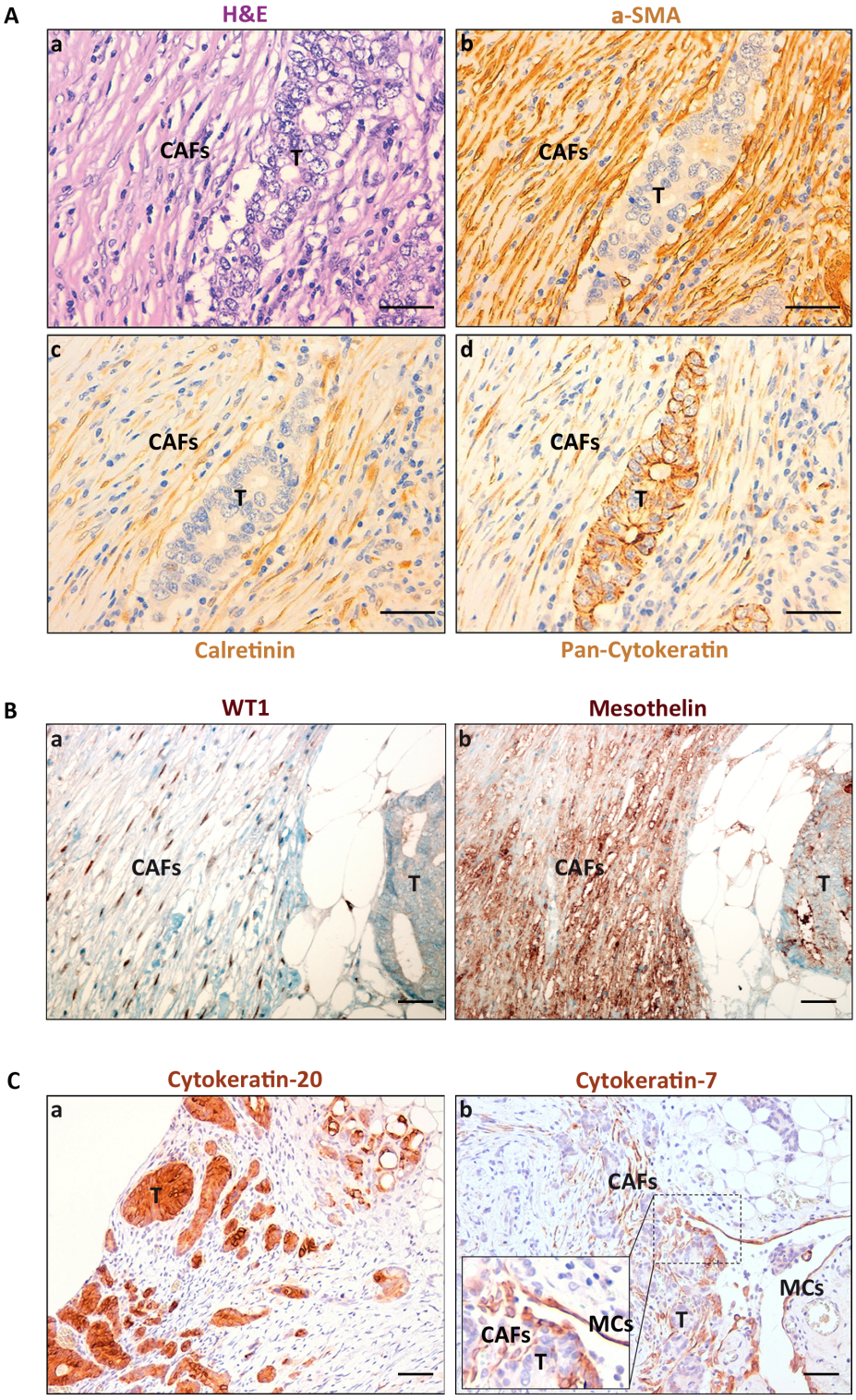

Figure 5. Analysis of human peritoneal carcinoma implants reveals the mesothelial origin for CAFs.

(A) (a) H&E staining shows an ovarian cancer micrometastasis in the submesothelial area, surrounded by spindle-like cells; (b–d) IHC analysis of serial sections reveals overlapped expression of α-SMA and the mesothelial markers calretinin and cytokeratin in fibroblastic cells surrounding the tumour implant; (d) cytokeratins also stain the metastasizing cells, revealing

their epithelial nature. Scale bars = 25 µm. **(B)** Serial sections of a peritoneal implant of an endometrial cancer biopsy reveal the presence of (a) fibroblastic cells expressing nuclear WT1 and (b) mesothelin detected within the endometrial tumour mass. Scale bars = 100 µm. **(C)** Biopsy of peritoneal metastasis from a patient diagnosed with colon carcinoma: (a) multiple tumour nodules express cytokeratin-20 while stromal cells close to metastatic implants are negative for this marker; (b) in contrast, fibroblast-like cells surrounding tumour implants express the mesothelial marker cytokeratin-7; inset shows a higher magnification of the delimited area. Scale bars = 100 µm. T, tumour.

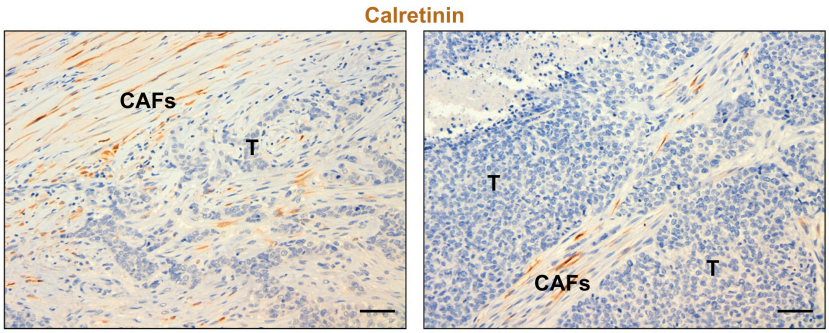

Figure 6. Analysis of human lung cancer-derived metastasis in the pleura.

Calretinin-positive fibroblasts coexist with large-cell lung carcinoma implants in pleura. These results support the mesothelial origin of CAFs. T, tumour. Scale bars = 100 µm.

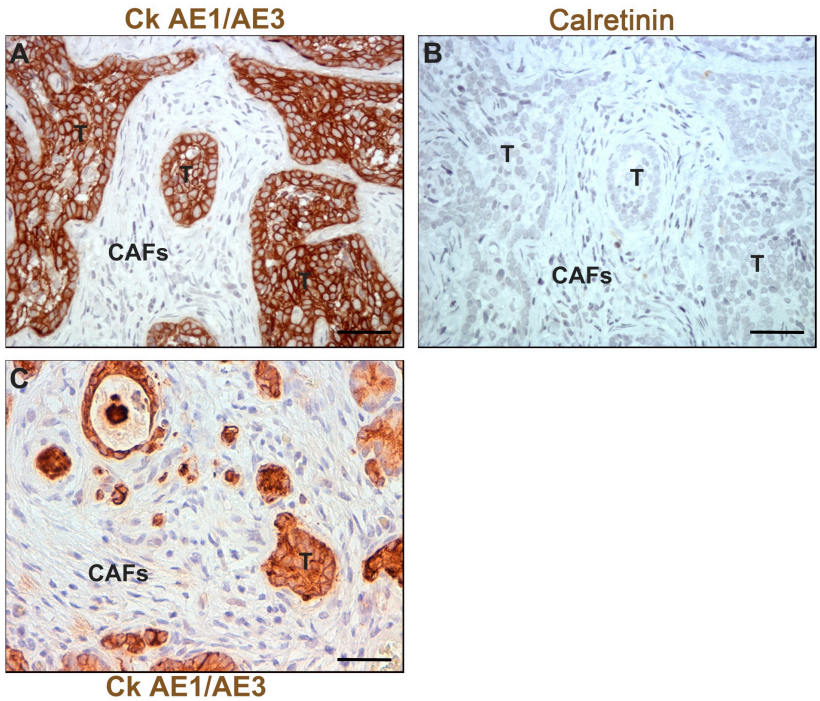

Figure 7. MC markers are not expressed in CAFs of tumours located outside the coelomic cavities.

(A, B) Serial sections of a cutaneous basal cell carcinoma show CAFs negative for mesothelial markers (cytokeratin AE1/AE3 and calretinin) accompanying the tumour. **(C)** An infiltrating breast carcinoma positive for cytokeratin AE1/AE3 shows proximal CAFs negative for this mesothelial marker. Scale bars = 25 µm. T, tumour.

It has been shown that during the MMT, MCs acquired the ability to produce large amounts of VEGF (Aroeira et al. 2005; Pérez-Lozano et al. 2013). Thus, it can be hypothesized that CAFs derived from MCs may play a role in tumour vascularization. Quantification of the number of vessels in biopsies from peritoneal implants derived from different human cancers revealed a significant increase (p=0.002) in CD34-positive vessels in the areas of tumour micrometastasis compared with tumour-free zones from the same biopsies (Figure 8A–C). To confirm that MC-derived CAFs participate in tumour angiogenesis, tumours that express low levels of VEGF were used. As shown in Figure Figure 9A, an endometrial adenocarcinoma expressed low amounts of VEGF. In contrast, MC-derived CAFs (cytokeratin-positive) appeared to be high producers of VEGF (Figure 9B).

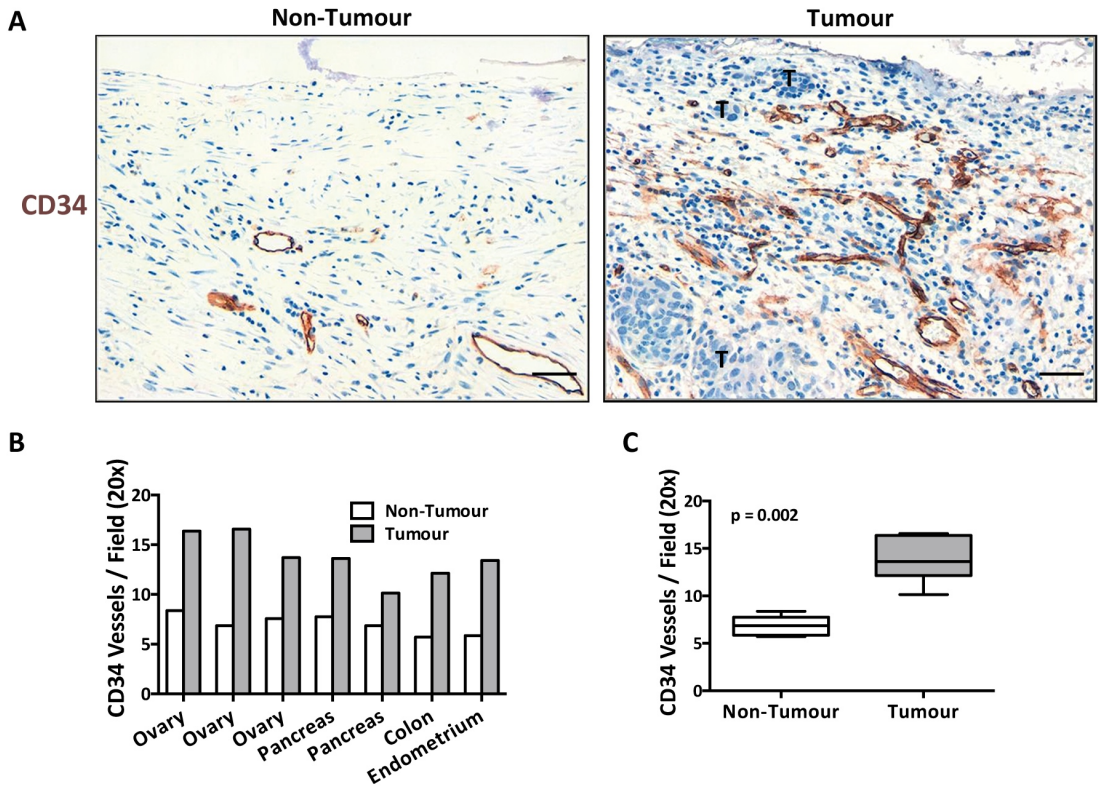

Figure 8. Vessel number increases in areas adjacent to micrometastases.

(A) Representative specimen of ovary cancer metastasis in peritoneum. The "Non-Tumour" image shows a submesothelial area from the biopsy without evidence of tumour implants and with a low number of vessels, which were mostly confined to the deeper compact zone. The "Tumour" image depicts a submesothelial area with micrometastases and elevated number of CD34-positive vessels. Scale bars = 100 µm. **(B)** Separate analysis of three ovarian, two pancreatic, one colorectal and one endometrial-derived metastases consistently shows the differences. **(C)** Quantification of CD34-positive vessels observed in tumour implant areas

compared to distant zones without evidence of peritoneal metastases. Box plot graphic depicts 25th and 75th percentiles, median, minimum and maximum values; differences were statistically significant (p = 0.002). Scale bars = 25 µm. T, tumour.

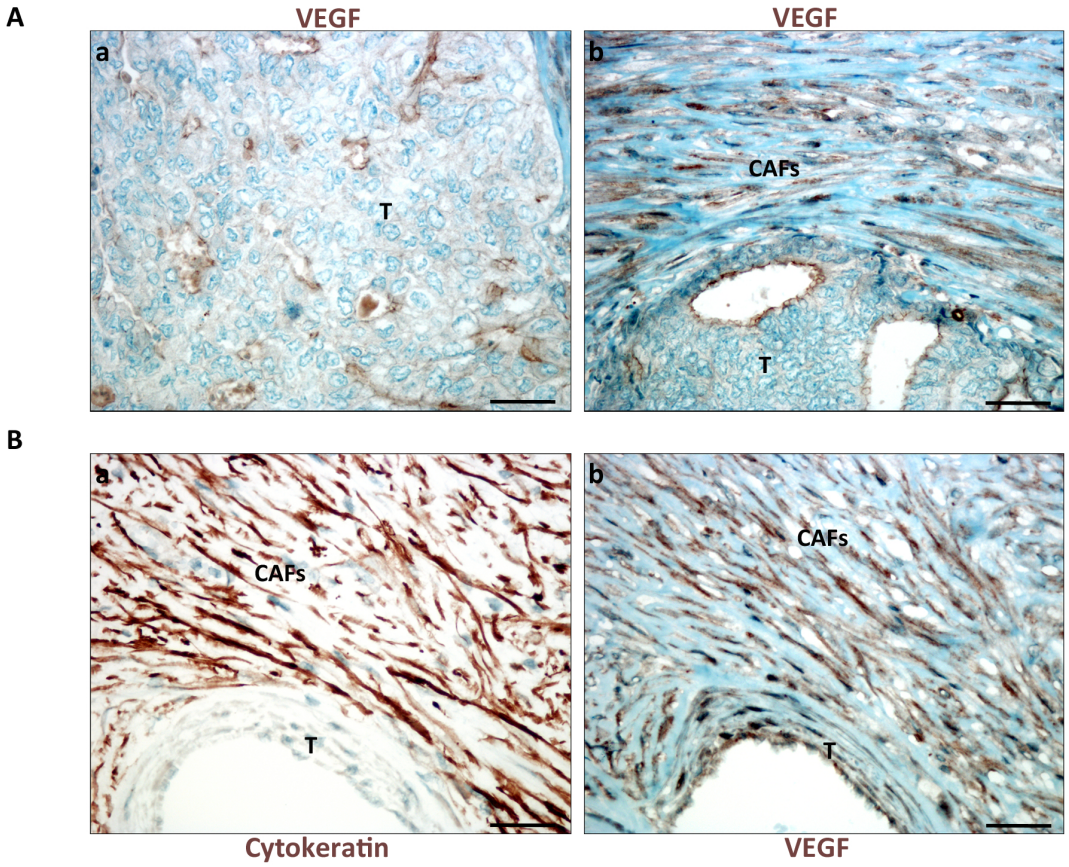

Figure 9. MC-derived CAFs accumulate close to micrometastases and express large amounts of VEGF.

(A) Representative case of endometrial adenocarcinoma metastasis in peritoneum: (a) tumour implant shows low expression levels of VEGF, which is mostly limited to endothelial cells in angiogenesis areas; (b) spindle-shaped CAFs surrounding the tumour mass express high levels of VEGF. Scale bars = 25 µm. **(B)** (a, b) Serial sections of the same case confirm that MC-derived CAFs (cytokeratin-positive) proximal to the tumour produce large amounts of VEGF. Scale bars = 25 µm. T, tumour.

2. CAFs originate from MCs in a mouse model of peritoneal dissemination

Parietal peritoneal tissues stained with H&E showed a fibro-proliferative response at the sites of small tumour implants, with submesothelial accumulation of spindle-like cells and fibrosis, which were absent in tumour-free zones of the same samples (Figure 10A, B). Immunohistochemistry analysis showed intense cytokeratin staining of metastasizing cells and a weak cytokeratin staining in MCs located nearby, indicating that these MCs were undergoing a

MMT, which implied the downregulation of cytokeratin expression. Surrounding the micrometastatic nodules there was a prominent accumulation of α-SMA-positive fibroblasts. In the peritoneal region without metastatic implants there was no expression of α-SMA other than that in the smooth muscle cells of the vessel walls, and the expression of cytokeratin was limited to the preserved mesothelium (Figure 10C–F). WT1 was used as an additional mesothelial marker in order to confirm the origin of CAFs. Immunohistochemistry analysis showed nuclear staining of WT1 in the preserved mesothelium of tumour-free regions and in submesothelial CAFs surrounding tumour implants (Figure 10G, H). Immunofluorescence techniques confirmed the presence of fibroblast-like cells that were double positive for WT1 and α-SMA (Figure 11). Western blot analysis demonstrated that SKOV-3 cells were negative for WT1 and α-SMA, and confirmed the down-regulation of cytokeratin and induction of α-SMA during the MMT (Figure 12).

Blood vessels of parietal tissues were stained with anti-CD31 antibody. There was a dramatic increase in the number of vessels in areas adjacent to micrometastases when compared with tumour-free regions (Figure 13A, B). The new vessels were mainly located in the upper sub-mesothelial zone, where MC-derived CAFs expressing high levels of VEGF (Figure 13C, D) tended to accumulate, suggesting that MCs could, indeed, play an important role in tumour vascularization.

Analysis of peritoneal specimens with larger implants showed that, at advanced stages of peritoneal dissemination, the expression of cytokeratin was restricted to carcinoma cells. Nevertheless, WT1- and α-SMA-positive cells could be observed, not only in the proximity of carcinoma implants, but also integrated within the tumour stroma (Figure 14). Peritoneal metastases were also observed in the omental tissue, where cytokeratin- and α-SMA-positive spindle cells were found in the interstitial stroma, surrounding tumour implants (Figure 15).

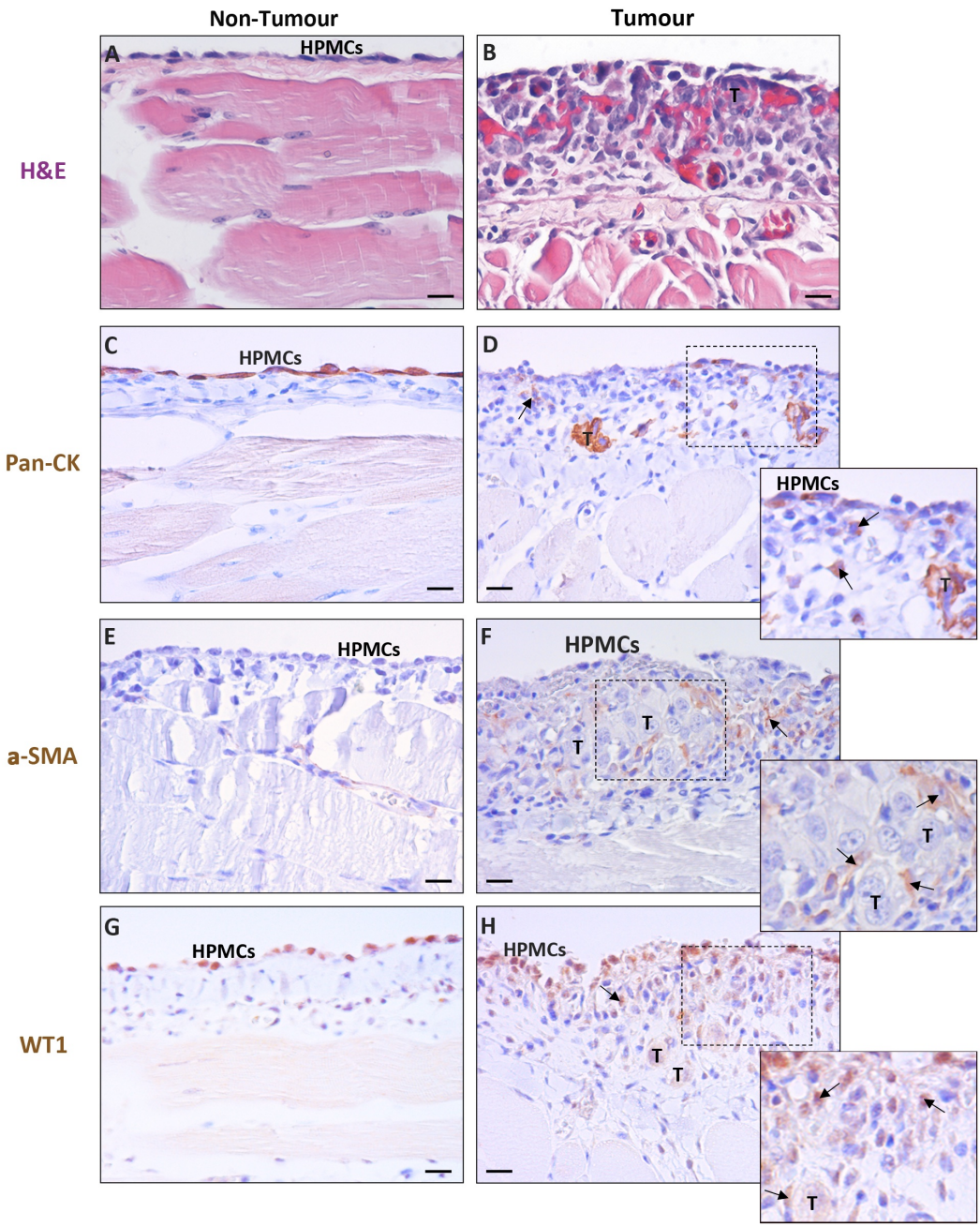

Figure 10. CAFs originate from MCs in a mouse model of peritoneal dissemination.

Immunohistochemistry of parietal peritoneum samples, 4 weeks after i.p. injection of SKOV-3 cells. **(A, B)** H&E staining shows areas distant from tumour implants (Non-Tumour) with a conserved histological structure, no evidence of fibrosis and with a preserved MC monolayer. At the places of tumour implants there is a fibro-proliferative response, with the accumulation of spindle-like cells. **(C, D)** Cytokeratin expression in the preserved mesothelium of "Non-Tumour" regions. In the proximity of tumour implants, there is an intense cytokeratin staining in metastasizing tumour cells, but a weak cytokeratin staining in MCs and in some fibroblast-like cells. **(E, F)** In the "Non-Tumour" areas there is no expression of α-SMA other than that in the smooth muscle cells of the vessel walls. Surrounding the tumour implants there is accumulation of α-SMA-positive fibroblasts. **(G, H)** Nuclear staining of WT1 (an additional MC marker) in the preserved mesothelium of tumour-free regions and in submesothelial CAFs

surrounding tumour implants. Arrows indicate MC-derived CAFs in the proximity of submesothelial tumour implants. Insets show higher magnifications of the delimited areas. Scale bars = 25 µm. T, tumour; Pan-CK, pan-cytokeratin.

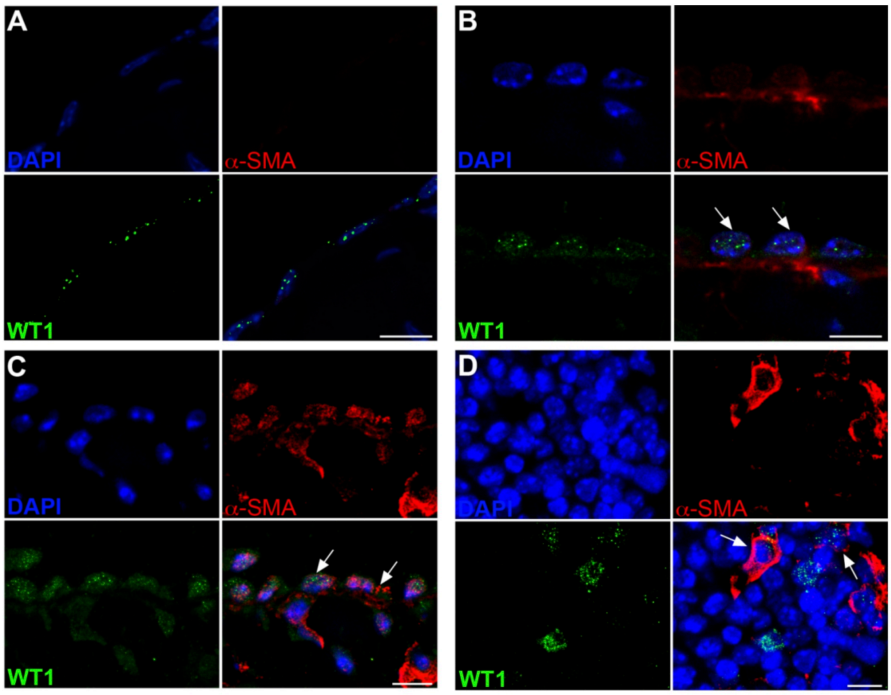

Figure 11. Mesothelial-derived CAFs co-express WT1 and α-SMA in the mouse model of peritoneal dissemination.

(A) Peritoneal tissue from a non-tumour-bearing mouse shows nuclear WT1 confined to the preserved MC monolayer, where there is no expression of α-SMA. **(B)** Distant areas from tumour micro-implants show MCs forming a monolayer and expressing nuclear WT1 (green). MCs lining the peritoneum are exposed to factors produced by the tumour and, as a consequence, MCs with an apparently preserved structure begin to express low levels of α-SMA (red). **(C)** In areas close to the micrometastasis, MCs co-expressing WT1 (green) and α-SMA (red) change their original localization on the peritoneal surface and start to invade the submesothelial compact zone. **(D)** CAFs co-expressing WT1 and α-SMA are embedded in the parenchyma of a micrometastasis cohabiting with tumour cells negative for both markers. Arrows indicate MC-derived CAFs co-expressing WT1 and α-SMA. Scale bars = 10 µm.

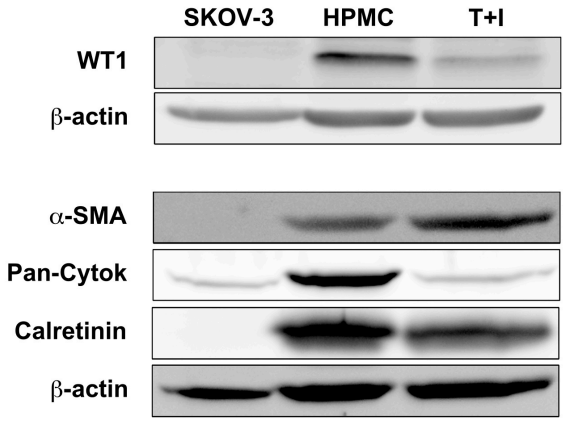

Figure 12. Expression pattern of mesothelial markers in primary HPMCs, either treated or not with TGF-β1 plus IL-1β, and in SKOV-3 cells.

Western blot analysis shows that SKOV-3 cells are negative for WT1, *α*-SMA and calretinin. The expression of pan-cytokeratin in SKOV-3 cells reveals its epithelial origin. On the contrary, HPMCs express WT1, pan-cytokeratin and calretinin. The levels of these markers are dramatically down-regulated in HPMCs treated with TGF-β1 + IL-1β (T+I). The molecule *α*-SMA is increased in HPMCs transdifferentiated *in vitro*. Expression of β-actin is employed as a loading control.

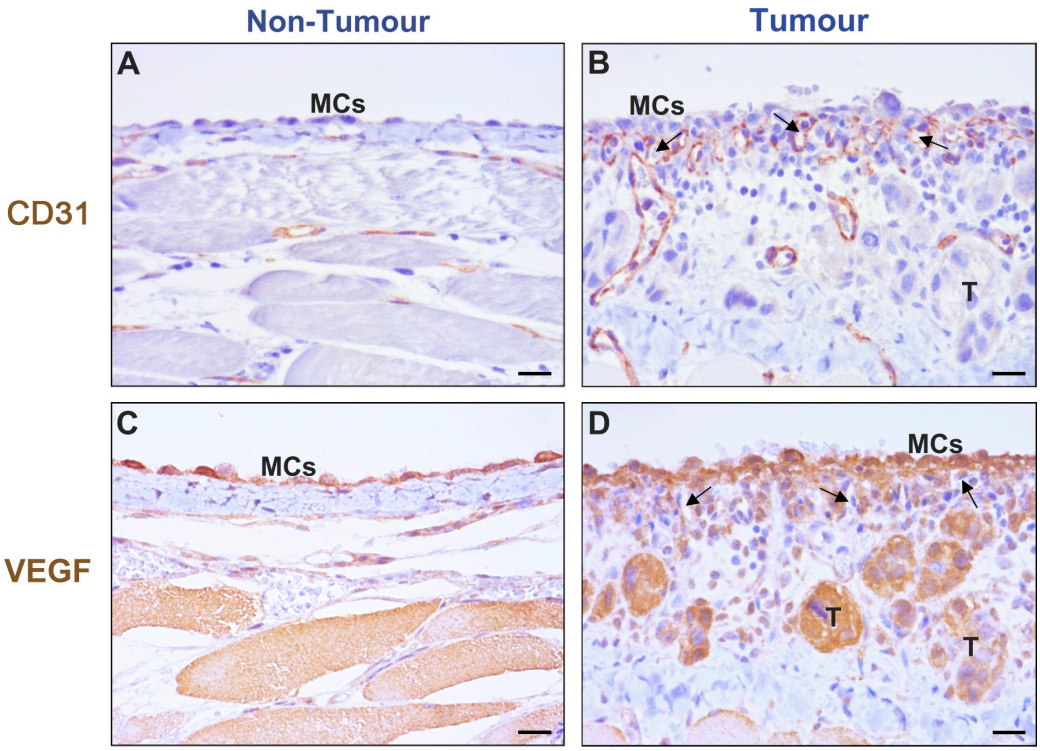

Figure 13. Increased angiogenesis is found in sites where MC-derived CAFs expressing high amounts of VEGF accumulate.

(A, B) CD31 staining reveals that non-tumour zones do not possess a high number of vessels. At the sites of tumour implants, there is a dramatic increase of vessel density, particularly located in the upper compact zone where MC-derived CAFs tend to accumulate. **(C, D)** VEGF

is expressed in a preserved mesothelium distant from tumour implants. At tumour zones, MCs and MC-derived CAFs, as well as cancer cells proximal to vascularized areas, express high levels of VEGF. Arrows indicate angiogenesis zones. Scale bars = 25 µm. T, tumour.

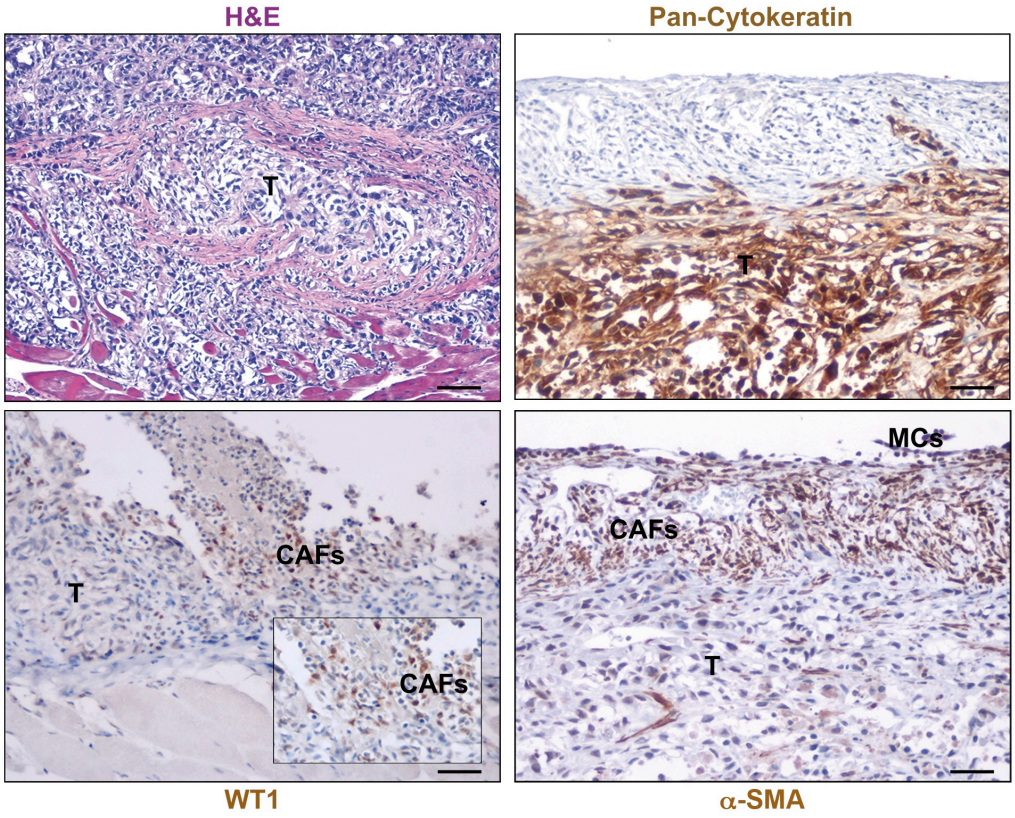

Figure 14. Large tumour implants coexist with fibrotic areas where CAFs express mesothelial markers.

H&E analysis of advanced peritoneal disseminations (8 weeks after i.p. SKOV-3 cell injection) shows larger metastatic masses coexisting with widespread areas of fibrosis. IHC studies reveal the existence of CAFs expressing mesothelial markers, not only in the proximity of carcinoma implants but also integrated within the tumour stroma. The expression of cytokeratin is restricted exclusively to carcinoma cells. However, extended WT1 and α-SMA staining can be observed cohabiting with the large peritoneal tumours. The inset shows a higher magnification of the WT1 nuclear staining. Scale bars = 100 µm. T, tumour.

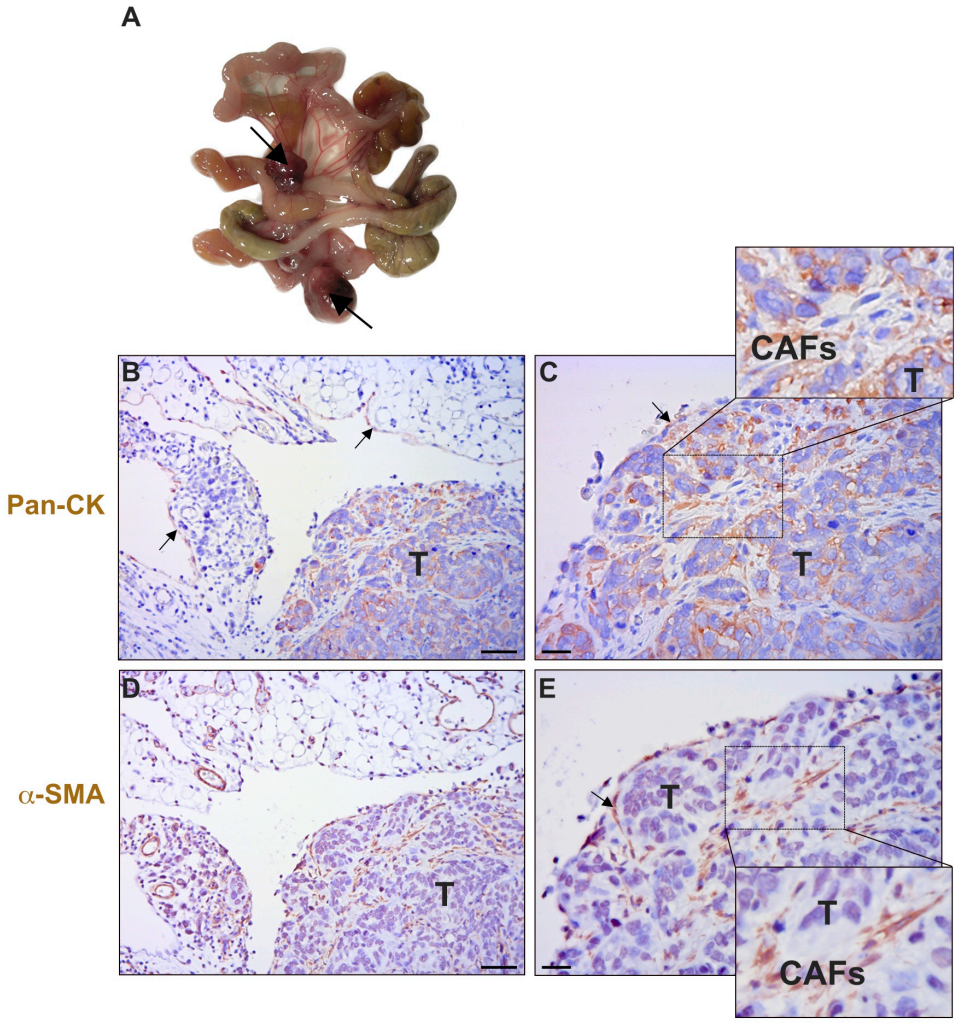

Figure 15. Analysis of omental metastasis in the mouse model of peritoneal dissemination. **(A)** Visceral macroscopic metastases are observed in mice i.p. inoculated with SKOV-3 cells. **(B)** Immunohistochemical analyses of omental tissues reveal that MCs positive for cytokeratin are lining omentum in tumour-free areas. **(C)** Fibroblastic cells (CAFs) express pan-cytokeratin in the stroma interstices between cancer cells. **(D)** α-SMA is negative in MCs lining tumour-free omental tissue. (E) A higher magnification of the tumour mass shows spindle-like cells positive for α-SMA embedded in the tumour parenchyma. Scale bars = 100 µm (B, D) and 25 µm (C, E). Arrows indicate MCs expressing cytokeratin or α-SMA; T, tumour.

3. Conditioned medium from carcinoma cells induces MMT in vitro

Incubation of HPMCs with SKOV-3-cell-conditioned medium induced the acquisition of a spindle-like morphology that was evident at 72 h and more pronounced at 6 days, with a similar appearance to that of HPMCs treated with TGF-β1 plus IL-1β (T+I) (Figure 16A). To verify the mesenchymal conversion of HPMCs, the expression patterns of MMT markers were analysed by quantitative RT–PCR in cells treated with conditioned medium for 72 h. Under

these conditions, the expression of E-cadherin was repressed and, conversely, the expression of Snail was induced when compared with control medium-treated cells (Figure 16B, C). The expression of other MMT markers (fibronectin, collagen I, VEGF and TGF-β1) was upregulated in HPMCs treated with conditioned medium compared to control cells (Figure 16D-G). The molecular reprogramming was more profound after 6 days of treatment with SKOV-3-conditioned medium (data not shown).

Similar experiments were performed using the colorectal adenocarcinoma cell line HT29. Treatment of HPMCs with supernatant from HT29 cultures induced the acquisition of a spindle-like morphology, but this was evident only at 6 days (Figure 17). Repression of E-cadherin and the up- regulation of fibronectin and collagen-I also reached statistical significance at 6 days (Figure 17B–D).

TGF-β1 is a key molecule in the mesenchymal conversion of MCs. Accordingly, experiments blocking the TGFβ type I receptor were performed. Quantitative RT-PCR analysis revealed that the selective inhibitor GW788388 blocked the induction of Snail, collagen I and fibronectin mediated by TGF-β1- or SKOV-3-conditioned medium (Figure 18).

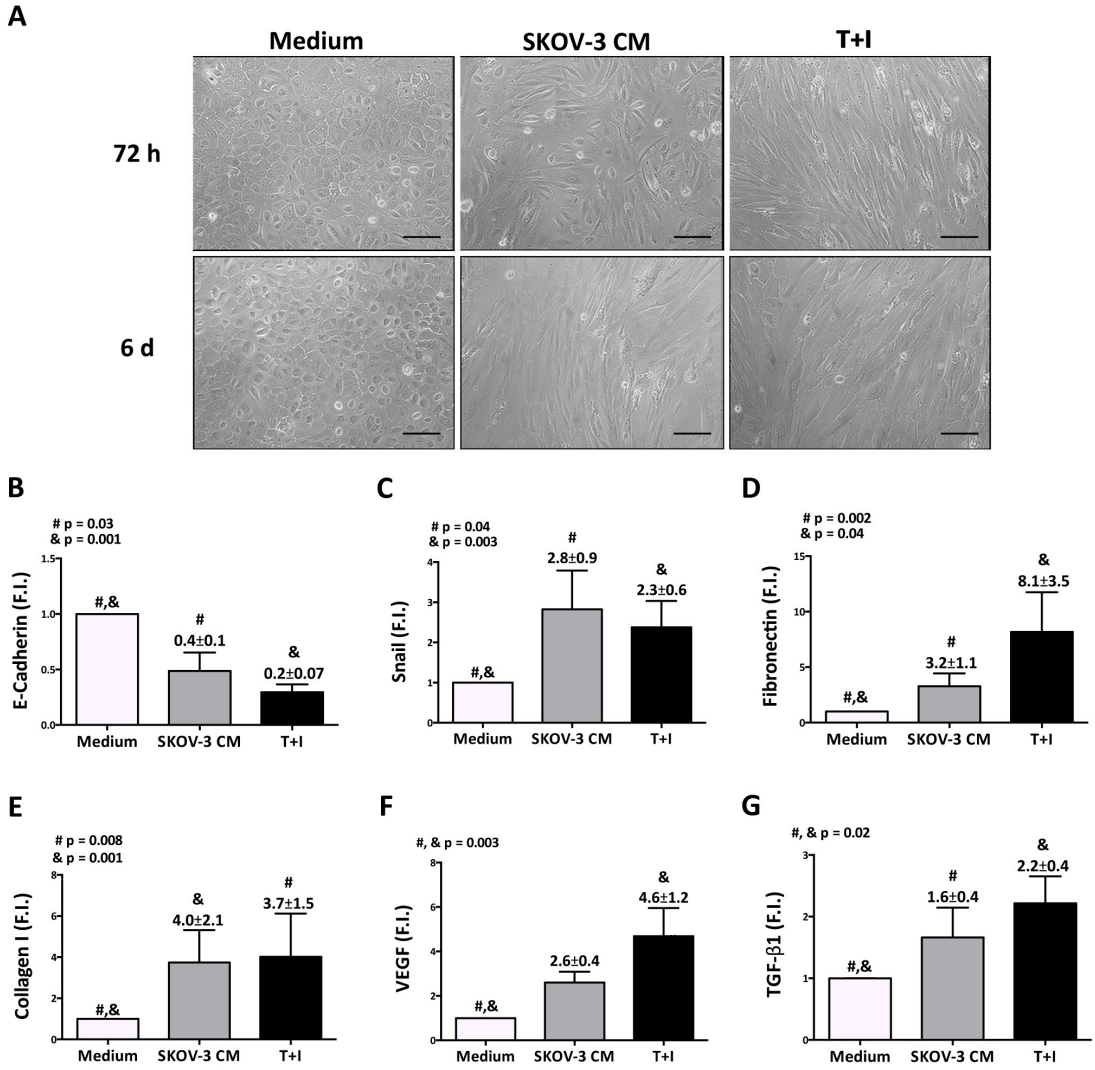

Figure 16. Conditioned medium from SKOV-3 cells induces MMT in vitro.

(A) Treatment of HPMCs with conditioned media (CM) from SKOV-3 cells induces the acquisition of a spindle-like phenotype that is evident at 72 h and more pronounced at 6 days. The morphology alteration of HPMCs is similar to that observed in cells treated with TGF-β1 plus IL-1β (T+I). Scale bars = 100 µm. **(B, C)** The mesenchymal conversion of HPMCs treated with conditioned medium is verified at the molecular level by qRT–PCR analysis of recognized MMT markers. The expression of E-cadherin is repressed in HPMCs treated for 72 h with SKOV-3-derived conditioned medium when compared with control medium-treated HPMCs. On the contrary, the expression of Snail is upregulated in HPMCs treated with conditioned medium. **(D–G)** The expression of other MMT-associated markers including the matrix components fibronectin and collagen I, as well as the growth factors VEGF and TGF-β1, are also significantly up-regulated in HPMCs treated with conditioned medium. Bar graphics represent mean ± SEM. Symbols represent the statistical differences between groups. FI, fold induction.

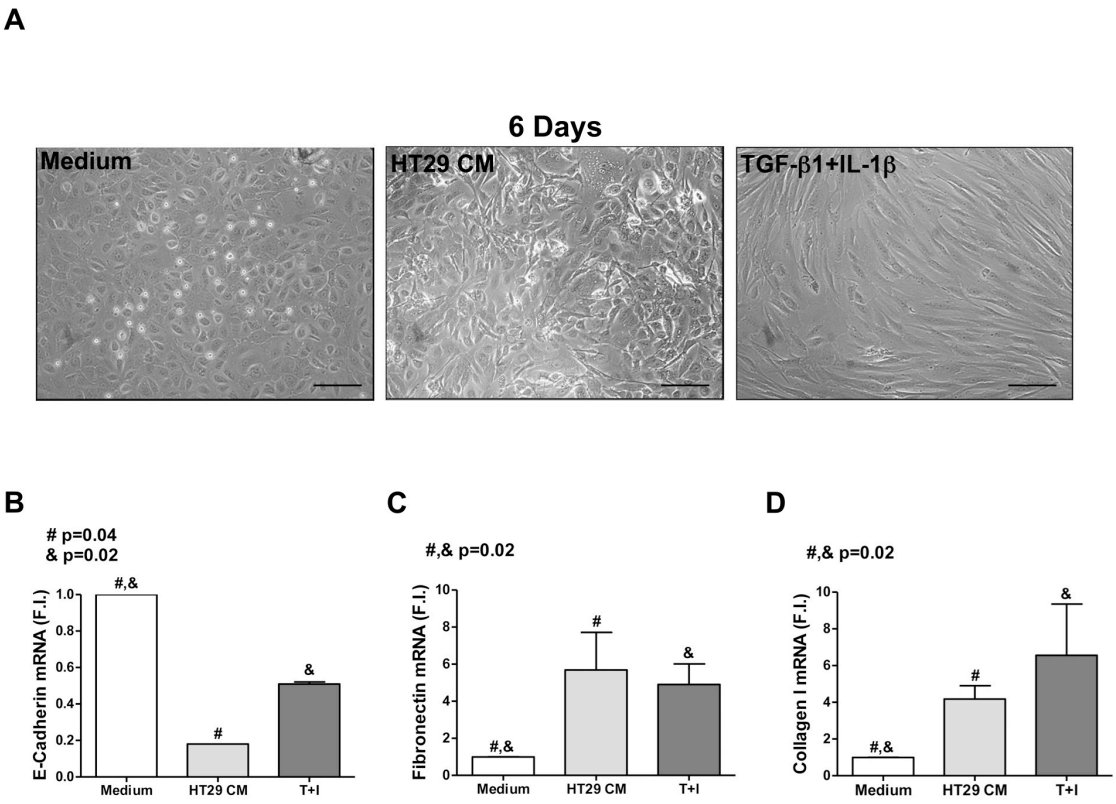

Figure 17. Conditioned medium from HT29 cells induces a MMT *in vitro*.

(A) Conditioned medium (CM) obtained from the colorectal adenocarcinoma cell line HT29 was applied for 6 days to HPMCs to induce MMT. The treatment induced the acquisition of a spindle-like morphology in HPMCs. Scale bars = 100 µm. (B–D) MMT molecular reprogramming, including the repression of E-cadherin and the up-regulation of mesenchymal markers such as fibronectin and collagen-I, reach statistical significance at 6 days of exposure to HT29-conditioned medium. Bar graphics represent mean ± SEM; symbols represent the statistical differences between groups. FI, fold induction; T+I, TGF-β1 plus IL-1β.

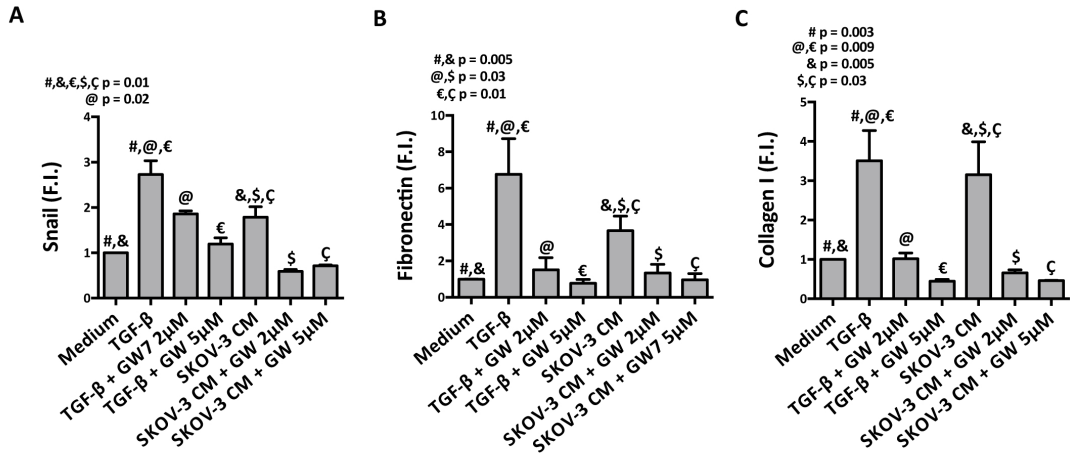

Figure 18. Blockade of TGF-β receptor I inhibitor interferes with the MMT.

HPMCs were treated for 72 h with TGF-β1 (1 ng/ml) or SKOV-3-conditioned medium (CM) in the presence or absence of 2 or 5 µm GW788388 (GW). (A, B) Quantitative RT–PCR shows

that GW788388 blocks the induction of fibronectin and collagen I mediated by TGF-β1 or SKOV-3-conditioned medium; (C) GW788388 also blocks the up-regulation of the MMT-associated molecule Snail. Bar graphics represent mean ± SEM. Symbols represent the statistical differences between groups. FI, fold induction.

4. Mesenchymal conversion of MCs enhances the adhesion of tumour cells

Adhesion experiments demonstrated that SKOV-3 cells had a significantly higher interaction capacity with mesenchymal-like HPMCs (stimulated with T+I) than with untreated HPMCs (Figure 19A, B). It was then investigated whether β1-integrins mediated the increased adhesion of tumour cells to HPMCs that were undergoing a MMT. Treatment of cells with the blocking anti-β1 antibody Lia1/2 disrupted both the basal adhesion of SKOV-3 cells to untreated HPMCs and the increased adhesion to transdifferentiated HPMCs. Conversely, treatment with the activating anti-β1 integrin antibody TS2/16 dramatically enhanced the adhesion of tumour cells to untreated HPMCs and to HPMCs T+I. Other blocking antibodies specific for the adhesion molecules VLA-1 (5E8D9) and β2-integrin (Lia3/2) did not affect the adhesion of tumour cells to HPMCs (Figure 19C). Our data demonstrated that the MMT promoted the adhesion of tumour cells and suggested that activated β1-integrin mediated, at least partially, the tumour cell–mesothelium interaction.

To explore whether the enhanced adhesion of tumour cells to mesenchymal-like HPMCs was due to exposure of underlying matrix or to an increased cell–cell interaction, scanning electron microscopy imaging analysis was carried out. The images showed SKOV-3 cells, maintaining a round-shaped morphology, laid on the monolayer of HPMCs with cobblestone features (Figure 19D). In contrast, SKOV-3 cells spread on transdifferentiated HPMCs, losing their round shape. Tumour cells emitted pseudopodial protrusions across the cytoplasmic extensions of mesenchymal-like HPMCs (Figure 19E). Detailed analysis of the images revealed that the enhanced adhesion of tumour cells was mostly due to increased cell–cell interaction and not to the underlying matrix exposed through the intercellular spaces.

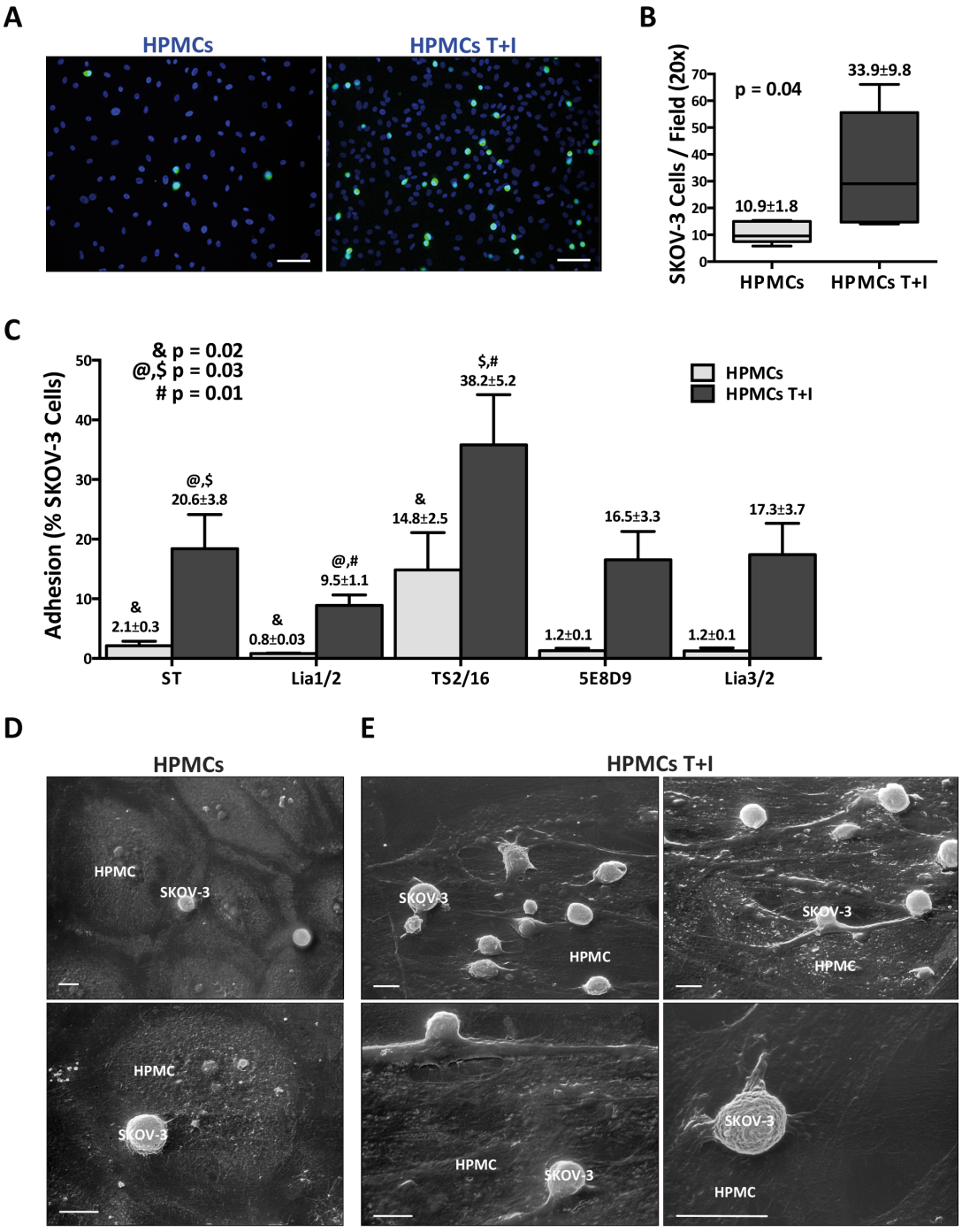

Figure 19. Tumour cells adhere mainly to the transdifferentiated MC monolayer through cell–cell interactions.

(A) Representative images show CFSE-labelled SKOV-3 cells (green) adhered on DAPI-stained HPMC monolayers that have or have not been pretreated with T+I. Scale bars = 100 μm. **(B)** Cancer cells adhere more efficiently to mesenchymal-like HPMCs than to HPMCs with epithelial morphology. Box plot graphic represents mean ± SEM of number of adhered SKOV-3 cells/field, 25th and 75th percentiles, median, minimum and maximum values. Differences are statistically significant ($p = 0.04$). (C) β1-integrins mediate the increased adhesion of tumour cells to transdifferentiated HPMCs. HPMCs were treated with the blocking anti-β1 antibody Lia1/2, activating anti-β1 antibody TS2/16, blocking antibodies specific for the adhesion

molecules VLA-1 (5E8D9) and β2-integrin (Lia3/2). Bar graphic represents mean ± SEM of percentage of adhered cells, considering the number of cells prior to washing as 100%. Symbols represent the statistical differences between groups; T+I, TGF-β1 plus IL-1β. (D) High-resolution images of co-cultures were obtained by scanning electron microscopy. SKOV-3 cells laid on a monolayer of HPMCs with epithelial-like morphology. Cancer cells adhered to control monolayers maintain a round-shaped morphology. **(E)** Transdifferentiated MC monolayers show a disorganized structure on which numerous cancer cells spread out and lose their round aspect. At high magnification, SKOV-3 cells display pseudopodial protrusions across the cytoplasmic extensions of mesenchymal-like HPMCs. Scale bars = 10 μm. T+I, TGF-β1 plus IL-1β.

5. MCs and tumour cells mutually stimulate their invasive capacity

Next, it was assessed whether mesenchymal HPMCs could promote the invasion of tumour cells. SKOV-3 cells seeded on a collagen I matrix did not show invasive capacity. On the contrary, carcinoma cells seeded on matrix harbouring HPMCs with an epithelial-like phenotype showed an increase in their invasive capacity. This effect was much more evident when HPMCs with a mesenchymal phenotype were embedded in the matrix (Figure 20A, B). The number of invading SKOV-3 cells increased significantly ($p=0.003$) when mesenchymal HPMCs were present in the matrix, compared with embedded epithelial-like HPMCs (Figure 20C). Histological analysis revealed that the MC monolayer was preserved in tumour-free regions but it was disrupted in areas with micrometastases, where CAFs expressing mesothelial markers could be observed (Figure 5C inset). These data suggested that tumour cells might, in turn, promote HPMCs to invade the stroma. *In vitro* invasion assays were performed to analyse the effect of carcinoma cells on the invasion capacity of HPMCs. SKOV-3 cells embedded in a collagen I matrix were able to attract the HPMCs from the monolayer into the matrix. In contrast, HPMCs seeded on collagen I matrix without cancer cells remained mainly as a monolayer (Figure 21A–C). The number of invading HPMCs showed a significant increase ($p=0.03$) when SKOV-3 cells were present in the matrix (Figure 21D).

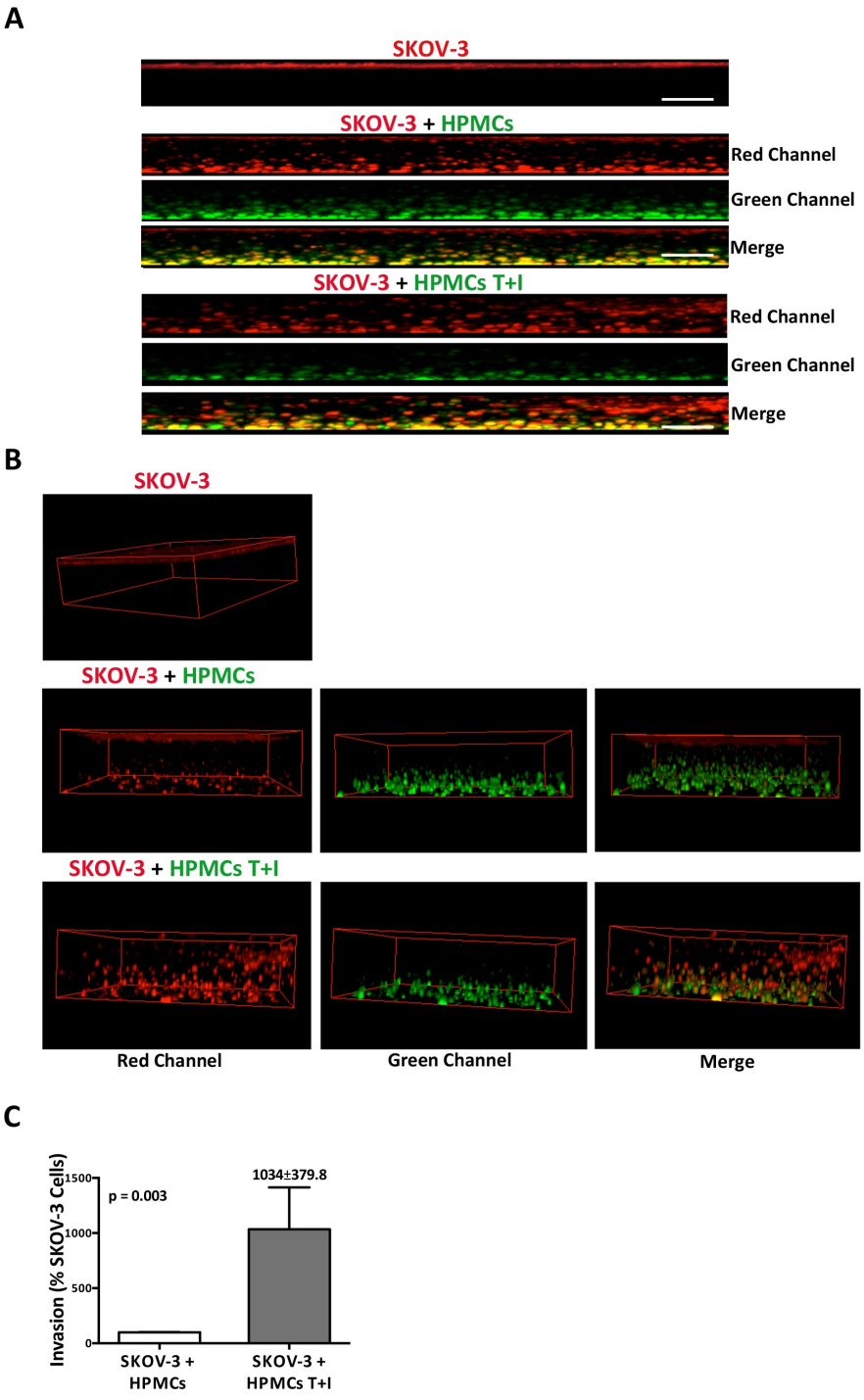

Figure 20. Mesenchymal-like HPMCs strongly stimulate the invasive capacity of carcinoma cells.

(A, B) Transverse projection and 3D reconstructions of confocal laser scanning microscopy show that SKOV-3 cells (red) seeded on a collagen I matrix do not invade after 5 days. In contrast, carcinoma cells seeded on matrix harbouring CFSE- and propidium iodide-labelled HPMCs (green + red), with either epithelial-like (HPMCs) or mesenchymal-like (HPMCs T+I) phenotype, show a significant increase in invasive capacity. This effect is much more evident when HPMCs with a mesenchymal phenotype are embedded in the matrix. Scale bars = 100 µm. **(C)** Quantification analyses of SKOV-3 invading cells were performed by subtracting

CFSE-labelled HPMCs (green) from the total propidium iodide-stained cells (red) that invaded the matrix. Thus, the invasion of SKOV-3 corresponds to red cells in the merge panel, since embedded HPMCs are yellow (green + red). Results show the percentage of invading SKOV-3 cells in gels containing HPMCs versus gels containing HPMCs pretreated with T+I. Bar graphics represent mean ± SEM; the difference is statistically significant (p = 0.003). T+I, TGF-β1 plus IL-1β.

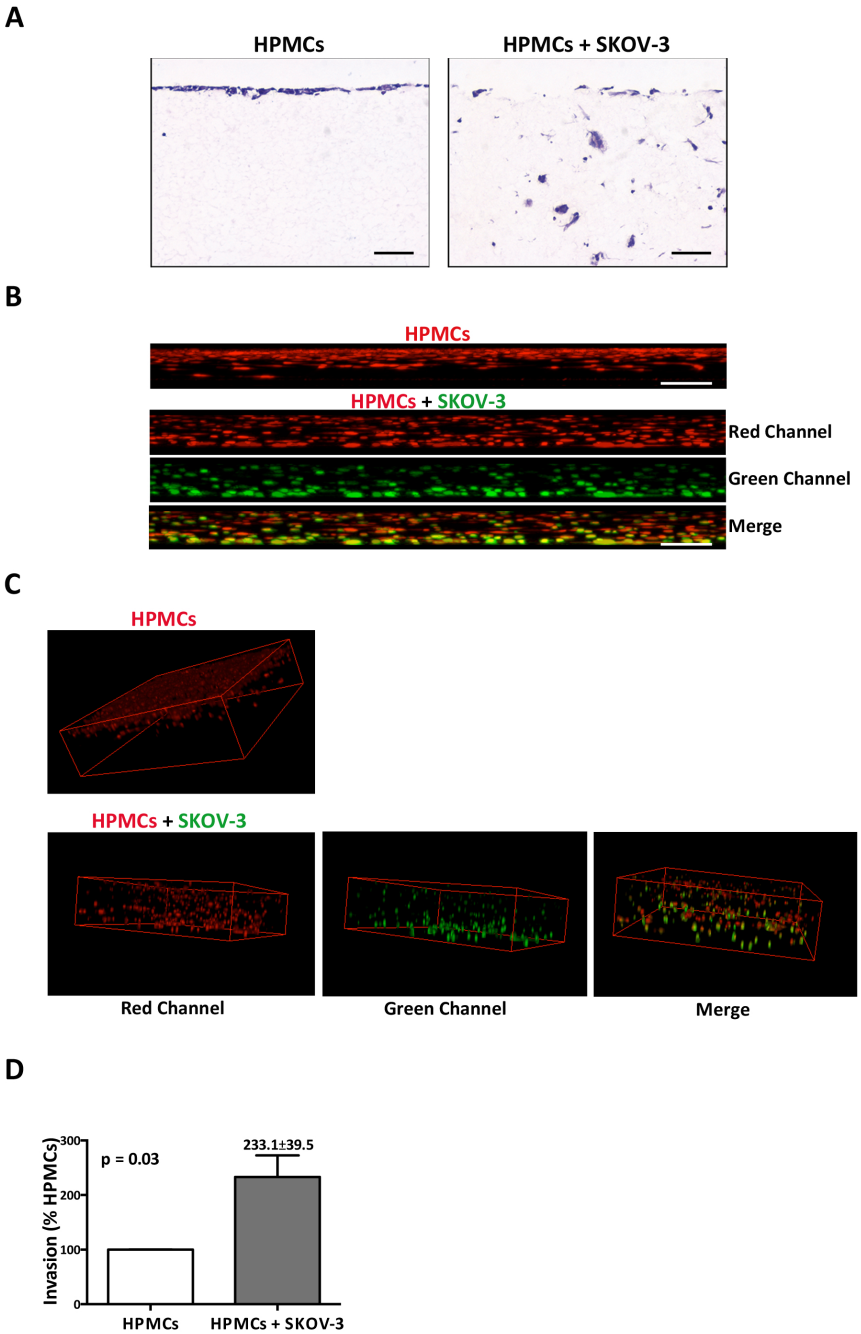

Figure 21. Tumour cells embedded in the matrix induce MC invasion.

(A) H&E sections of paraffin-embedded gels show the disruption of the MC monolayer when SKOV-3 cells are present in a collagen I matrix, mimicking a metastatic submesothelium. **(B)** Confocal images display transverse projections of CFSE- and propidium iodide-labelled SKOV-

3 cells (green + red) embedded in a collagen I matrix. Carcinoma cells are able to attract HPMCs (red) from the monolayer into the matrix. However, HPMCs seeded on collagen I matrixes without cancer cells remain mainly as a monolayer. **(C)** Reconstructions in 3D of confocal laser scanning microscopy. **(D)** Quantification analyses of invading HPMCs were performed by subtracting CFSE-labelled SKOV-3 cells (green) from the total propidium iodide-stained cells (red) that invaded the matrix. Thus, the invasion of HPMCs corresponds to red cells in the merge panel, since embedded SKOV-3 cells are yellow (green + red). Results show the percentage of invading HPMCs in gels containing SKOV-3 cells versus gels without tumour cells. Bar graphics represent mean ± SEM; the difference is statistically significant ($p = 0.03$). Scale bars = 100 μm.

6. Ascitic fluid-derived mesothelial cells undergo a mesothelial-to-mesenchymal transition

Once it had been established that there is a mesenchymal conversion of MCs in the peritoneum and that the MMT played a role in the adhesion and invasion of cancer cells, the characterisation of MCs isolated from the ascitic fluid of ovarian cancer patients with peritoneal metastasis was performed. In culture, some ascitic fluid-derived MCs (AFMCs) had a fibroblast-like morphology, similar to that of HPMCs T+I (Figure 22A a). Positive immunofluorescence staining for calretinin confirmed the mesothelial cell type (Figure 22A b), and α-SMA staining indicated that AFMCs had converted into myofibroblasts (Figure 22A b). Analysis of conventional MMT-related markers by quantitative RT-PCR showed the expression of E-cadherin was repressed and, conversely, the expression of Snail, TGF-β1 and VEGF was induced in AFMCs compared to control HPMCs (Figure 22B a-d). The difference in these markers was significant, except for TGF-β1, where a tendency to a higher expression in AFMCs can be observed. This pattern is indicative of an *in vivo* MMT taking place in AFMCs. The expression of extracellular matrix (ECM) proteins was also considered. Although a tendency to a higher expression in AFMCs compared to controls was observed in the case of fibronectin (Figure 22B e), there were no differences for collagen I (Figure 22B f). These data suggest that AFMCs have converted into CAFs.

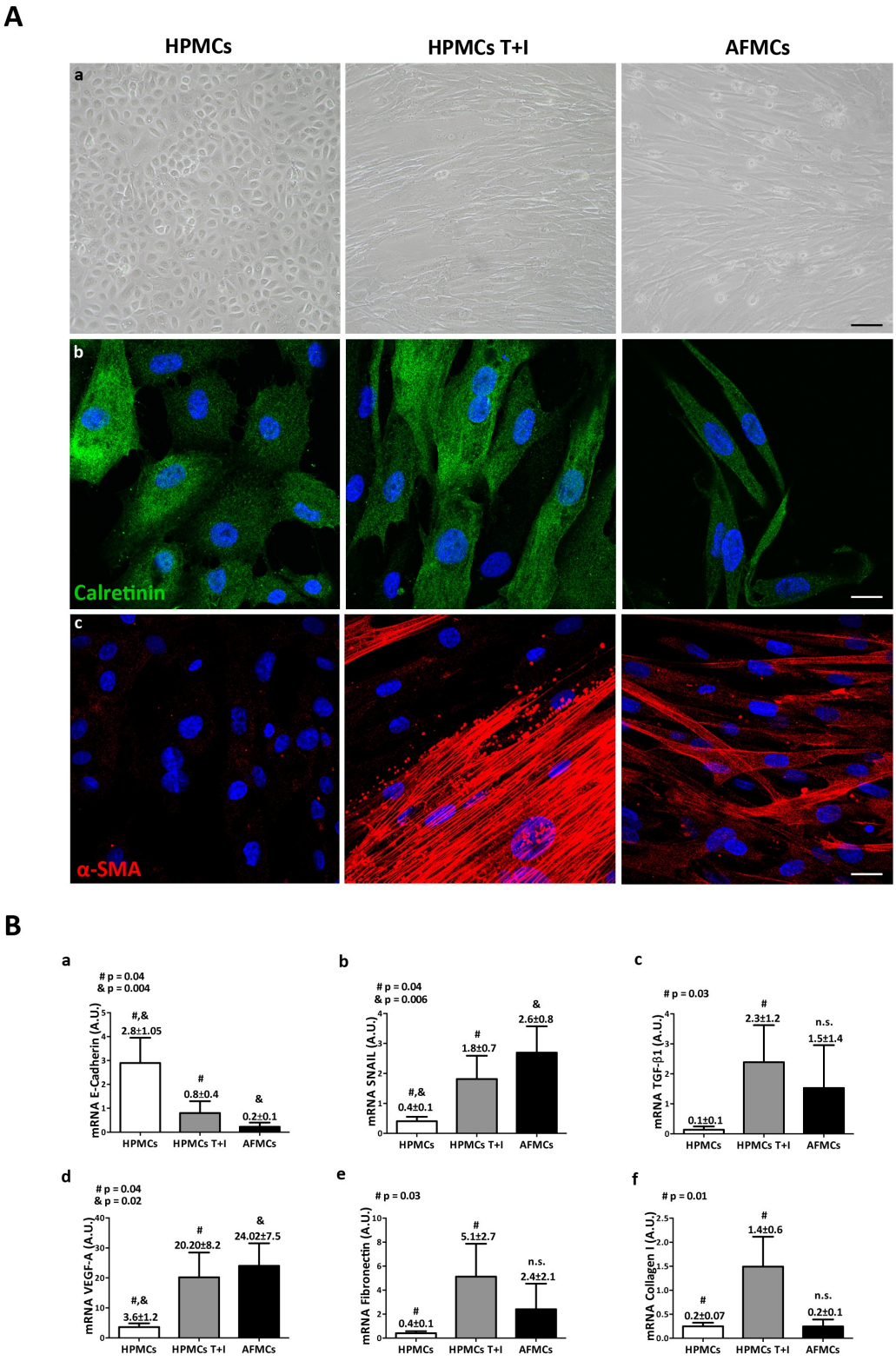

Figure 22. AFMCs undergo a MMT.

(A) (a) Representative phase contrast microscopy images of HPMCs, HPMCs T+I and AFMCs in culture. Scale bar = 100 µm. (b) Immunofluorescence staining for calretinin, confirming mesothelial cell type, and (c) α-SMA, indicating myofibroblast conversion of AFMCs. Scale bars = 25 µm. **(B)** Transcript levels of MMT markers analysed by real time qRT-PCR in

HPMCs (n=8), HPMCs T+I (n=8) and AFMCs (n=5). **(a-d)** E-cadherin expression is repressed and, conversely, the expression of Snail, TGF-β1 and VEGF is induced in AFMCs and HPMCs T+I compared to control HPMCs. All were significant except for TGF-β1. (e, f) The expression of other MMT markers, collagen and fibronectin, is not significantly different between AFMCs and controls. Bar graphics represent mean ± SEM. Symbols represent the statistical differences between groups. A.U., arbitrary units; T+I, TGF-β1 plus IL-1β.

7. Ascitic fluid-derived mesothelial cells promote tumour growth of ovarian cancer cells in a subcutaneous xenograft mouse model

In order to study the role of transdifferentiated AFMCs in tumour growth, a subcutaneous xenograft mouse model was used. Although SKOV-3-luciferase cells are efficient in establishing peritoneal metastases, a preliminary assay showed that cancer cells alone are unable to grow when subcutaneously inoculated (Figure 23A). The differential behaviour of cancer cells in these two different microenvironments suggests that MC-derived CAFs may be key players in peritoneal metastasis. Therefore, SKOV-3-luciferase cells were subcutaneously co-inoculated with control HPMCs in the left flank, and with either HPMCs T+I (Figure 23B) or AFMCs (Figure 23C) in the right flank. Bioluminiscence monitoring showed that tumour growth was significantly increased in tumours in the right flank, where MCs that had undergone a MMT had been co-injected.

8. Identification of a mesothelial-to-mesenchymal gene signature in ascitic fluid-derived mesothelial cells

RNA-sequencing analysis was carried out on control HPMCs and AFMCs. Expression data for each gene within each sample was used to create a heatmap for cluster classification, which revealed a clear separation between HPMCs and AFMCs (Figure 24A). Ensembl ID of differentially-expressed genes, i.e., genes with a q-value < 0.05 and a fold change higher than 2, were submitted to IPA® for functional annotation, identification of upstream regulators, and mapping to canonical pathways.

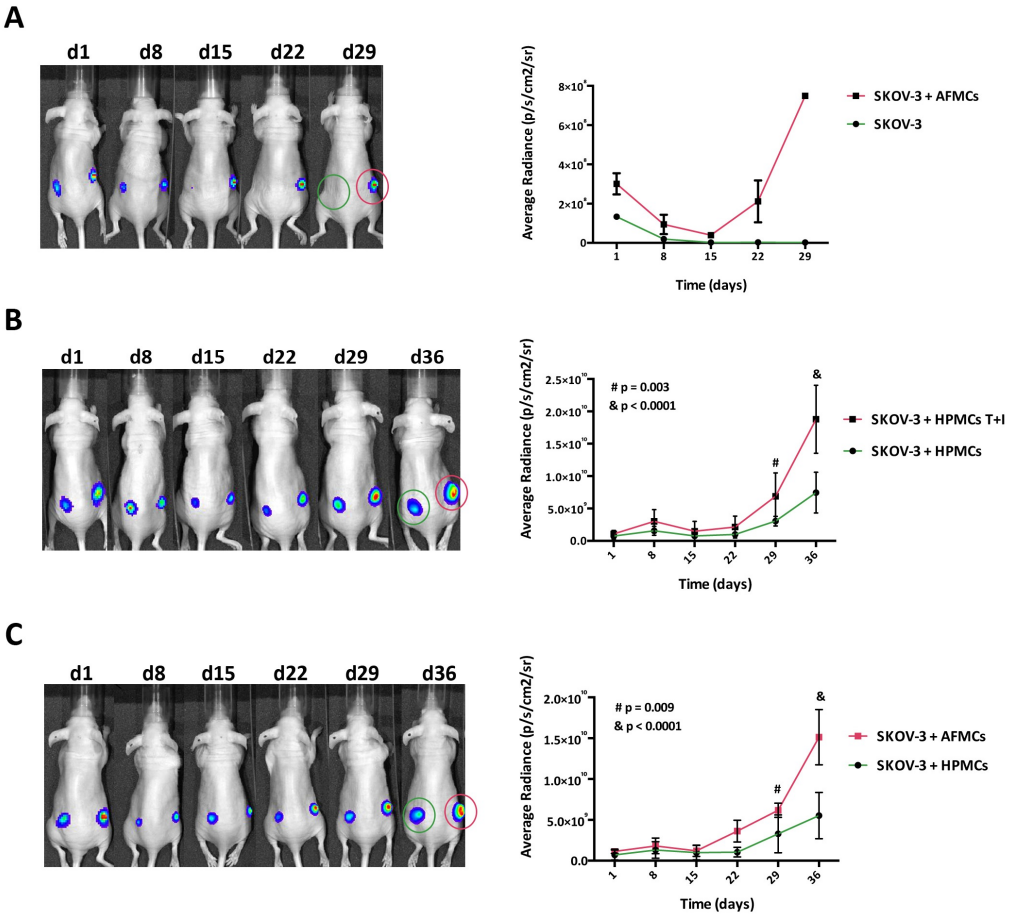

Figure 23. AFMCs favour tumour progression in a subcutaneous xenograft mouse model. **(A)** Preliminary assay of subcutaneous inoculation of SKOV-3-luciferase cells in left flank and co-inoculation with AFMCs in the right flank, indicating SKOV-3 cells alone do not grow subcutaneously. **(B, C)** SKOV-3-luciferase cells were co-inoculated with control HPMCs in the left flank of nude mice, and with either T+I HPMCs (B) (n=8) or AFMCs (C) (n=6) in the right flank. Bioluminiscence monitoring showed that tumour growth was significantly increased in tumours in the right flank, where HPMCs that had undergone a MMT had been used. Graphs represent mean average radiance of SKOV-3-luciferase cells ± SEM. Symbols represent the statistical differences between groups. T+I, TGF-β1 plus IL-1β.

The analysis revealed 1997 upregulated genes and 1646 downregulated genes in AFMCs relative to their expression in control HPMCs. A summary of the top 100 up-regulated and top 100 down-regulated genes in AFMCs, along with the fold change for each gene is presented in Supplementary Tables 1 and 2, respectively. Among the canonical pathways that were significantly differentially regulated, many were directly related to MMT: hepatic stellate cell activation, regulation of EMT pathway, caveolar-mediated endocytosis signalling, vitamin D receptor/retinoid X receptor (VDR/RXR) activation, inhibition of angiogenesis by

thrombospondin 1 (TSP1), tight junction signalling, and signalling pathways for integrin-linked kinase (ILK), TGF-β, HGF, thrombin, peroxisome proliferator-activated receptor (PPAR), p38 and NF-κB. Other pathways are related to steps involved in tumour progression (integrin signalling, inhibition of matrix metalloproteases) or have been associated to ovarian cancer (signalling pathways for IL-6, IL-8 and IL-10) (Figure 24B). Upstream regulators represented in our dataset were identified and, interestingly, the top 3 (TNF, TGF-β1 and IL-1β) are known inducers of MMT (Figure 24C).

A

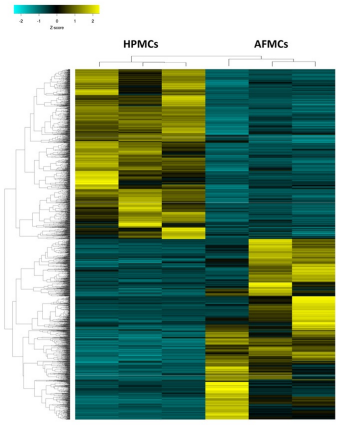

B

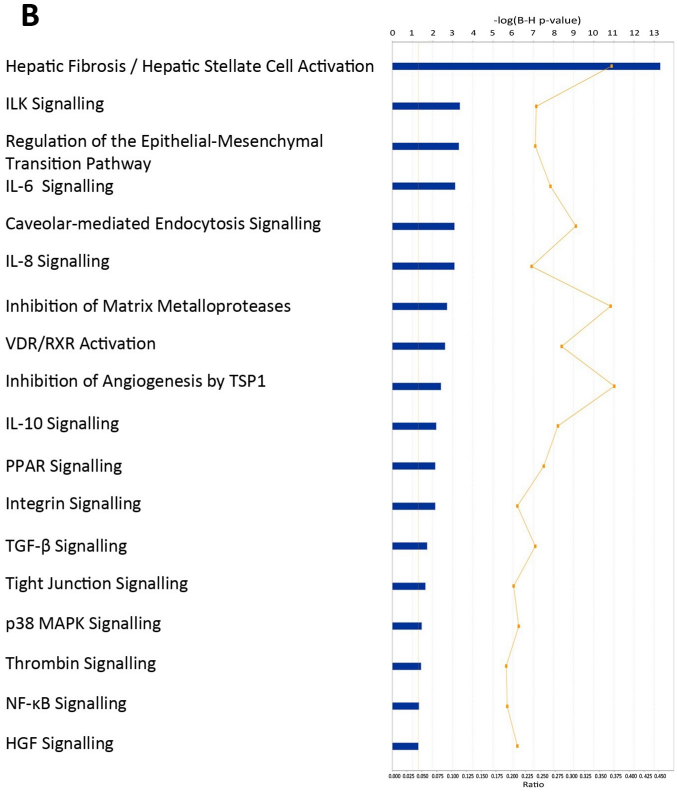

C

Symbol	Gene name	Exp Log Ratio	Molecule Type	Predicted Activation State	Activation z-score	p-value of overlap
TNF	Tumor necrosis factor	7.971	cytokine	Activated	9.536	3.93E-79
TGFB1	Transforming growth factor, beta 1	1.476	growth factor	Activated	5.952	3.47E-74
IL1B	Interleukin 1 beta	8.091	cytokine	Activated	8.121	1.69E-61

Figure 24. RNA-seq analysis of AFMCs.

(A) Heatmap representing the differentially expressed genes in HPMCs and AFMCs. **(B)** Significantly differentially regulated canonical pathways analysed by IPA. The y-axis indicates the statistical significance, calculated using the Benjamini-Hochberg correction (-log(p-value) = 1.3). The yellow threshold line represents this cutoff. **(C)** Top 3 upstream regulators in the dataset. P-value of overlap ($p < 0.05$) represents the statistical significance of genes in the dataset to overlap with the list of downstream targets of a given regulator. The activation z-score (z-score $\geq |2|$) infers the activation state of the transcriptional regulator based on published findings.

9. Mesothelial-to-mesenchymal transition via TGF-β1 in the peritoneum renders peritoneum more susceptible to metastasis

Previously, MCs that had undergone a MMT were shown to promote an increased invasion and attachment of cancer cells. Based on this, it was hypothesized that a peritoneum where a MMT had taken place could be more receptive to metastasis. Given that TGF-β1 is a key MMT inducer and also appeared as a key regulator in the RNA-seq data of AFMCs, it was of interest to study its role in intraperitoneal tumour progression. Thus, the peritoneum of mice was pre-conditioned, in order to induce an early MMT, by overexpressing TGF-β1 with i.p. adenoviral delivery, followed by SKOV-3-luciferase cell i.p. inoculation. Then, mice were monitored for 41 days with via *in vivo* bioluminiscence imaging. Tumour growth and progression were significantly higher in mice whose peritoneum had undergone a MMT, compared to those where a control adenovirus—and, hence, no induced MMT—had been used (Figure 25).

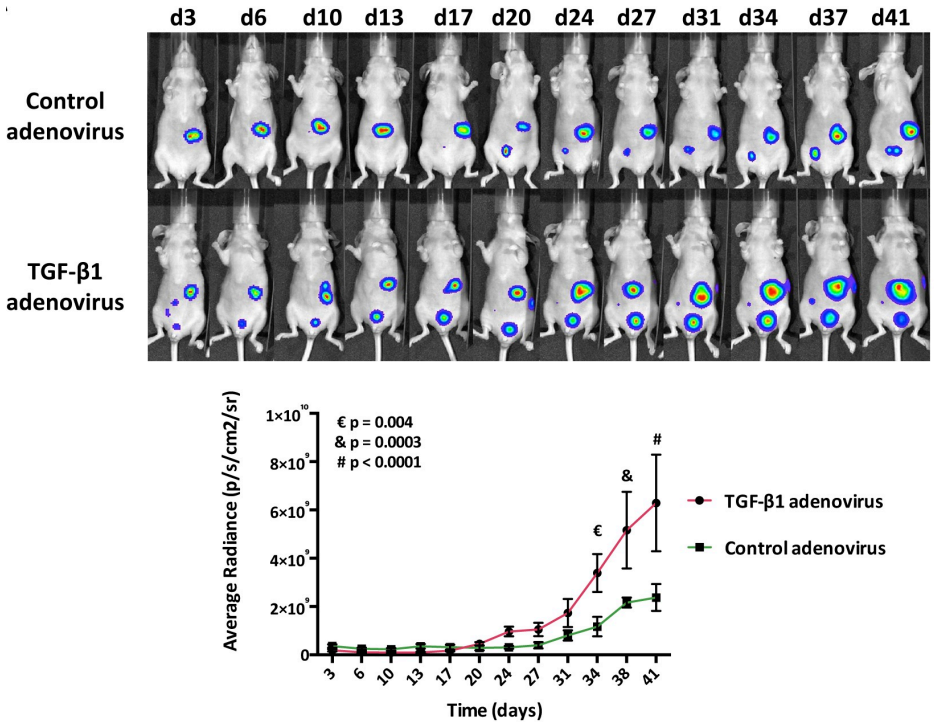

Figure 25. Overexpression of TGF-β in the peritoneum supports tumour progression.
In vivo monitoring of SKOV-3-luciferase cells in nude mice pre-conditioned with adenovirus encoding for TGF-β1 or control. Graph represents mean average radiance of SKOV-3-luciferase cells ± SEM. Symbols represent the statistical differences between groups. n=6 per group.

Although ovarian cancer cells secrete a high concentration of TGF-β1, many other cytokines and factors that are also present in the ascitic fluid could have an effect on the peritoneum. In a preliminary experiment, it was observed that pre-conditioning the peritoneum of mice for 2 days with conditioned medium from SKOV-3 cells decreased E-cadherin expression in the mesothelial monolayer, indicating that an early MMT had taken place (Figure 26A). In order to study the role of TGF-β1 in conditioned medium in the context of metastasis, mice were pre-treated with a TGF-β1 receptor I inhibitor (GW788388) and then with conditioned medium from SKOV-3 cells, followed by SKOV-3-luciferase cell i.p. delivery. Monitoring of tumour progression for 41 days by *in vivo* bioluminiscence imaging, showed that tumour growth was significantly higher in mice where an early MMT had been induced with cancer cell medium (Figure 26B). Interestingly, when the TGF-β1 receptor I was inhibited and cancer cell medium was used, tumour growth was maintained at levels comparable to those of mice with no induced MMT (control medium). These results suggest that, despite other cytokines also having possible roles in tumour growth and metastasis, blocking the TGF-β1 pathway is sufficient to see a significant and dramatic change in tumour progression.

10. Crosstalk between mesothelial-derived carcinoma-associated fibroblasts and cancer cells takes place via TGF-β1/pSmad3 pathway

MC-derived CAFs and cancer cells produce large amounts of TGF-β1. It has been described that TGF-β1 can induce a MMT via Smad-dependent and/or Smad-independent pathways. On this note, Smad3 is an important downstream mediator in the Smad-dependent signalling of TGF-β1 and, once phosphorylated, activates gene transcription in the nucleus. However, the response to TGF-β1 through Smad3 has not been analysed in MC-derived CAFs. Thus, double immunofluorescence staining for α-SMA and phosphorylated Smad3 (pSmad3) was carried out in MC cultures. Our results showed that control HPMCs were negative for both markers (Figure 27A a). However, nuclear expression of pSmad3 was observed in α-SMA-positive HPMCs T+I and AFMCs (Figure 27A b, c).

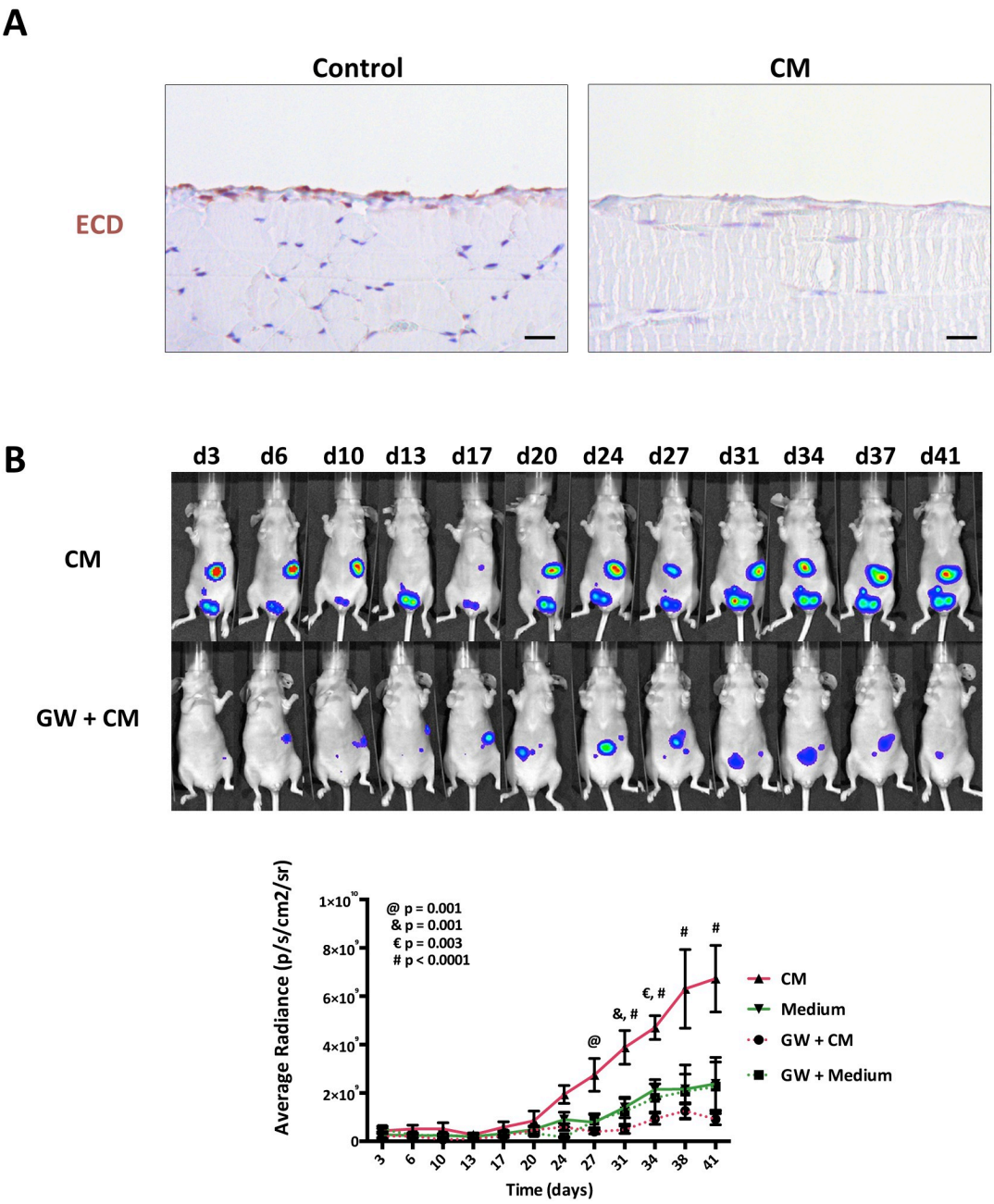

Figure 26. Blockade of TGF-β receptor I blocks the tumour growth induced by cancer cell media.

(A) Immunohistochemistry staining for E-cadherin (ECD) on the peritoneum of a mouse sacrificed 2 days after being pre-conditioned with cancer cell medium (CM) shows early MMT. Scale bars = 25 µm. **(B)** *In vivo* monitoring of SKOV-3-luciferase cells in nude mice pre-conditioned with CM control medium together with the TGF-β receptor I inhibitor GW788388 (GW) or vehicle. n=6 per group. Graphs represent mean average radiance of SKOV-3-luciferase cells ± SEM. Symbols represent the statistical differences between groups.

Quantification of the percentage of pSmad3-positive nuclei revealed a significant increase in HPMCs T+I and AFMCs (p = 0.0043, p = 0.0002, respectively) (Figure 27B).

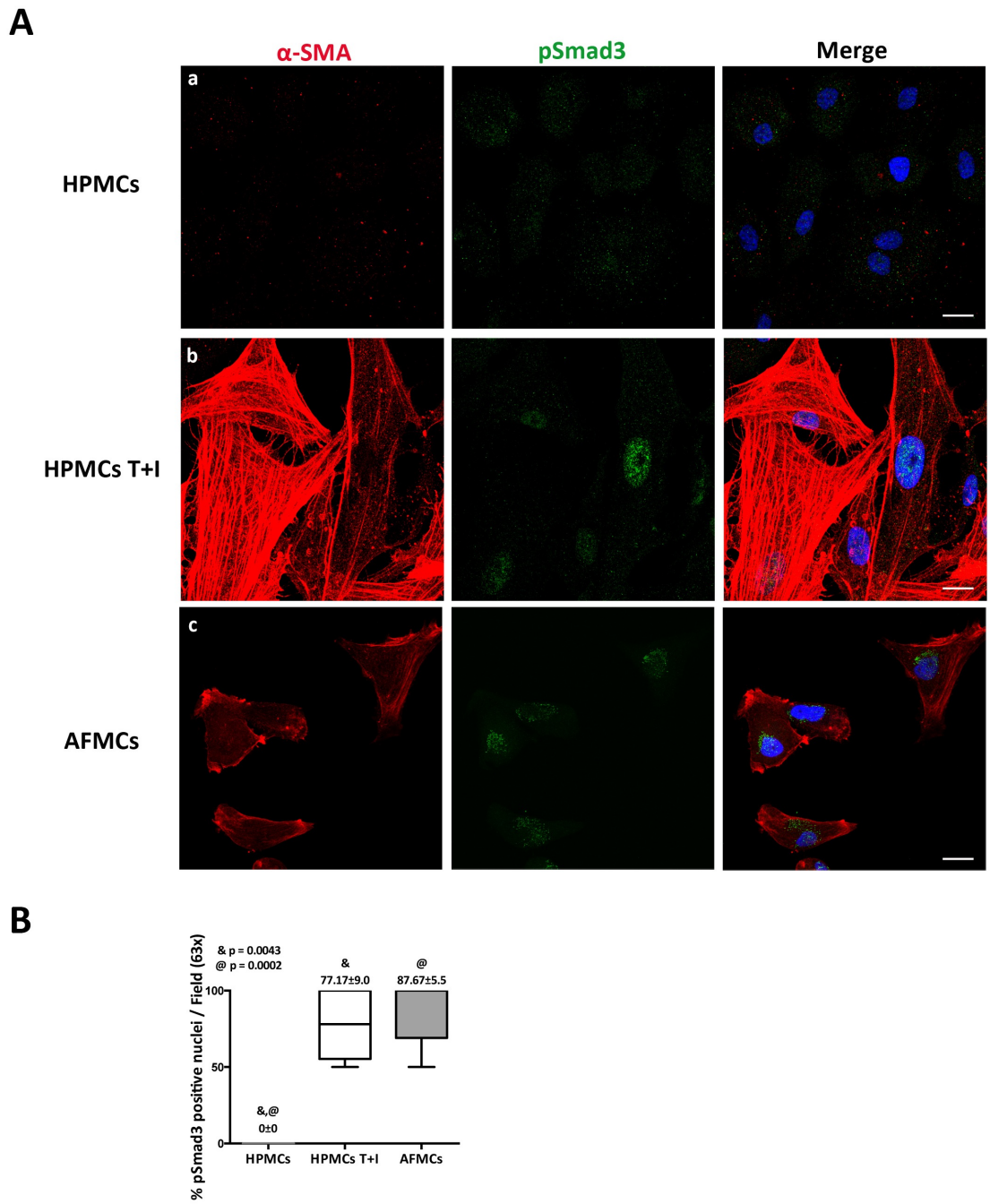

Figure 27. TGF-β1/Smad3 pathway is activated in AFMCs, inducing a MMT.

(A) Double immunofluorescence staining for α-SMA and pSmad3 in HPMCs (a), HPMCs T+I (b) and AFMCs (c) indicates a MMT has taken place through Smad-dependent TGF-β1 pathway activation in transdifferentiated AFMCs. (d) Percentage of pSmad3-positive nuclei. Scale bars = 25 µm. **(B)** Quantification of percentage of pSmad3-positive nuclei. Box plot graphic depicts 25th and 75th percentiles, median, minimum and maximum values; symbols represent the statistical differences between groups. T+I, TGF-β1 plus IL-1β.

Knowing that the TGF-β1 route was activated in both transdifferentiated HPMCs and AFMCs, its activation state was verified in ovarian cancer cells. HPMCs and SKOV-3 cells were treated with TGF-β1 for 1 and 6 hours. As expected, by immunofluorescence pSmad3 is shown to be translocated to the nucleus in HPMCs (Figure 28A, B, E, F). Surprisingly, in the cases in which ovarian cancer cells were exposed to TGF-β1, pSmad3 remained cytoplasmic (Figure 28C, D, G, H). These results suggest that the TGF-β1/Smad3 pathway could be truncated in ovarian cancer cells.

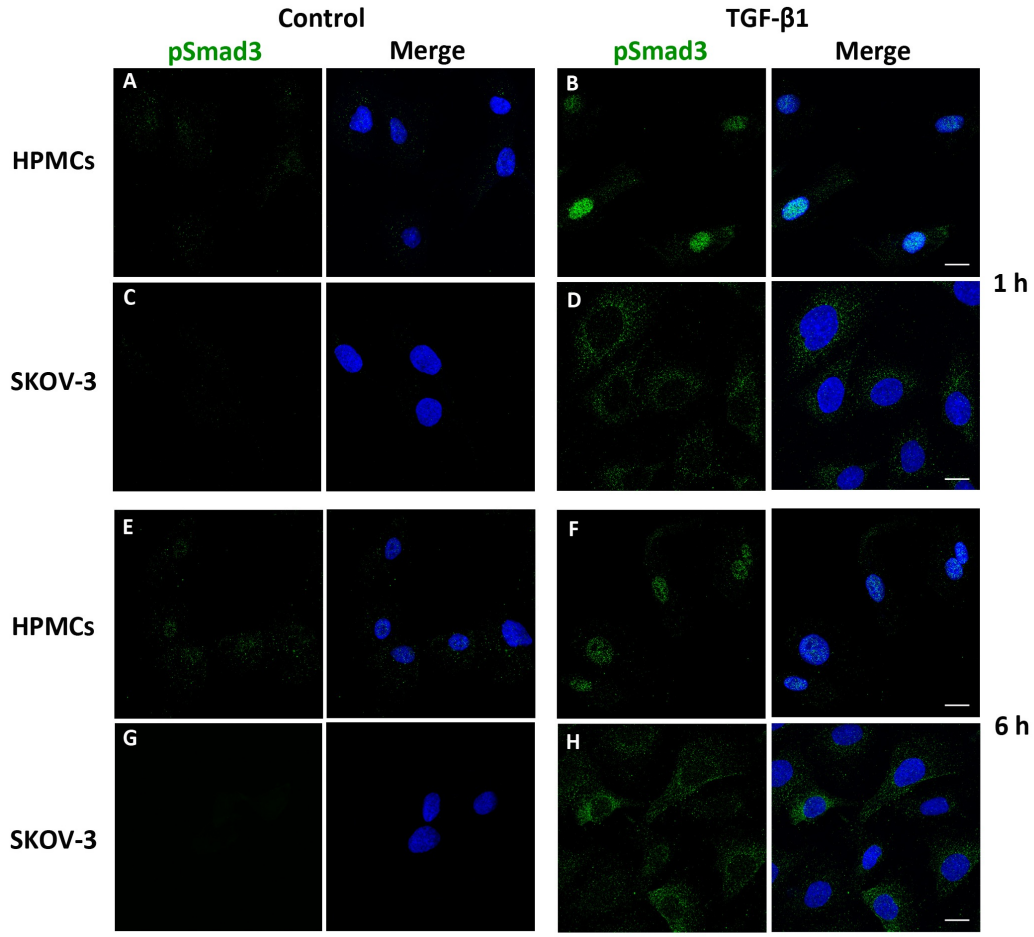

Figure 28. TGF-β1/Smad3 pathway is truncated in SKOV-3 cells.
Treatment of SKOV-3 cells and HPMCs with TGF-β1 (4 ng/ml) for 1 and 6 hours. Inmunofluorescence images show that, upon TGF-β1 treatment, pSmad3 translocates to the nucleus in HPMCs (A, B, E, F), and remains cytoplasmic in ovarian cancer cells (C, D, G, H). Scale bars = 25 μm.

In order to corroborate the nuclear localization of pSmad3 in peritoneal CAFs, serial sections of mouse tissues were analysed by immunohistochemistry, staining for α-SMA and

pSmad3. The peritoneum of non-tumour-bearing mice showed a preserved mesothelial monolayer that was negative for both markers (Figure 29A, B). However, in tumour-bearing mice, the peritoneum was positive for pSmad3 but still negative for α-SMA in areas distant to the tumour microimplants (Figure 29C, D). Interestingly, in areas close to the micrometastasis, positive α-SMA and nuclear pSmad3 staining are overlapped in the submesothelial fibrotic zone (Figure 29E, F). In tumour areas, an accumulation of CAFs (α-SMA positive) expressing nuclear pSmad3 was observed surrounding cancer cells where, similarly to the previous *in vitro* assay, pSmad3 remained cytoplasmic (Figure 29G, H).

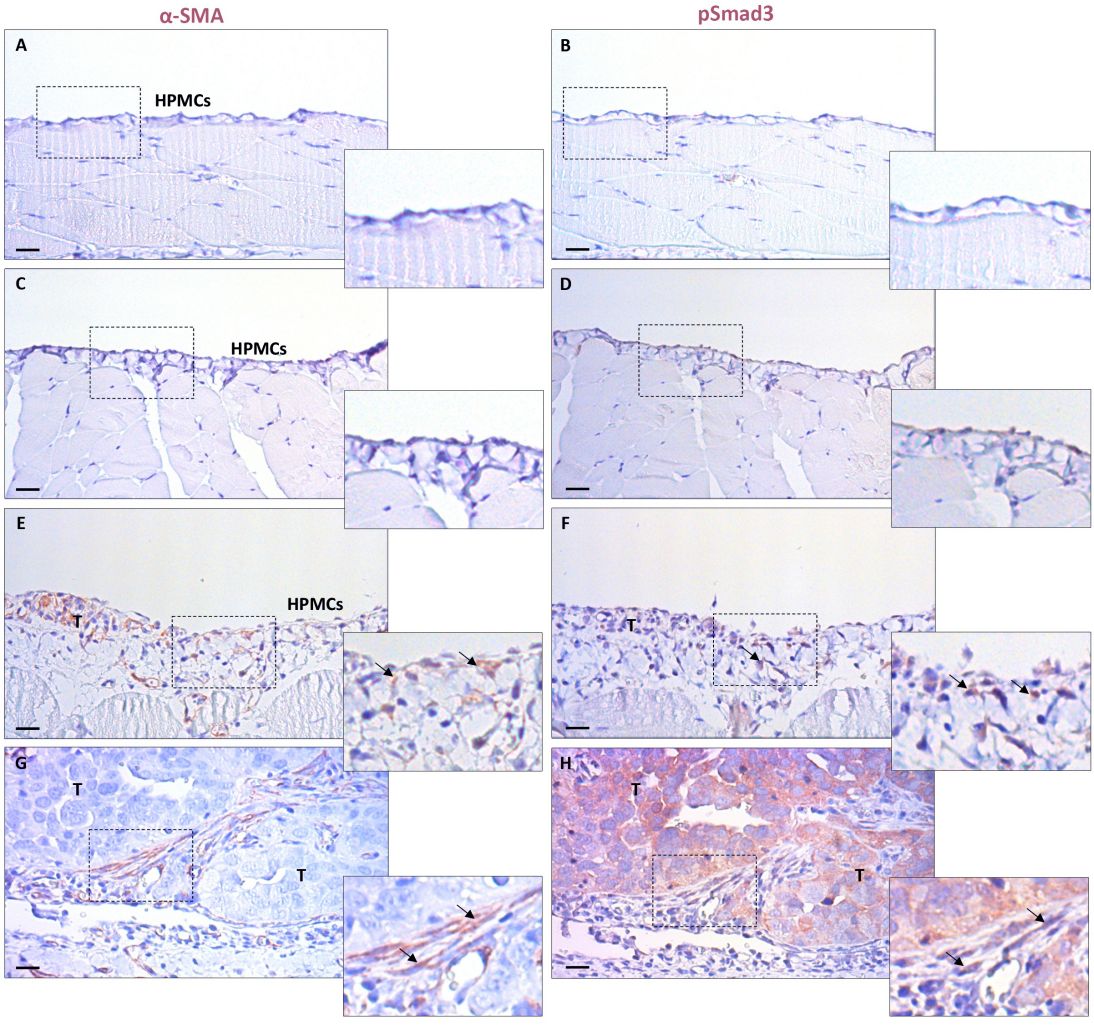

Figure 29. Immunohistochemical analysis of mouse peritoneal tissues.
Staining of serial sections was performed for α-SMA and pSmad3. (**A, B)** Peritoneum of a control mouse showing a preserved mesothelium and negative expression for both markers. **(C-H)** Same sample from a mouse with ovarian cancer implants in the peritoneum: **(C, D)** Preserved and nuclear pSmad3-positive mesothelial monolayer in an area distant to the tumour

cells. **(E, F)** Submesothelial CAFs expressing α-SMA are accumulated in an area closer to the tumour site and overlap with nuclear pSmad3-positive cells. **(G, H)** Peritoneal metastasis where ovarian cancer cells show cytoplasmic expression of pSmad3, and adjacent CAFs (α-SMA-positive) express nuclear pSmad3. Scale bars = 50 µm (A-F) and 25 µm (G, H). Arrows indicate CAFs in the proximity of tumour implants expressing nuclear pSmad3. Insets show higher magnifications of the delimited areas. T, tumour.

The differential localisation of pSmad3 in MC-derived CAFs and cancer cells was also analysed by immunohistochemistry in serial sections of peritoneal implant biopsies from patients with ovarian cancer, staining for calretinin, α-SMA and pSmad3. The peritoneum of control donors showed a calretinin-positive preserved mesothelial monolayer with no staining for α-SMA or pSmad3 (Figure 30A-C). However, in ovarian cancer patients, preserved mesothelial areas distant to tumour cells showed nuclear expression of pSmad3, indicating that the TGF-β1 pathway had been activated (Figure 30D-F). It can be hypothesized that an early-stage MMT is taking place in these cells, but an invasive phenotype has not been acquired yet, hence the monolayer structure and lack of α-SMA expression. In the tumour stroma, there was an accumulation of cells with a fibroblastic phenotype. Some of these cells with spindle-like morphology are triple positive for calretinin, α-SMA and nuclear pSmad3, confirming mesothelial cells have undergone a MMT, invaded the stroma, and transdifferentiated into CAFs (Figure 30G-I). Ovarian cancer peritoneal nodules from the same patient were pSmad3-negative (Figure 30I) or showed pSmad3 staining limited to the cytoplasmic compartment, in contrast with the surrounding MC-derived CAFs presenting nuclear pSmad3 expression (Figure 30J-L).

11. Lentiviral knockdown of Smad3 in the peritoneum reduces metastasis

Having observed that the TGF-β1/pSmad3 pathway is relevant in the communication between ovarian cancer cells and HPMCs, lentiviral particles containing Smad3 shRNA were administered to mice in order to knock down its expression, followed by SKOV-3-luciferase cell i.p. inoculation. Mice were then monitored for 41 days via *in vivo* bioluminiscence imaging. Tumour growth and progression were significantly reduced in mice whose peritoneum had been knocked down of Smad3 expression (Figure 16).

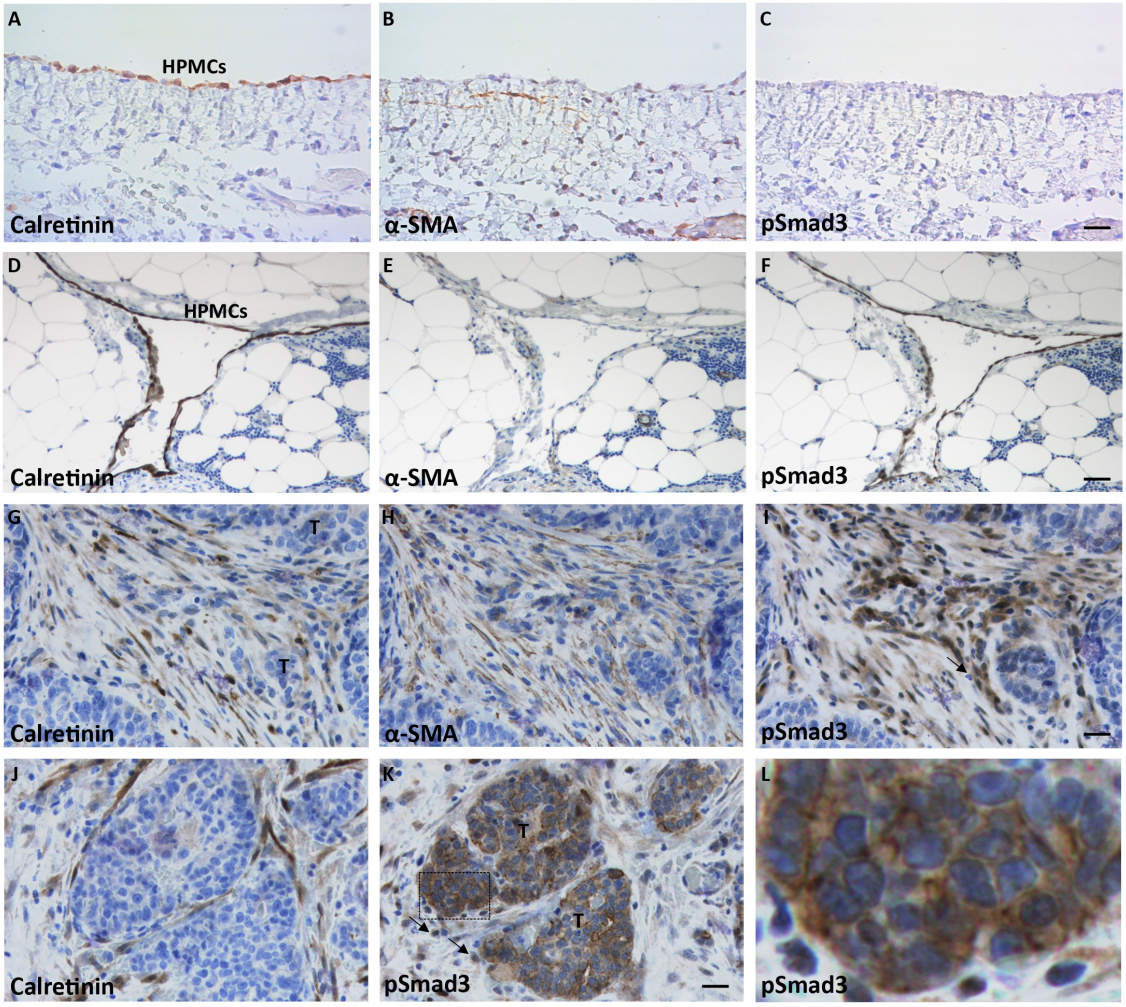

Figure 30. Immunohistochemical analysis of human peritoneal implants of ovarian cancer. Staining of serial sections was performed for calretinin, α-SMA and pSmad3. **(A-C)** Peritoneum of a control donor showing a preserved mesothelium and negative expression for both markers. **(D-L)** Same sample of ovarian cancer implant in the peritoneum. **(D-F)** Preserved mesothelial monolayer (calretinin-positive) in an area distant to the tumour cells, positive for nuclear pSmad3. **(G-I)** Submesothelial tumour implant showing surrounding stromal CAFs (α-SMA-positive) derived from MCs (calretinin-positive) and expressing nuclear pSmad3. **(J,K)** Micrometastasis, showing ovarian cancer cells with cytoplasmic expression of pSmad3, and -MC-derived CAFs surrounding the tumour and expressing nuclear pSmad3. **(L)** Higher magnification of the cytoplasmic pSmad3 staining in tumour cells. Scale bars = 25 µm (A-C, G-K), and 50 µm (D-F). Arrows indicate MC-derived CAFs, expressing nuclear pSmad3 in the proximity of tumour implants. Insets show higher magnifications of the delimited areas. T, tumour.

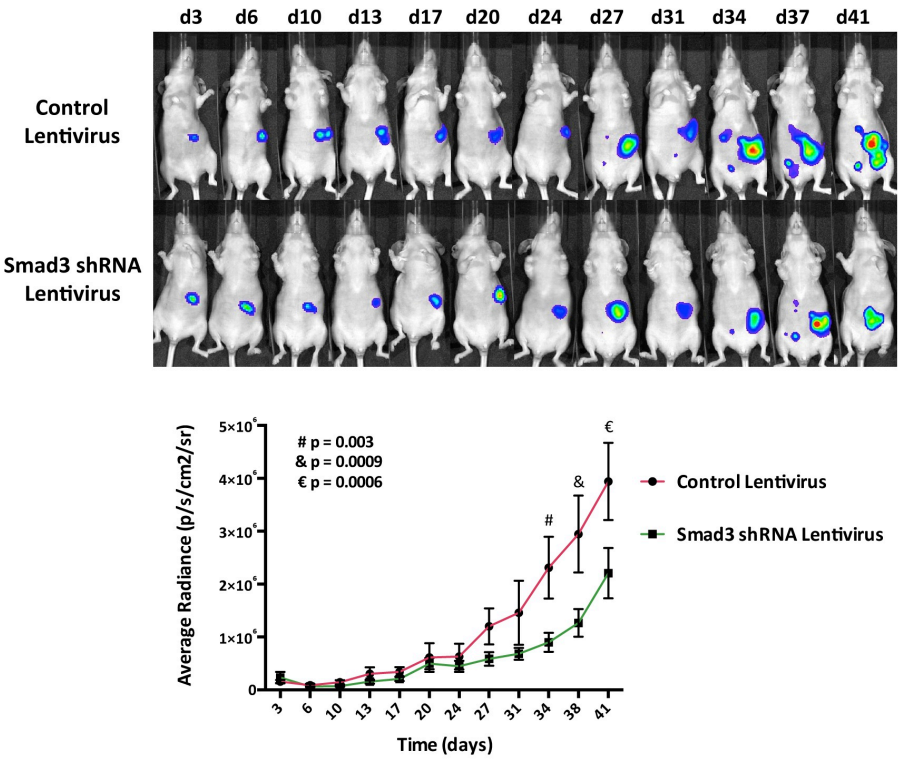

Figure 31. Lentiviral knockdown of Smad3 reduces tumour progression.

In vivo monitoring of SKOV-3-luciferase cells in nude mice pre-conditioned with lentiviral particles producing Smad3 shRNA or control. Graph represents mean average radiance of SKOV-3-luciferase cells ± SEM. Symbols represent the statistical differences between groups. n=9 per group.

DISCUSSION

CAFs deriving from various sources play an important role in facilitating tumour progression. In this work it is shown, for the first time, that in peritoneal implants of abdominal cancers, such as ovarian and colorectal, a proportion of CAFs derives from MCs via a MMT that is induced by cancer cells. The mesenchymal conversion of MCs favours the adhesion and invasion of metastasizing tumour cells and promotes the growth of secondary tumour implants. The MMT has been widely studied in the context of peritoneal dialysis, and has been suggested to play an important role in modifying the peritoneal structure, associated with fibrosis and angiogenesis (Aroeira et al. 2007; López-Cabrera 2014). A population of CAFs was observed to express several mesothelial markers: calretinin, WT1, mesothelin, and cytokeratin. The presence of CAFs expressing these mesothelial markers, in both human biopsies and mouse peritoneal samples, indicates that a subpopulation of CAFs originates from MCs during peritoneal tumour dissemination. Additionally, there is a marked fibro-proliferative response and increased angiogenesis at the places of tumour implants, where MC-derived CAFs accumulate. These results suggest that MMT plays important roles in transforming the tumour stroma at the secondary site in the peritoneum. When metastasizing to the peritoneum, cancer cells can attach to the MC monolayer or to the exposed submesothelial matrix. It has been proposed that tumour cells prefer the ECM for first attachment, predominantly binding to "milky spots" during the initial stages of peritoneal metastasis. In this regard, *in vitro* adhesion experiments demonstrate that cancer cells adhere better to mesenchymal than to epithelial-like MC monolayers. This is in agreement with other reports, where cancer cell adhesion was increased to mesothelial cells that had undergone a MMT (Jiang et al. 2013), or expressed the CAF marker FAP (Miao et al. 2014). Similarly, treatment of MCs with TNF-α induces a fibroblast-like conversion (Zhu et al. 2002) which increases the adhesion to cancer cells (Yu et al. 2010). In contrast to the "milky spot" preference regarded until now, scanning electron microscopy analysis suggested that the enhanced adhesion of tumour cells to mesenchymal MCs is due to an increased cell–cell interaction and not to a mere exposure of the underlying matrix. Hence, the MMT could play a role in conferring an advantage on metastatic cells for

attachment to the peritoneal membrane. The use of different β1 inhibitors indicated that this cancer cell–mesothelium interaction is mediated, at least in part, by β1-integrins, which is in agreement with reports by others (Takatsuki et al. 2004; Watanabe et al. 2012; Chen et al. 2015). However, other adhesion molecules have also been described to be participating in this interaction; although, their role throughout the mesenchymal conversion of MCs would require further analysis (Casey and Skubitz 2000; Ziprin et al. 2003; Rump et al. 2004; Alkhamesi et al. 2005; Ksiazek et al. 2010; Wagner et al. 2011)

Histological analysis shows that MC-derived CAFs accumulate in areas with micrometastases, coinciding also with prominent new vessel formation, but not in tumour-free regions, suggesting that tumour cells promote the invasion of adjacent MCs. On this note, MCs have been reported to create the invasion front of cancer cells (Satoyoshi et al. 2015a). Interestingly, in areas distant to micrometastasis, where the mesothelial monolayer is preserved, the nuclear localisation of pSmad3 suggests a mesenchymal conversion may be underway, but an invasive phenotype has not been acquired yet, which can be explained by the lack of α-SMA expression. The *in vitro* invasion assays demonstrate that carcinoma cells embedded in the matrix enhance the invasive capacity of MCs, which could be a consequence of the MMT. In this context, it is demonstrated that MCs with a mesenchymal phenotype markedly stimulate the invasion of ovarian carcinoma SKOV-3 cells, more so than MCs with an epithelial-like phenotype. The pro-invasive capacity acquired by mesenchymal MCs is in accordance with CAFs' known properties (Karagiannis et al. 2012). Thus, these results suggest that mesenchymal MCs and carcinoma cells establish a feed-forward cycle by mutually stimulating their invasiveness. This is in agreement with other reports of cancer cells stimulating MC invasiveness (Nakamura et al. 2015) and vice versa (Ren et al. 2006; Heyman et al. 2010; Kenny et al. 2014).

Given that the mesenchymal conversion of peritoneal MCs exerted an effect on ovarian cancer cells, it was of interest to study and characterise the MCs suspended in the ascitic fluid of ovarian cancer patients. These AFMCs were expressing the myofibroblast/CAF marker α-SMA, indicating they had undergone a MMT. Additionally, the TGF-β downstream effector pSmad3 was expressed in the nucleus, where it can modify gene transcription. It is also interesting to note that, in RT-PCR data, the transcription factor Snail is induced, which leads to a decrease in the E-cadherin levels. The angiogenesis-promoting factor VEGF is overexpressed; however, the ECM proteins collagen I and fibronectin were not significantly affected. RNA-seq analysis provided a more detailed pattern of the changes taking place in AFMCs. A sizeable proportion of the pathways that were significantly differentially regulated was directly associated to MMT (TGF-β signalling) or its consequences (loss of tight junctions, angiogenesis). The most differentially regulated pathway regards the hepatic stellate cell activation which, interestingly, MCs have been reported to convert into through a MMT (Li et al. 2013). Other molecules in these pathways have relevant roles in the MMT context: ILK mediates TGF-β1-induced EMT and myofibroblast differentiation (Li et al. 2003; Vi et al. 2010); Caveolin-1 is implicated in the internalization of TGF-β receptor type I, blocks the phosphorylation of Smad2, and its deficiency induces MMT (Razani et al. 2001; Strippoli et al. 2015); vitamin D regulates the TGF-β-induced EMT (Pervin et al. 2013; Fischer and Agrawal 2014; Li et al. 2015; Larriba and de Herreros 2016); a PPAR agonist (rosiglitazone) protects the peritoneal membrane *in vivo* (Sandoval et al. 2010; Bunt et al. 2013)*;* thrombin has been shown to promote cancer cell invasion by inducing EMT (Zhong et al. 2013) and the expression of β1-integrin and MMP-9 (Radjabi et al. 2008); p38 and NF-κB regulate EMT (Strippoli et al. 2008; 2010; 2012); and, recently, HGF secreted by ovarian cancer cells has been implicated in inducing a MMT and favouring invasion of MCs (Nakamura et al. 2015). During MMT, there is an increased angiogenesis and upregulation of MMPs (López-Cabrera 2014). In the RNA-seq data, two pathways that inhibit these processes appear as differentially regulated. However, this does not necessarily implicate that these processes are indeed inhibited, e.g. molecules implicated in the

inhibition of angiogenesis have a different regulation in AFMCs, which may lead to a blockade of this inhibiting pathway and, thus, promotion of angiogenesis. Supporting this, pro-angiogenic factors such as VEGF-A, VEGF-B, FGF-2, PDGF-A and PDGF-B, and MMPs 1, 2, 3, 7 and 9 appear upregulated in AFMCs in the RNA-seq data. Other pathways that are differentially regulated include signalling of various molecules present in the ascitic fluid and associated with ovarian cancer progression and poor prognosis: IL-6, IL-8 and IL-10 (Moradi et al. 1993; Santin et al. 2001; Mustea et al. 2006; Giuntoli et al. 2009; Lane et al. 2011; Matte et al. 2012). In this context, only IL-6 has been reported to be highly produced by HPMCs (Offner et al. 1995) compared to ovarian cancer cells. These data show, for the first time, that AFMCs secrete an array of inflammatory cytokines that will affect cancer progression. Overall, these pathways provide an overview of the changes taking place in AFMCs, and allow to conclude that these cells have undergone a MMT. The mesenchymal conversion will, in turn, transform the environment, rendering it more favourable for tumour progression by continuing to promote a MMT in an inflammatory and immunosuppressive context. On this note, the inflammatory cytokines IL-1β and TNF-α have been reported to work synergistically with TGF-β1 in upregulating VEGF (Catar et al. 2013) and IL-6 production in MCs (Offner et al. 1995). The fact that, in the RNA-seq data, IL-1β and TNF-α have a higher activation z-score than TGF-β1 as upstream regulators, could point to the MMT taking place in AFMCs as a link between the inflammatory environment present in the ascitic fluid and the induction of angiogenesis. However, a larger sample size of AFMCs is necessary to conclude these differential MMT outcomes. Patient heterogeneity is very high, which could also explain why the ECM proteins do not appear as upregulated in the RT-PCR data.

In agreement with the MMT they have undergone, when co-injected with ovarian cancer cells, AFMCs favoured tumour growth in a subcutaneous xenograft mouse model, compared to control HPMCs with no MMT, indicating this transition plays a role in tumour progression.

TGF-β1 is a key molecule controlling MMT and peritoneal fibrosis (López-Cabrera 2014) and, given that the MMT is driving the transformation of AFMCs, it was speculated that targeting the TGF-β1 pathway could interfere with the accumulation of CAFs. An *in vivo* assay of overexpression of TGF-β1 by adenoviral delivery indicated tumour progression was owed, at least partially, to TGF-β1. Previously, *in vitro* blockade of the TGF-β1 receptor was shown to prevent the mesenchymal conversion of MCs treated with conditioned medium from SKOV-3 cells. Further confirmation was attained when blocking this receptor *in vivo* translated into a dramatic decrease in tumour growth. These results are supported by reports of *in vivo* TGF-β1 blockade reducing peritoneal metastasis and improving survival in mice (Yamamura et al. 2011; Miao et al. 2013). The Smad-dependent pathway was considered to be activated in AFMCs, based on the nuclear localisation of pSmad3, a necessary step for the following transcriptional regulation (Derynck and Zhang 2003). Interestingly, biopsies of ovarian cancer implants in the peritoneum showed a differential localisation of pSmad3 between cancer cells and the MC-derived CAFs that surround them, being cytoplasmic in the former, and nuclear in the latter. Despite SKOV-3 cells producing high amounts of TGF-β1 (measurement in their conditioned medium was 1141.6 ± 169.3 pg/ml versus 369.4 ± 27.2 pg/ml in HT-29 cells), the Smad-dependent pathway was truncated in these cells: pSmad3 remained in the cytoplasm, unable to selectively activate or repress gene transcription in the nucleus, whereas in transdifferentiated MCs translocation was observable after 1 hour. Finally, knocking down Smad3 expression in mice resulted in reduced intraperitoneal tumour growth, indicating the Smad-dependent pathway is relevant *in vivo*.

All of these data point to the MMT being a key player in the initiation and progression of peritoneal metastasis, which is the result of a multi-directional communication between cancer cells, MCs and CAFs. Cancer cells trigger the conversion of MCs into CAFs via a MMT, creating a suitable metastatic niche that renders the peritoneum more receptive for further metastatic implants, promotes cancer cell adhesion to and invasion through the peritoneum, and

facilitates tumour growth. MC-derived CAFs accumulate in the submesothelial compact zone, providing the tumour with the adequate blood support, ECM components and/or proliferating signals to progress to advanced stages (Figure 32).

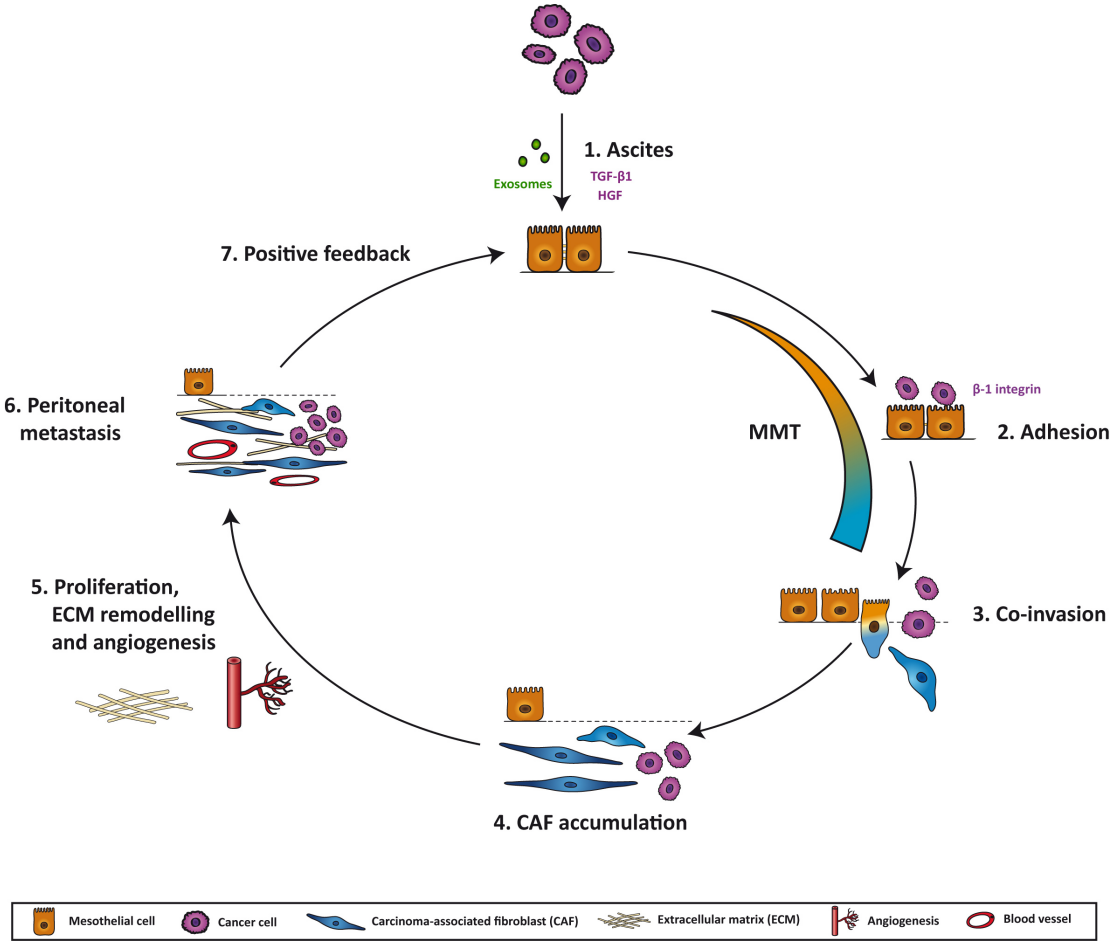

Figure 32. Model for transformation of the pre-metastatic niche by mesothelial-to-mesenchymal transition in the peritoneum.

(1) Cancer cells at the primary site secrete an array of exosomes, cytokines, chemokines and growth factors that accumulate in the ascitic fluid. Some of these molecules, such as transforming growth factor-beta1 (TGF-β1) or hepatocyte growth factor (HGF), induce changes in the mesothelial cells (MCs), triggering a mesothelial-to-mesenchymal transition (MMT), through which they lose apico-basal polarity and cell-cell adhesion, and acquire myofibroblastic properties. **(2)** Cancer cells adhere via β1 integrins to the MCs that line the peritoneum. This adhesion is increased when a MMT has taken place. **(3)** In later stages of MMT, MCs have converted into carcinoma-associated fibroblasts (CAFs) that represent the invasion front into the stroma, followed by cancer cells. **(4)** After invading, MC-derived CAFs accumulate in the peritoneal stroma. **(5)** CAFs produce factors that affect peritoneal implant progression: they induce angiogenesis via secretion of VEGF, among other factors; they transform the extracellular matrix (ECM) by producing collagen, fibronectin and other structural proteins, and they remodel the ECM via matrix metalloproteinases (MMPs); they also stimulate proliferation of cancer cells. **(6)** The metastatic niche in the peritoneum is created as a result of the clearance of the MC monolayer, myofibroblast conversion of MCs, invasion of MCs and cancer cells, accumulation of CAFs, increased vascularization, ECM remodelling and proliferation of cancer

cells. **(7)** Cancer cells in the new site, together with CAFs, will continue to produce factors that modify the stroma and induce changes in both cancer cells and MCs, thereby creating a positive feedback loop. *Modified from A Rynne-Vidal et al., Cancers 2015.*

Mesothelial-to-mesenchymal transition as a potential therapeutic target in peritoneal metastasis.

CAFs' proven tumour-promoting capacities have raised interest in exploiting them as drug targets for anticancer therapy (Micke and Ostman 2005). The MMT that drives the conversion of MCs into CAFs points to a possible alternative target in the treatment of metastases that disseminate via the peritoneum, since this process can be modulated. Therapeutic strategies could be designed towards avoiding the accumulation of mesothelial-derived CAFs in the compact zone. This could be achieved by targeting the MMT-inducing stimuli in the peritoneal cavity, by blocking or reverting the MMT itself, and/or by treating the MMT-associated effects, such as tumour cell adhesion and invasion, ECM accumulation or synthesis of pro-angiogenic factors (Figure 33).

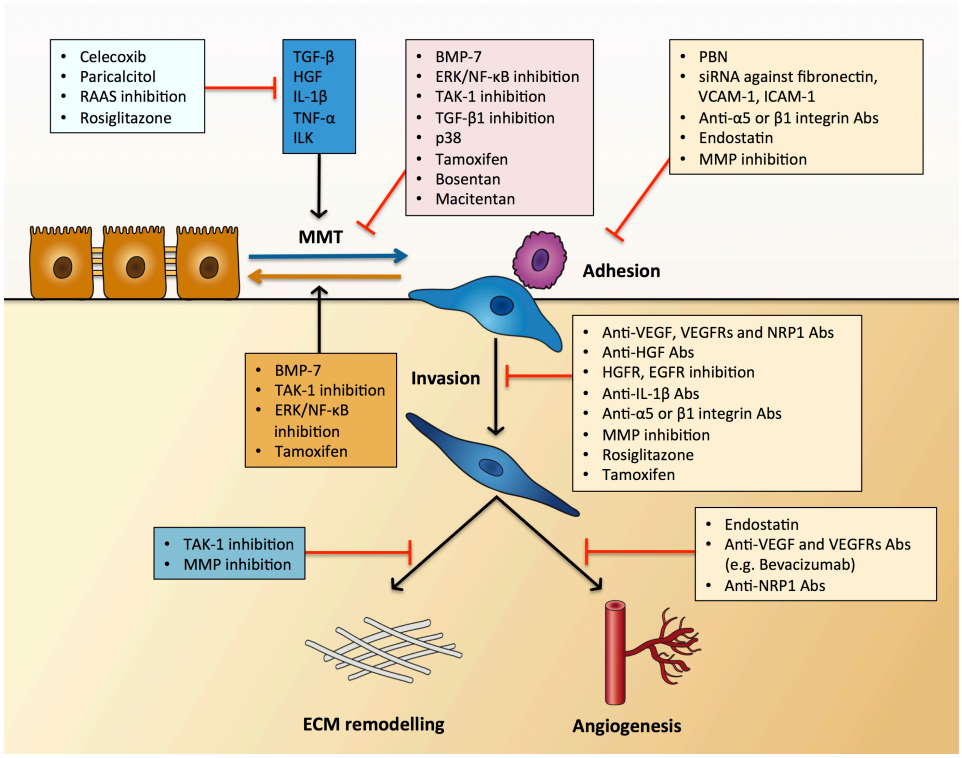

Figure 33. Targets for therapeutic strategies in the treatment of peritoneal metastasis. Different steps can be targeted, such as the MMT-promoting stimuli, the MMT itself, or the adhesion, invasion, angiogenesis and ECM remodelling associated with it. Abs, antibodies.

One approach would be the use of pharmacological agents that preserve the mesothelium against several stimuli. The MMT can result from molecular inflammatory signals associated with the intraperitoneal ascitic environment, and previous studies of MMT in peritoneal dialysis have demonstrated that using pharmacological agents (celecoxib, rosiglitazone) that target inflammation can preserve the peritoneal membrane. In this context, celecoxib is a potent anti-inflammatory drug whose mechanism of action is based on the inhibition of cyclooxygenase (COX)-2, which is expressed at high levels by MCs that undergo MMT. COX-2 has been widely implicated in inflammatory responses, as well as in fibrotic and angiogenic processes in animal peritoneal dialysis models (Aroeira et al. 2009; Fabbrini et al. 2009). Interestingly, expression of COX-2 is also elevated in tumour cells of colorectal and ovarian carcinomas (Menczer 2009; Rizzo 2011). Multiple clinical studies show the effectiveness of specific inhibitors of COX-2 in preventing or delaying re-occurrence of cancer, including metastases, in high risk patients (Arber et al. 2006; Baron et al. 2006; Solomon et al. 2006; Midgley et al. 2010)., Rosiglitazone is an activating agonist of the inflammation regulator PPAR-γ whose use *in vivo* protects the peritoneal membrane in the context of peritoneal dialysis (Sandoval et al. 2010) and, combined with gemcitabine, reduces peritoneal metastasis, TGF-β production and cancer cell invasion (Bunt et al. 2013). On a separate note, vitamin D also has a role in immune regulation, and an activator (paricalcitol) of its receptor VDR has been shown to protect the peritoneal membrane, reduce fibrosis and attenuate the TGF-β-induced EMT in peritoneal dialysis (González-Mateo et al. 2014; Kang et al. 2014). Finally, in an inflammatory environment, the components of the renin-angiotensin-aldosterone system (RAAS) are upregulated in mesothelial cells; and blockade of this system has proven to protect the peritoneal membrane (Duman et al. 2004; Nessim et al. 2010).

Another therapeutic approach could be directed to interfere with or modify the MMT. Regarding this idea, TGF-β1 is a master molecule in the induction of MMT and is highly accumulated in malignant ascitic fluids. Our data demonstrate that interfering with the TGF-β1

pathway, both *in vitro* and *in vivo*, blocks the conversion of MCs into CAFs and diminishes tumour growth and metastasis. Also, *in vivo* experiments showed that using a TGF-β1 blocking agent prevented peritoneal dissemination of gastric cancer cells by preserving the mesothelial monolayer structure (Miao et al. 2013). Although further studies are needed in this regard, it should be considered that agents directly blocking TGF-β1 cannot be easily employed in the clinical practice, at least for long-term treatments, because TGF-β1 has important modulating functions of the immune and inflammatory responses (Wang et al. 2010; Yoshimura et al. 2010). In the present work, the mesenchymal conversion of MCs is reported to be taking place, at least partially, in a TGF-β1 Smad-dependent manner, although further downstream studies of this signalling pathway in MMT would provide more specific strategies for the preservation of peritoneal membrane with fewer side effects. In this context, the use of bone morphogenetic protein (BMP)-7 (an endogenous negative regulator of this process) has been shown to block/reverse MMT *in vitro, ex vivo* and *in vivo*, reducing fibrosis, angiogenesis, invasion and the acquisition of a mesenchymal phenotype by MCs (Vargha et al. 2006; Loureiro et al. 2010). Further, receptor antagonists (bosentan and macitentan) of endothelin-1 (ET-1), a TGF-β1 transcriptional target, attenuated the MMT, fibrosis and angiogenesis induced by peritoneal dialysis (Busnadiego et al. 2015). Additionally, the TGF-β1 Smad-independent signalling pathways play a role in MMT, and prevention/reversion has been attained by targeting TAK-1 (Strippoli et al. 2012), ERKs-1/2, and NF-κB (Strippoli et al. 2008; 2010; Jang et al. 2012). Further characterization of the involvement of these molecules in peritoneal metastasis could provide a wider range of possible molecular targets. On a related note, the recent description of HGF as an inducer of MMT in peritoneal metastasis could also open new therapeutic strategies focused on this signalling pathway. Regarding this idea, *in vitro* experiments have shown that the use of blocking antibodies against HGF, and inhibitors of HGF receptor (HGFR) and epidermal growth factor receptor (EGFR) block the migration of HPMCs (Matte et al. 2014b) and ovarian cancer cells (Sowter et al. 1999). Finally, tamoxifen is a synthetic modulator of the estrogen receptor that is known to act in peritoneal tissue. Its efficacy in preserving the

peritoneal structure was tested in a mouse model of peritoneal dialysis, where it reduced peritoneal thickness, angiogenesis and invasion of the compact zone by transdifferentiated MCs (Loureiro et al. 2013). With regard to ovarian cancer, hormone treatment with tamoxifen is often used in conjunction with chemotherapy and other therapies (Serkies et al. 2013).

Targeting adhesion of cancer cells to the mesothelium could also be considered as a therapeutic strategy for peritoneal metastasis, given that blocking antibodies or siRNA directed against either ICAM-1 (Ranieri et al. 2013), VCAM-1 (Slack-Davis et al. 2009), fibronectin (Kenny et al. 2008) or their integrin ligands significantly decreased the adhesion and invasion of ovarian cancer cells through the MC monolayer, and dramatically reduced metastases in a mouse model (Kenny et al. 2014). The use of blocking antibodies or siRNA against α5 or β1 integrins have shown significantly reduced adhesion, invasion, tumour burden and peritoneal metastasis (Sawada et al. 2008; Mitra et al. 2011; Watanabe et al. 2012; Kenny et al. 2014). On this note, the angiogenesis inhibitor endostatin targets the α5β1 integrin, and its use prevented the attachment of cancer cells to the mesothelium (Yokoyama et al. 2007). Interestingly, it has been reported that the oxidative stress that accompanies senescent MCs may facilitate the adhesion and dissemination of cancer cells; and the use of an antioxidant (PBN) significantly reduced this attachment (Ksiazek et al. 2009; 2010). Senescence also mediates the interaction of tumour cells and MCs via binding of α5β1 integrin to fibronectin, respectively (Ksiazek et al. 2009). Additionally, higher production levels of TGF-β1 by MCs have been associated with oxidative stress, but also with age of the patients, suggesting there may be an accumulation of senescent MCs *in vivo* (Ksiazek 2013). Moreover, adhesion of ovarian cancer cells to the mesothelium is also mediated by MMPs (Burleson et al. 2004; Kenny et al. 2008) and their inhibition in ovarian cancer cells prior to inoculation in mice resulted in reduced metastasis. Therefore, strategies directed towards MMP inhibition would also be of interest in the treatment of peritoneal metastases and may prevent the accumulation of MC-derived CAFs in the submesothelial stroma (Egeblad and Werb 2002; Gialeli et al. 2010; Cathcart et al. 2015).

Recently, it has been demonstrated that invasion capacity of MCs that have undergone a MMT is governed, at least partially, by the VEGF/VEGF receptors/co-receptors axis. It was shown that blocking antibodies directed against VEGF or the co-receptor neuropilin-1 efficiently reduced the invasion of MCs *in vitro* (Pérez-Lozano et al. 2013). With regard to VEGF, this work points to its enhanced expression as one of the most evident effects associated to MMT during peritoneal metastasis. Therefore, therapeutic intervention may also be directed at preventing peritoneal tumour vascularization via interrupting VEGF expression or its effects on the stromal endothelial cell (Wu et al. 2012). In fact, Sako *et al.* showed that peritoneal dissemination of gastric cancer was significantly suppressed when adenovirus expressing a soluble form of the VEGF receptor Flt-1 was administered intraperitoneally to mice (Sako et al. 2004). Various anti-angiogenic therapies directed against VEGF or its receptors are presently being considered for the treatment of advanced abdominal cancers (Masoumi Moghaddam et al. 2011; Gadducci et al. 2015). Particularly, the use of Bevacizumab, a monoclonal antibody targeting VEGF, showed an improvement of patient survival in both colorectal (Mulder et al. 2011) and ovarian cancer (Perren et al. 2011). Additionally, tamoxifen also inhibits the invasion capacity of mesenchymal-like MCs via the inhibition of matrix metalloproteinase-2 (MMP-2) (Loureiro et al. 2013), and blocking of MMP-2 in MCs has been shown to reduce invasion by gastric cancer cells *in vitro* (Mizutani et al. 2000).

In conclusion, targeting the MMT could constitute an alternative target in the treatment of cancers that disseminate through and metastasize in the peritoneum. Further characterization of the molecules involved requires development; however, analysis of the pathways that are differentially regulated in AFMCs could provide insight into new therapeutic options. Additionally, strategies that interfere with the MMT in peritoneal dialysis could be considered for the metastasis scenario, since the effects of MMT (MC invasion, fibroblast accumulation, ECM deposition and angiogenesis) in the peritoneum seem to be similar in both pathologies.

CONCLUSIONS

1. Mesothelial cells (MCs) convert into carcinoma-associated fibroblasts through a mesothelial-to-mesenchymal (MMT) transition induced by cancer cells.

2. Adhesion to and invasion through the peritoneum is favoured by the mesenchymal conversion of mesothelial cells.

3. MC-derived CAFs and SKOV-3 cells mutually stimulate their invasive capacity.

4. Mesothelial cells in the ascitic fluid of patients with ovarian cancer have undergone a MMT and favour tumour progression.

5. The TGF-β1-induced MMT promotes peritoneal metastasis.

6. MMT in the peritoneum takes place, at least partially, via a Smad-dependent TGF-β1 signalling pathway.

7. The TGF-β1 signalling pathway appears to be truncated in ovarian cancer cells, which rely on the MC-derived CAFs for transforming the pre-metastatic niche.

8. Therapeutic strategies directed towards blocking and/or reversing the MMT could open the door to new treatments for peritoneal metastasis.

CONCLUSIONES

1. Las células mesoteliales (MCs) se convierten en fibroblastos asociados a cáncer (CAFs) mediante una transición mesotelio-mesénquima inducida por las células cancerosas.

2. La conversión mesenquimal de las células mesoteliales favorece la adhesión y la invasión a través del peritoneo.

3. Los CAFs derivados de MCs y las células SKOV-3 estimulan mutuamente su capacidad invasiva.

4. Las MCs del líquido ascítico de pacientes con cáncer de ovario han sufrido una MMT y favorecen la progresión tumoral.

5. La MMT inducida por TGF-β1 promueve la metástasis peritoneal.

6. La MMT en el peritoneo se induce, al menos parcialmente, por la vía Smad-dependiente de la señalización de TGF-β1.

7. La vía de señalización de TGF-β1 aparece truncada en las células de cáncer ovario, que dependen de los CAFs derivados de MCs para transformar el nicho pre-metastásico

8. Las estrategias terapéuticas dirigidas a bloquear o revertir la MMT podrían abrir la puerta a nuevos tratamientos para la metástasis peritoneal.

REFERENCES

Adam RA, Adam YG. Malignant ascites: past, present, and future. Journal of the American College of Surgeons. 2004 Jun;198(6):999–1011.

Aguilera A, Yanez-Mo M, Selgas R, Sanchez-Madrid F, Lopez Cabrera M. Epithelial to mesenchymal transition as a triggering factor of peritoneal membrane fibrosis and angiogenesis in peritoneal dialysis patients. Curr Opin Investig Drugs. 2005 ed. 2005 Mar;6(3):262–8.

Al-Alem L, Curry TEJ. Ovarian cancer: involvement of the matrix metalloproteinases. Reproduction. 2015 ed. 2015 Aug;150(2):R55–64.

Alkhamesi NA, Ziprin P, Pfistermuller K, Peck DH, Darzi AW. ICAM-1 mediated peritoneal carcinomatosis, a target for therapeutic intervention. Clin Exp Metastasis. 2005 ed. 2005;22(6):449–59.

Arber N, Eagle CJ, Spicak J, Rácz I, Dite P, Hajer J, et al. Celecoxib for the prevention of colorectal adenomatous polyps. N Engl J Med. 2006 Aug 31;355(9):885–95.

Aroeira LS, Aguilera A, Sanchez-Tomero JA, Bajo MA, del Peso G, Jimenez-Heffernan JA, et al. Epithelial to mesenchymal transition and peritoneal membrane failure in peritoneal dialysis patients: pathologic significance and potential therapeutic interventions. J Am Soc Nephrol. 2007 ed. 2007 Jul;18(7):2004–13.

Aroeira LS, Aguilera A, Selgas R, Ramirez-Huesca M, Perez Lozano ML, Cirugeda A, et al. Mesenchymal conversion of mesothelial cells as a mechanism responsible for high solute transport rate in peritoneal dialysis: role of vascular endothelial growth factor. Am J Kidney Dis. 2005 ed. 2005 Nov;46(5):938–48.

Aroeira LS, Lara-Pezzi E, Loureiro J, Aguilera A, Ramírez-Huesca M, González-Mateo G, et al. Cyclooxygenase-2 mediates dialysate-induced alterations of the peritoneal membrane. Journal of the American Society of Nephrology. 2009 Mar;20(3):582–92.

Arroyo AG, Sánchez-Mateos P, Campanero MR, Martín-Padura I, Dejana E, Sanchez-Madrid F. Regulation of the VLA integrin-ligand interactions through the beta 1 subunit. J Cell Biol. 1992 May;117(3):659–70.

Ayantunde AA, Parsons SL. Pattern and prognostic factors in patients with malignant ascites: a retrospective study. Ann Oncol. 2007 May;18(5):945–9.

Ayhan A, Gultekin M, Taskiran C, Dursun P, Firat P, Bozdag G, et al. Ascites and epithelial ovarian cancers: a reappraisal with respect to different aspects. International Journal of Gynecological Cancer. 2007 Jan;17(1):68–75.

Bakrin N, Classe JM, Pomel C, Gouy S, Chene G, Glehen O. Hyperthermic intraperitoneal chemotherapy (HIPEC) in ovarian cancer. J Visc Surg. 2014 Oct;151(5):347–53.

Baron JA, Sandler RS, Bresalier RS, Quan H, Riddell R, Lanas A, et al. A randomized trial of rofecoxib for the chemoprevention of colorectal adenomas. Gastroenterology. 2006 Dec;131(6):1674–82.

Belotti D, Calcagno C, Garofalo A, Caronia D, Riccardi E, Giavazzi R, et al. Vascular endothelial growth factor stimulates organ-specific host matrix metalloproteinase-9 expression and ovarian cancer invasion. Mol Cancer Res. 2008 Apr;6(4):525–34.

Bhome R, Bullock MD, Saihati Al HA, Goh RW, Primrose JN, Sayan AE, et al. A top-down view of the tumor microenvironment: structure, cells and signaling. Front Cell Dev Biol. 2015 ed. 2015;3:33.

Bhowmick NA, Neilson EG, Moses HL. Stromal fibroblasts in cancer initiation and progression. Nature. 2004 ed. 2004 Nov 18;432(7015):332–7.

Birkedal-Hansen H, Moore WG, Bodden MK, Windsor LJ, Birkedal-Hansen B, DeCarlo A, et al. Matrix metalloproteinases: a review. Crit Rev Oral Biol Med. 1993rd ed. 1993;4(2):197–250.

Bochet L, Lehuédé C, Dauvillier S, Wang YY, Dirat B, Laurent V, et al. Adipocyte-derived fibroblasts promote tumor progression and contribute to the desmoplastic reaction in breast cancer. Cancer Res. 2013 Sep 15;73(18):5657–68.

Bunt SK, Mohr AM, Bailey JM, Grandgenett PM, Hollingsworth MA. Rosiglitazone and Gemcitabine in combination reduces immune suppression and modulates T cell populations in pancreatic cancer. Cancer Immunol Immunother. 2013 Feb;62(2):225–36.

Burleson KM, Hansen LK, Skubitz APN. Ovarian carcinoma spheroids disaggregate on type I collagen and invade live human mesothelial cell monolayers. Clin Exp Metastasis. 2004 May 18;21(8):685–97.

Busnadiego Ó, Loureiro-Álvarez J, Sandoval P, Lagares D, Dotor J, Pérez-Lozano ML, et al. A pathogenetic role for endothelin-1 in peritoneal dialysis-associated fibrosis. Journal of the American Society of Nephrology. 2015 Jan;26(1):173–82.

Cai J, Tang H, Xu L, Wang X, Yang C, Ruan S, et al. Fibroblasts in omentum activated by tumor cells promote ovarian cancer growth, adhesion and invasiveness. Carcinogenesis. 2011 Dec 28;33(1):20–9.

Calon A, Espinet E, Palomo-Ponce S, Tauriello DVF, Iglesias M, Céspedes MV, et al. Dependency of Colorectal Cancer on a TGF-β-Driven Program in Stromal Cells for Metastasis Initiation. Cancer Cell. 2012 Nov;22(5):571–84.

Calon A, Tauriello DVF, Batlle E. TGF-beta in CAF-mediated tumor growth and metastasis. Semin Cancer Biol. 2014 Apr;25:15–22.

Campanero MR, Arroyo AG, Pulido R, Ursa A, de Matías MS, Sánchez-Mateos P, et al. Functional role of alpha 2/beta 1 and alpha 4/beta 1 integrins in leukocyte intercellular adhesion induced through the common beta 1 subunit. Eur J Immunol. 1992 Dec;22(12):3111–9.

Cappellesso R, Tinazzi A, Giurici T, Simonato F, Guzzardo V, Ventura L, et al. Programmed cell death 4 and microRNA 21 inverse expression is maintained in cells and exosomes from ovarian serous carcinoma effusions. Cancer Cytopathology. 2014 May 28;122(9):685–93.

Casey RC, Skubitz AP. CD44 and beta1 integrins mediate ovarian carcinoma cell migration toward extracellular matrix proteins. Clin Exp Metastasis. 2001st ed. 2000;18(1):67–75.

Catar R, Witowski J, Wagner P, Annett Schramm I, Kawka E, Philippe A, et al. The proto-oncogene c-Fos transcriptionally regulates VEGF production during peritoneal inflammation. Kidney Int. 2013 Dec;84(6):1119–28.

Cathcart J, Pulkoski-Gross A, Cao J. Targeting Matrix Metalloproteinases in Cancer: Bringing New Life to Old Ideas. Genes Dis. 2015 Mar 1;2(1):26–34.

Chambers AF, Groom AC, MacDonald IC. Dissemination and growth of cancer cells in metastatic sites. Nat Rev Cancer. 2002 Aug;2(8):563–72.

Chegini N. TGF-beta system: the principal profibrotic mediator of peritoneal adhesion formation. Semin Reprod Med. 2008 ed. 2008 Jul;26(4):298–312.

Chen CN, Chang CC, Lai HS, Jeng YM, Chen CI, Chang KJ, et al. Connective tissue growth factor inhibits gastric cancer peritoneal metastasis by blocking integrin alpha3beta1-dependent adhesion. Gastric Cancer. 2015 Jul 2;3(18):504–15.

Choi D-S, Park JO, Jang SC, Yoon YJ, Jung JW, Choi D-Y, et al. Proteomic analysis of microvesicles derived from human colorectal cancer ascites. Proteomics. 2011 Jun 1;11(13):2745–51.

Cirri P, Chiarugi P. Cancer-associated-fibroblasts and tumour cells: a diabolic liaison driving cancer progression. Cancer Metastasis Rev. 2011 ed. 2012 Jun;31(1-2):195–208.

Clark R, Krishnan V, Schoof M, Rodriguez I, Theriault B, Chekmareva M, et al. Milky spots promote ovarian cancer metastatic colonization of peritoneal adipose in experimental models. Am J Pathol. 2013 ed. 2013 Aug;183(2):576–91.

Davidowitz RA, Selfors LM, Iwanicki MP, Elias KM, Karst A, Piao H, et al. Mesenchymal gene program-expressing ovarian cancer spheroids exhibit enhanced mesothelial clearance. J Clin Invest. 2014 ed. 2014 Jun;124(6):2611–25.

de Caestecker M. The transforming growth factor-beta superfamily of receptors. Cytokine Growth Factor Rev. 2004 Feb;15(1):1–11.

de Cuba EM, Kwakman R, van Egmond M, Bosch LJ, Bonjer HJ, Meijer GA, et al. Understanding molecular mechanisms in peritoneal dissemination of colorectal cancer : future possibilities for personalised treatment by use of biomarkers. Virchows Arch. 2012 ed. 2012 Sep;461(3):231–43.

De Vlieghere E, Gremonprez F, Verset L, Marien L, Jones CJ, De Craene B, et al. Tumor-environment biomimetics delay peritoneal metastasis formation by deceiving and redirecting disseminated cancer cells. Biomaterials. 2015 ed. 2015 Jun;54:148–57.

Deb A, Ubil E. Cardiac fibroblast in development and wound healing. J Mol Cell Cardiol. 2014 May;70:47–55.

Demir AY, Groothuis PG, Dunselman GAJ, Schurgers L, Evers JLH, de Goeij AFPM. Molecular characterization of soluble factors from human menstrual effluent that induce epithelial to mesenchymal transitions in mesothelial cells. Cell Tissue Res. 2005 Aug 5;322(2):299–311.

Derynck R, Akhurst RJ. Differentiation plasticity regulated by TGF-beta family proteins in development and disease. Nat Cell Biol. 2007 Sep;9(9):1000–4.

Derynck R, Zhang YE. Smad-dependent and Smad-independent pathways in TGF-beta family signalling. Nature. 2003 Oct 9;425(6958):577–84.

Desmoulière A, Gabbiani G. Modulation of Fibroblastic Cytoskeletal Features During Pathological Situations: The Role of Extracellular Matrix and Cytokines. Cell Motility and the Cytoskeleton. 1994 Jun 20;29:195–203.

Desmoulière A, Geinoz A, Gabbiani F, Gabbiani G. Transforming Growth Factor-beta1 Induces a-SmoothMuscle Actin Expression in Granulation Tissue Myofibroblasts and in Quiescent and Growing Cultured Fibroblasts. The Journal of Cell Biology. 1993 Jul 1;122(1):103–11.

Desmoulière A, Guyot C, Gabbiani G. The stroma reaction myofibroblast: a key player in the control of tumor cell behavior. Int J Dev Biol. 2004 ed. 2004;48(5-6):509–17.

Devuyst O, Margetts PJ, Topley N. The pathophysiology of the peritoneal membrane. Journal of the American Society of Nephrology. 2010 ed. 2010 Jul;21(7):1077–85.

Di Paolo N, Sacchi G. Atlas of peritoneal histology. Perit Dial Int. 2000 ed. 2000;20 Suppl 3:S5–96.

Ding B, Kilpatrick DL. Lentiviral vector production, titration, and transduction of primary neurons. Methods Mol Biol. 2013 Apr;1018:119–31.

Direkze NC, Hodivala-Dilke K, Jeffery R, Hunt T, Poulsom R, Oukrif D, et al. Bone marrow contribution to tumor-associated myofibroblasts and fibroblasts. Cancer Res. 2004 Dec 1;64(23):8492–5.

Dulauroy S, Di Carlo SE, Langa F, Eberl G, Peduto L. Lineage tracing and genetic ablation of ADAM12(+) perivascular cells identify a major source of profibrotic cells during acute tissue injury. Nat Med. 2012 Aug;18(8):1262–70.

Duman S, Wieczorowska-Tobis K, Styszynski A, Kwiatkowska B, Breborowicz A, Oreopoulos DG. Intraperitoneal enalapril ameliorates morphologic changes induced by hypertonic peritoneal dialysis solutions in rat peritoneum. Adv Perit Dial. 2004;20:31–6.

Egeblad M, Werb Z. New functions for the matrix metalloproteinases in cancer progression. Nat Rev Cancer. 2002 Mar;2(3):161–74.

Evans RA, Tian YC, Steadman R, Phillips AO. TGF-β1-mediated fibroblast-myofibroblast terminal differentiation-the role of Smad proteins. Exp Cell Res. 2003 Jan 15;282(2):90–100.

Fabbrini P, Schilte MN, Zareie M, Wee ter PM, Keuning ED, Beelen RHJ, et al. Celecoxib treatment reduces peritoneal fibrosis and angiogenesis and prevents ultrafiltration failure in experimental peritoneal dialysis. Nephrology Dialysis Transplantation. 2009 Dec;24(12):3669–76.

Feng X-H, Derynck R. Specificity and Versatility in TGF-beta signaling through Smads. Ann Rev Cell Dev Biol. 2005 Jul 1;21:659–93.

Fischer KD, Agrawal DK. Vitamin D regulating TGF-β induced epithelial-mesenchymal transition. Respir Res. 2014;15:146.

Fredj S, Bescond J, Louault C, Delwail A, Lecron J-C, Potreau D. Role of interleukin-6 in cardiomyocyte/cardiac fibroblast interactions during myocyte hypertrophy and fibroblast proliferation. J Cell Physiol. 2005 Aug;204(2):428–36.

Freedman RS, Deavers M, Liu J, Wang E. Peritoneal inflammation - A microenvironment for Epithelial Ovarian Cancer (EOC). J Transl Med. 2004 ed. 2004 Jun 25;2(1):23.

Gadducci A, Lanfredini N, Sergiampietri C. Antiangiogenic agents in gynecological cancer: State of art and perspectives of clinical research. Crit Rev Oncol Hematol. 2015 Jun 16;:[Epubaheadofprint].

Gialeli C, Theocharis AD, Karamanos NK. Roles of matrix metalloproteinases in cancer progression and their pharmacological targeting. FEBS Journal. 2010 Nov 19;278(1):16–27.

Giuntoli RL, Webb TJ, Zoso A, Rogers O, Diaz-Montes TP, Bristow RE, et al. Ovarian cancer-associated ascites demonstrates altered immune environment: implications for antitumor immunity. Anticancer Res. 2009 Aug;29(8):2875–84.

Glehen O, Cotte E, Brigand C, Arvieux C, Sayag-Beaujard AC, Gilly FN. Nouveautés thérapeutiques dans la prise en charge des carcinoses péritonéales d'origine digestive : chirurgie de cytoréduction et chimiothérapie intrapéritonéale. [Therapeutic innovations in the management of peritoneal carcinomatosis from digestive origin: cytoreductive surgery and intraperitoneal chemotherapy]. Rev Med Interne. 2005 ed. 2006 May;27(5):382–91.

Glockzin G, Schlitt HJ, Piso P. Peritoneal carcinomatosis: patients selection, perioperative complications and quality of life related to cytoreductive surgery and hyperthermic intraperitoneal chemotherapy. World J Surg Oncol. 2009 ed. 2009;7:5.

González-Mateo GT, Fernández-Millara V, Bellón T, Liappas G, Ruíz-Ortega M, López-Cabrera M, et al. Paricalcitol reduces peritoneal fibrosis in mice through the activation of regulatory T cells and reduction in IL-17 production. PLoS ONE. 2014;9(10):e108477.

Göritz C, Dias DO, Tomilin N, Barbacid M, Shupliakov O, Frisén J. A pericyte origin of spinal cord scar tissue. Science. 2011 Jul 8;333(6039):238–42.

Graves LE, Ariztia EV, Navari JR, Matzel HJ, Stack MS, Fishman DA. Proinvasive properties of ovarian cancer ascites-derived membrane vesicles. Cancer Res. 2004 Oct 1;64(19):7045–9.

Hagiwara A, Takahashi T, Sawai K, Taniguchi H, Shimotsuma M, Okano S, et al. Milky spots as the implantation site for malignant cells in peritoneal dissemination in mice. Cancer Res. 1993 Feb 1;53(3):687–92.

Hanahan D, Weinberg RA. Hallmarks of Cancer: The Next Generation. Cell. 2011 Mar;144(5):646–74.

Heath RM, Jayne DG, O'Leary R, Morrison EE, Guillou PJ. Tumour-induced apoptosis in human mesothelial cells: a mechanism of peritoneal invasion by Fas Ligand/Fas interaction. Br J Cancer. 2004 ed. 2004 Apr 5;90(7):1437–42.

Hennessy BT, Coleman RL, Markman M. Ovarian cancer. Lancet. 2009 Oct 17;374(9698):1371–82.

Heyman L, Leroy-Dudal J, Fernandes J, Seyer D, Dutoit S, Carreiras F. Mesothelial vitronectin stimulates migration of ovarian cancer cells. Cell Biol Int. 2010 May;34(5):493–502.

Ishii G, Sangai T, Oda T, Aoyagi Y, Hasebe T, Kanomata N, et al. Bone-marrow-derived myofibroblasts contribute to the cancer-induced stromal reaction. Biochem Biophys Res Commun. 2003 Sep 12;309(1):232–40.

Iwanicki MP, Davidowitz RA, Ng MR, Besser A, Muranen T, Merritt M, et al. Ovarian Cancer Spheroids Use Myosin-Generated Force to Clear the Mesothelium. Cancer Discovery. 2011 Jul 17;1(2):144–57.

Jang Y-H, Shin H-S, Choi HS, Ryu E-S, Kim MJ, Min SK, et al. Effects of dexamethasone on the TGF-b1-induced epithelial-to-mesenchymal transition in human peritoneal mesothelial cells. Laboratory Investigation. Nature Publishing Group; 2012 Dec 3;93(2):194–206.

Jiang C-G, Lv L, Liu F-R, Wang Z-N, Na D, Li F, et al. Connective tissue growth factor is a positive regulator of epithelial-mesenchymal transition and promotes the adhesion with gastric cancer cells in human peritoneal mesothelial cells. Cytokine. 2013 Jan;61(1):173–80.

Jimenez-Heffernan JA, Aguilera A, Aroeira LS, Lara-Pezzi E, Bajo MA, del Peso G, et al. Immunohistochemical characterization of fibroblast subpopulations in normal peritoneal tissue and in peritoneal dialysis-induced fibrosis. Virchows Arch. 2004 ed. 2004 Mar;444(3):247–56.

John A, Tuszynski G. The role of matrix metalloproteinases in tumor angiogenesis and tumor metastasis. Pathol Oncol Res. 2001st ed. 2001;7(1):14–23.

Jotzu C, Alt E, Welte G, Li J, Hennessy BT, Devarajan E, et al. Adipose tissue-derived stem cells differentiate into carcinoma-associated fibroblast-like cells under the influence of tumor-derived factors. Anal Cell Pathol (Amst). 2010;33(2):61–79.

Kalluri R, Weinberg RA. The basics of epithelial-mesenchymal transition. The Journal of Clinical Investigation. American Society for Clinical Investigation; 2009 Jun 1;119(6):1420–8.

Kalluri R, Zeisberg M. Fibroblasts in cancer. Nat Rev Cancer. 2006 ed. 2006 May;6(5):392–401.

Kang SH, Kim SO, Cho KH, Park JW, Yoon KW, Do JY. Paricalcitol ameliorates epithelial-to-mesenchymal transition in the peritoneal mesothelium. Nephron Exp Nephrol. 2014;126(1):1–7.

Karagiannis GS, Poutahidis T, Erdman SE, Kirsch R, Riddell RH, Diamandis EP. Cancer-associated fibroblasts drive the progression of metastasis through both paracrine and mechanical pressure on cancer tissue. Mol Cancer Res. 2012 Nov;10(11):1403–18.

Karki S, Surolia R, Hock TD, Guroji P, Zolak JS, Duggal R, et al. Wilms' tumor 1 (Wt1) regulates pleural mesothelial cell plasticity and transition into myofibroblasts in idiopathic pulmonary fibrosis. The FASEB Journal. 2014 Feb 27;28(3):1122–31.

Kenny HA, Chiang C-Y, White EA, Schryver EM, Habis M, Romero IL, et al. Mesothelial cells promote early ovarian cancer metastasis through fibronectin secretion. J Clin Invest. 2014 Sep 9;124(10):4614–28.

Kenny HA, Kaur S, Coussens LM, Lengyel E. The initial steps of ovarian cancer cell metastasis are mediated by MMP-2 cleavage of vitronectin and fibronectin. J Clin Invest. 2008 ed. 2008 Apr;118(4):1367–79.

Kenny HA, Krausz T, Yamada SD, Lengyel E. Use of a novel 3D culture model to elucidate the role of mesothelial cells, fibroblasts and extra-cellular matrices on adhesion and invasion of ovarian cancer cells to the omentum. Int J Cancer. 2007 ed. 2007 Oct 1;121(7):1463–72.

Kenny HA, Lengyel E. MMP-2 functions as an early response protein in ovarian cancer metastasis. Cell Cycle. 2009 ed. 2009 Mar 1;8(5):683–8.

Kessenbrock K, Plaks V, Werb Z. Matrix metalloproteinases: regulators of the tumor microenvironment. Cell. 2010 ed. 2010 Apr 2;141(1):52–67.

Kidd S, Spaeth E, Watson K, Burks J, Lu H, Klopp A, et al. Origins of the tumor microenvironment: quantitative assessment of adipose-derived and bone marrow-derived stroma. PLoS ONE. 2012;7(2):e30563.

Kitadai Y. Cancer-stromal cell interaction and tumor angiogenesis in gastric cancer. Cancer Microenviron. 2009 ed. 2010 Dec;3(1):109–16.

Kojima M, Higuchi Y, Yokota M, Ishii G, Saito N, Aoyagi K, et al. Human subperitoneal fibroblast and cancer cell interaction creates microenvironment that enhances tumor progression and metastasis. PLoS ONE. 2014 ed. 2014 Feb;9(2):e88018.

Kolomeyevskaya N, Eng KH, Khan ANH, Grzankowski KS, Singel KL, Moysich K, et al. Gynecologic Oncology. Gynecol Oncol. Elsevier Inc; 2015 Jun 3;:1–6.

Koppe MJ, Boerman OC, Oyen WJ, Bleichrodt RP. Peritoneal carcinomatosis of colorectal origin: incidence and current treatment strategies. Ann Surg. 2006 ed. 2006 Feb;243(2):212–22.

Ksiazek K. Mesothelial cell: a multifaceted model of aging. Ageing Res Rev. 2013 Mar;12(2):595–604.

Ksiazek K, Mikula-Pietrasik J, Catar R, Dworacki G, Winckiewicz M, Frydrychowicz M, et al. Oxidative stress-dependent increase in ICAM-1 expression promotes adhesion of colorectal and pancreatic cancers to the senescent peritoneal mesothelium. Int J Cancer. 2010 Jul 15;127(2):293–303.

Ksiazek K, Mikula-Pietrasik J, Korybalska K, Dworacki G, Jörres A, Witowski J. Senescent Peritoneal Mesothelial Cells Promote Ovarian Cancer Cell Adhesion. The American Journal of Pathology. 2009 Apr;174(4):1230–40.

Lane D, Matte I, Rancourt C, Piché A. Prognostic significance of IL-6 and IL-8 ascites levels in ovarian cancer patients. BMC Cancer. 2011;11:210.

Larriba MJ, de Herreros AG. Vitamin D and the Epithelial to Mesenchymal Transition. Stem Cells 2016.

Lazard D, Sastre X, Frid MG, Glukhova MA, Thiery J-P, Koteliansky VE. Expression of smooth muscle-specific proteins in myoepithelium and stromal myofibroblasts ofnormal and malignant human breast tissue. Proceedings of the National Academy of Sciences.

1993 Feb 1;90:999–1003.

Lee IK, Vansaun MN, Shim JH, Matrisian LM, Gorden DL. Increased metastases are associated with inflammation and matrix metalloproteinase-9 activity at incision sites in a murine model of peritoneal dissemination of colorectal cancer. J Surg Res. 2012 ed. 2013 Apr;180(2):252–9.

Lee MA, Park JH, Rhyu SY, Oh ST, Kang WK, Kim HN. Wnt3a expression is associated with MMP-9 expression in primary tumor and metastatic site in recurrent or stage IV colorectal cancer. BMC Cancer. 2014 ed. 2014;14:125.

Lengyel E. Ovarian Cancer Development and Metastasis. The American Journal of Pathology. 2010 Sep;177(3):1053–64.

Li Y, Wang J, Asahina K. Mesothelial cells give rise to hepatic stellate cells and myofibroblasts via mesothelial-mesenchymal transition in liver injury. Proc Natl Acad Sci USA. 2013 Feb 5;110(6):2324–9.

Li Y, Yang J, Dai C, Wu C, Liu Y. Role for integrin-linked kinase in mediating tubular epithelial to mesenchymal transition and renal interstitial fibrogenesis. J Clin Invest. 2003 Aug;112(4):503–16.

Li Z, Guo J, Xie K, Zheng S. Vitamin D receptor signaling and pancreatic cancer cell EMT. Curr Pharm Des. 2015;21(10):1262–7.

Liotta LA, Kohn EC. The microenvironment of the tumour-host interface. Nature. 2001st ed. 2001 May 17;411(6835):375–9.

Loureiro J, Aguilera A, Selgas R, Sandoval P, Albar-Vizcaino P, Pérez-Lozano ML, et al. Blocking TGF-β1 Protects the Peritoneal Membrane from Dialysate-Induced Damage. Journal of the American Society of Nephrology. 2011 Aug 31;22(9):1682–95.

Loureiro J, Sandoval P, del Peso G, González-Mateo G, Fernández-Millara V, Santamaria B, et al. Tamoxifen ameliorates peritoneal membrane damage by blocking mesothelial to mesenchymal transition in peritoneal dialysis. PLoS ONE. 2013 Apr;8(4):e61165.

Loureiro J, Schilte M, Aguilera A, Albar-Vizcaino P, Ramirez-Huesca M, Perez Lozano ML, et al. BMP-7 blocks mesenchymal conversion of mesothelial cells and prevents peritoneal damage induced by dialysis fluid exposure. Nephrology Dialysis Transplantation. 2010 Mar 26;25(4):1098–108.

López-Cabrera M. Mesenchymal Conversion of Mesothelial Cells Is a Key Event in the Pathophysiology of the Peritoneum during Peritoneal Dialysis. Advances in Medicine. 2014;2014:1–17.

Manenti L, Paganoni P, Floriani I, Landoni F, Torri V, Buda A, et al. Expression levels of vascular endothelial growth factor, matrix metalloproteinases 2 and 9 and tissue inhibitor of metalloproteinases 1 and 2 in the plasma of patients with ovarian carcinoma. Eur J Cancer. 2003 Sep;39(13):1948–56.

Margetts PJ, Bonniaud P. Basic mechanisms and clinical implications of peritoneal fibrosis. Perit Dial Int. 2004 ed. 2003 Nov-Dec;23(6):530–41.

Margetts PJ, Bonniaud P, Liu L, Hoff CM, Holmes CJ, West-Mays JA, et al. Transient overexpression of TGF-b1 induces epithelial mesenchymal transition in the rodent peritoneum. J Am Soc Nephrol. 2005 Feb;16(2):425–36.

Masoumi Moghaddam S, Amini A, Morris DL, Pourgholami MH. Significance of vascular endothelial growth factor in growth and peritoneal dissemination of ovarian cancer. Cancer Metastasis Rev. 2011 Nov 20;31(1-2):143–62.

Massagué J, Gomis RR. The logic of TGF β signaling. FEBS Letters. 2006 Apr 21;580(12):2811–20.

Masunaga Y, Muto S, Asakura S, Akimoto T, Homma S, Kusano E, et al. Ascites from patients with encapsulating peritoneal sclerosis augments NIH/3T3 fibroblast proliferation. Ther Apher Dial. 2003 Oct;7(5):486–93.

Mathot L, Stenninger J. Behavior of seeds and soil in the mechanism of metastasis: a deeper understanding. Cancer Sci. 2012 ed. 2012 Apr;103(4):626–31.

Matte I, Lane D, Bachvarov D, Rancourt C, Piche A. Role of malignant ascites on human mesothelial cells and their gene expression profiles. BMC Cancer. 2014 ed. 2014a Apr;14:288.

Matte I, Lane D, Laplante C, Garde-Granger P, Rancourt C, Piché A. Ovarian cancer ascites enhance the migration of patient-derived peritoneal mesothelial cells viacMet pathway through HGF-dependent and -independent mechanisms. Int J Cancer. 2014b Dec 18;137(2):289–98.

Matte I, Lane D, Laplante C, Rancourt C, Piché A. Profiling of cytokines in human epithelial ovarian cancer ascites. Am J Cancer Res. 2012;2(5):566–80.

Menczer J. Cox-2 expression in ovarian malignancies: a review of the clinical aspects. Eur J Obstet Gynecol Reprod Biol. 2009 Oct;146(2):129–32.

Mendoza M, Khanna C. Revisiting the seed and soil in cancer metastasis. Int J Biochem Cell Biol. 2009 ed. 2009 Jul;41(7):1452–62.

Miao Z-F, Zhao T-T, Wang Z-N, Miao F, Xu Y-Y, Mao X-Y, et al. Transforming growth factor-beta1 signaling blockade attenuates gastric cancer cell-induced peritoneal mesothelial cell fibrosis and alleviates peritoneal dissemination both in vitro and in vivo. Tumour Biol. 2013 Dec 18;35(4):3575–83.

Miao Z-F, Zhao T-T, Wang Z-N, Miao F, Xu Y-Y, Mao X-Y, et al. Tumor-associated mesothelial cells are negative prognostic factors in gastric cancer and promote peritoneal dissemination of adherent gastric cancer cells by chemotaxis. Tumour Biol [Internet]. 2014 Mar 11;35(6):6105–11.

Micke P, Ostman A. Exploring the tumour environment: cancer-associated fibroblasts as targets in cancer therapy. Expert Opin Ther Targets. 2005 Dec;9(6):1217–33.

Midgley RS, McConkey CC, Johnstone EC, Dunn JA, Smith JL, Grumett SA, et al. Phase III randomized trial assessing rofecoxib in the adjuvant setting of colorectal cancer: final results of the VICTOR trial. Journal of Clinical Oncology. 2010 Oct 20;28(30):4575–80.

Mikula-Pietrasik J, Sosinska P, Kucinska M, Murias M, Maksin K, Malinska A, et al. Peritoneal mesothelium promotes the progression of ovarian cancer cells in vitro and in a mice xenograft model in vivo. Cancer Lett. 2014 ed. 2014 Dec 28;355(2):310–5.

Milliken D, Scotton C, Raju S, Balkwill F, Wilson J. Analysis of chemokines and chemokine receptor expression in ovarian cancer ascites. Clin Cancer Res. 2002 Apr;8(4):1108–14.

Mitra AK, Sawada K, Tiwari P, Mui K, Gwin K, Lengyel E. Ligand-independent activation of c-Met by fibronectin and α(5)β(1)-integrin regulates ovarian cancer invasion and metastasis. Oncogene. 2011 Mar 31;30(13):1566–76.

Mizutani K, Kofuji K, Shirouzu K. The significance of MMP-1 and MMP-2 in peritoneal disseminated metastasis of gastric cancer. Surg Today. Springer-Verlag; 2000 Jul;30(7):614–21.

Montori G, Coccolini F, Ceresoli M, Catena F, Colaianni N, Poletti E, et al. The treatment of peritoneal carcinomatosis in advanced gastric cancer: state of the art. Int J Surg Oncol. 2014 Feb;2014:1–7.

Moradi MM, Carson LF, Twiggs LB, Weinberg JB, Haney AF, Ramakrishnan S. Serum and ascitic fluid levels of interleukin-1, interleukin-6, and tumor necrosis factor-alpha in patients with ovarian epithelial cancer. Cancer. 1993 Oct 15;72(8):2433–40.

Mulder K, Scarfe A, Chua N, Spratlin J. The role of bevacizumab in colorectal cancer: understanding its benefits and limitations. Expert Opin Biol Ther. 2011 ed. 2011 Mar;11(3):405–13.

Mustea A, Könsgen D, Braicu EI, Pirvulescu C, Sun P, Sofroni D, et al. Expression of IL-10 in patients with ovarian carcinoma. Anticancer Res. 2006 Mar;26(2C):1715–8.

Na D, Lv ZD, Liu FN, Xu Y, Jiang CG, Sun Z, et al. Transforming growth factor beta1 produced in autocrine/paracrine manner affects the morphology and function of mesothelial cells and promotes peritoneal carcinomatosis. Int J Mol Med. 2010 ed. 2010 Sep;26(3):325–32.

Nakamura M, Ono YJ, Kanemura M, Tanaka T, Hayashi M, Terai Y, et al. Hepatocyte growth factor secreted by ovarian cancer cells stimulates peritoneal implantation via the mesothelial–mesenchymal transition of the peritoneum. Gynecol Oncol. Elsevier B.V; 2015 Sep 3;:[Epubaheadofprint].

Nash MA, Lenzi R, Edwards CL, Kavanagh JJ, Kudelka AP, Verschraegen CF, et al. Differential expression of cytokine transcripts in human epithelial ovarian carcinoma by solid tumour specimens, peritoneal exudate cells containing tumour, tumour-infiltrating lymphocyte (TIL)-derived T cell lines and established tumour cell lines. Clin Exp Immunol. 1998 ed. 1998 May;112(2):172–80.

Nessim SJ, Perl J, Bargman JM. Kidney International - Abstract of article: The renin-angiotensin-aldosterone system in peritoneal dialysis: is what is good for the kidney also good for the peritoneum[quest]. Kidney Int. 2010.

Offner FA, Obrist P, Stadlmann S, Feichtinger H, Klingler P, Herold M, et al. IL-6 secretion by human peritoneal mesothelial and ovarian cancer cells. Cytokine. 1995 Aug;7(6):542–7.

Ono YJ, Hayashi M, Tanabe A, Hayashi A, Kanemura M, Terai Y, et al. Estradiol-mediated hepatocyte growth factor is involved in the implantation of endometriotic cells via the mesothelial-to-mesenchymal transition in the peritoneum. Am J Physiol Endocrinol Metab. 2015 Jun 1;308(11):E950–9.

Otsuka G, Agah R, Frutkin AD, Wight TN, Dichek DA. Transforming growth factor beta 1 induces neointima formation through plasminogen activator inhibitor-1-dependent pathways. Arterioscler Thromb Vasc Biol. 2006 Apr;26(4):737–43.

Parsons SL, Lang MW, Steele RJ. Malignant ascites: a 2-year review from a teaching hospital. Eur J Surg Oncol. 1996 Jun 1;22(3):237–9.

Paulsson J, Micke P. Prognostic relevance of cancer-associated fibroblasts in human cancer. Semin Cancer Biol. 2014 ed. 2014 Apr;25:61–8.

Peng P, Yan Y, Keng S. Exosomes in the ascites of ovarian cancer patients: origin and effects on anti-tumor immunity. Oncol Rep. 2011 Mar;25(3):749–62.

Perren TJ, Swart AM, Pfisterer J, Ledermann JA, Pujade-Lauraine E, Kristensen G, et al. A phase 3 trial of bevacizumab in ovarian cancer. N Engl J Med. 2011 ed. 2011 Dec 29;365(26):2484–96.

Pervin S, Hewison M, Braga M, Tran L, Chun R, Karam A, et al. Down-regulation of vitamin D receptor in mammospheres: implications for vitamin D resistance in breast cancer and potential for combination therapy. PLoS ONE. 2013;8(1):e53287.

Pérez-Lozano ML, Sandoval P, Rynne-Vidal A, Aguilera A, Jiménez-Heffernan JA, Albar-Vizcaíno P, et al. Functional relevance of the switch of VEGF receptors/co-receptors during peritoneal dialysis-induced mesothelial to mesenchymal transition. PLoS ONE. 2013 Apr;8(4):e60776.

Polanska UM, Orimo A. Carcinoma-associated fibroblasts: Non-neoplastic tumour-promoting mesenchymal cells. J Cell Physiol [Internet]. 2013 Apr 18;228(8):1651–7. Available from: http://onlinelibrary.wiley.com/doi/10.1002/jcp.24347/pdf

Potenta S, Zeisberg E, Kalluri R. The role of endothelial-to-mesenchymal transition in cancer progression. Br J Cancer. 2008 ed. 2008 Nov 4;99(9):1375–9.

Radisky DC, Kenny PA, Bissell MJ. Fibrosis and cancer: do myofibroblasts come also from epithelial cells via EMT? J Cell Biochem. 2007 Jul 1;101(4):830–9.

Radjabi AR, Sawada K, Jagadeeswaran S, Eichbichler A, Kenny HA, Montag A, et al. Thrombin induces tumor invasion through the induction and association of matrix metalloproteinase-9 and beta1-integrin on the cell surface. J Biol Chem. 2008 Feb 1;283(5):2822–34.

Ranieri D, Raffa S, Parente A, Rossi Del Monte S, Ziparo V, Torrisi MR. High adhesion of tumor cells to mesothelial monolayers derived from peritoneal wash of disseminated gastrointestinal cancers. PLoS ONE. 2013;8(2):e57659.

Razani B, Zhang XL, Bitzer M, Gersdorff von G, Böttinger EP, Lisanti MP. Caveolin-1 regulates transforming growth factor (TGF)-beta/SMAD signaling through an interaction with the TGF-beta type I receptor. J Biol Chem. 2001 Mar 2;276(9):6727–38.

Ren J, Xiao Y-J, Singh LS, Zhao X, Zhao Z, Feng L, et al. Lysophosphatidic acid is constitutively produced by human peritoneal mesothelial cells and enhances adhesion, migration, and invasion of ovarian cancer cells. Cancer Res. 2006 Mar 15;66(6):3006–14.

Rizzo MT. Cyclooxygenase-2 in oncogenesis. Clinica Chimica Acta. 2011 Apr;412(9-10):671–87.

Roberts AB, Tian F, Byfield SD, Stuelten C, Ooshima A, Saika S, et al. Smad3 is key to TGF-β-mediated epithelial-to-mesenchymal transition, fibrosis, tumor suppression and metastasis. Cytokine Growth Factor Rev. 2006 Feb;17(1-2):19–27.

Ruiz-Villalba A, Simón AM, Pogontke C, Castillo MI, Abizanda G, Pelacho B, et al. Interacting resident epicardium-derived fibroblasts and recruited bone marrow cells form myocardial infarction scar. J Am Coll Cardiol. 2015 May 19;65(19):2057–66.

Rump A, Morikawa Y, Tanaka M, Minami S, Umesaki N, Takeuchi M, et al. Binding of ovarian cancer antigen CA125/MUC16 to mesothelin mediates cell adhesion. J Biol Chem. 2003rd ed. 2004 Mar 5;279(10):9190–8.

Sako A, Kitayama J, Koyama H, Ueno H, Uchida H, Hamada H, et al. Transduction of soluble Flt-1 gene to peritoneal mesothelial cells can effectively suppress peritoneal metastasis of gastric cancer. Cancer Res. 2004 ed. 2004 May 15;64(10):3624–8.

Sako A, Kitayama J, Yamaguchi H, Kaisaki S, Suzuki H, Fukatsu K, et al. Vascular endothelial growth factor synthesis by human omental mesothelial cells is augmented by fibroblast growth factor-2: possible role of mesothelial cell on the development of peritoneal metastasis. J Surg Res. 2003rd ed. 2003 Nov;115(1):113–20.

Sandoval P, Jiménez-Heffernan JA, Guerra-Azcona G, Pérez-Lozano ML, Rynne-Vidal A, Albar-Vizcaíno P, et al. Mesothelial-to-mesenchymal transition in the pathogenesis of post-surgical peritoneal adhesions. J Pathol. 2016 Jan;:epubaheadofprint.

Sandoval P, Loureiro J, González-Mateo G, Pérez-Lozano ML, Maldonado-Rodríguez A, Sánchez-Tomero JA, et al. PPAR-γ agonist rosiglitazone protects peritoneal membrane from dialysis fluid-induced damage. Laboratory Investigation. 2010 Oct;90(10):1517–32.

Santin AD, Bellone S, Ravaggi A, Roman J, Smith CV, Pecorelli S, et al. Increased levels of interleukin-10 and transforming growth factor-beta in the plasma and ascitic fluid of patients with advanced ovarian cancer. BJOG: An Internal Journal of Obs Gyn. 2001 Aug;108(8):804–8.

Satoyoshi R, Aiba N, Yanagihara K, Yashiro M, Tanaka M. Tks5 activation in mesothelial cells creates invasion front of peritoneal carcinomatosis. Oncogene. 2015a Jun 11;34(24):3176–87.

Satoyoshi R, Kuriyama S, Aiba N, Yashiro M, Tanaka M. Asporin activates coordinated invasion of scirrhous gastric cancer and cancer-associated fibroblasts. Oncogene. 2014 ed. 2015b Jan 29;34(5):650–60.

Sawada K, Mitra AK, Radjabi AR, Bhaskar V, Kistner EO, Tretiakova M, et al. Loss of E-cadherin promotes ovarian cancer metastasis via alpha 5-integrin, which is a therapeutic target. Cancer Res. 2008 Apr 1;68(7):2329–39.

Schropfer A, Kammerer U, Kapp M, Dietl J, Feix S, Anacker J. Expression pattern of matrix metalloproteinases in human gynecological cancer cell lines. BMC Cancer. 2010 ed. 2010;10:553.

Selcuklu SD, Donoghue MTA, Spillane C. miR-21 as a key regulator of oncogenic processes. Biochem Soc Trans. 2009 Aug;37(4):918–25.

Serkies K, Sinacki M, Jassem J. The role of hormonal factors and endocrine therapy in ovarian cancer. Contemp Oncol (Pozn). 2013 Mar;17(1):14–9.

Sheid B. Angiogenic effects of macrophages isolated from ascitic fluid aspirated from women with advanced ovarian cancer. Cancer Letters. 1992 Feb 28;62(2):153–8.

Shi Y, Massagué J. Mechanisms of TGF-beta signaling from cell membrane to the nucleus. Cell. 2003 Jun 13;113(6):685–700.

Shimoda M, Mellody KT, Orimo A. Carcinoma-associated fibroblasts are a rate-limiting determinant for tumour progression. Seminars in Cell & Developmental Biology. 2010 Feb;21(1):19–25.

Siegel RL, Miller KD, Jemal A. Cancer statistics, 2016. CA Cancer J Clin. 2016 Jan;66(1):7–30.

Slack-Davis JK, Atkins KA, Harrer C, Hershey ED, Conaway M. Vascular Cell Adhesion Molecule-1 Is a Regulator of Ovarian Cancer Peritoneal Metastasis. Cancer Res. 2009 Feb 3;69(4):1469–76.

Sodek KL, Murphy KJ, Brown TJ, Ringuette MJ. Cell–cell and cell–matrix dynamics in intraperitoneal cancer metastasis. Cancer Metastasis Rev. 2012 Apr 13;31(1-2):397–414.

Sohaib SA, Houghton SL, Meroni R, Rockall AG, Blake P, Reznek RH. Recurrent endometrial cancer: patterns of recurrent disease and assessment of prognosis. Clin Radiol. 2007 Jan;62(1):28–34.

Solomon SD, Pfeffer MA, McMurray JJV, Fowler R, Finn P, Levin B, et al. Effect of celecoxib on cardiovascular events and blood pressure in two trials for the prevention of colorectal adenomas. Circulation. 2006 Sep 5;114(10):1028–35.

Sowter HM, Corps AN, Smith SK. Hepatocyte growth factor (HGF) in ovarian epithelial tumour fluids stimulates the migration of ovarian carcinoma cells. Int J Cancer. 1999 Nov 12;83(4):476–80.

Stadlmann S, Amberger A, Pollheimer J, Gastl G, Offner FA, Margreiter R, et al. Ovarian carcinoma cells and IL-1beta-activated human peritoneal mesothelial cells are possible sources of vascular endothelial growth factor in inflammatory and malignant peritoneal effusions. Gynecol Oncol. 2005 Jun;97(3):784–9.

Strippoli R, Benedicto I, Foronda M, Pérez-Lozano ML, Sánchez-Perales S, López-Cabrera M, et al. p38 maintains E-cadherin expression by modulating TAK1-NF-kappa B during epithelial-to-mesenchymal transition. J Cell Sci. 2010 Dec 15;123(Pt 24):4321–31.

Strippoli R, Benedicto I, Lozano MLP, Cerezo A, López-Cabrera M, del Pozo MA. Epithelial-to-mesenchymal transition of peritoneal mesothelial cells is regulated by an ERK/NF-κ

B/Snail1 pathway. Dis Model Mech. 2008 Dec;1(4-5):264–74.

Strippoli R, Benedicto I, Pérez-Lozano ML, Pellinen T, Sandoval P, López-Cabrera M, et al. Inhibition of transforming growth factor-activated kinase 1 (TAK1) blocks and reverses epithelial to mesenchymal transition of mesothelial cells. PLoS ONE. 2012 Feb;7(2):e31492.

Strippoli R, Loureiro J, Moreno V, Benedicto I, Perez Lozano ML, Barreiro O, et al. Caveolin-1 deficiency induces a MEK-ERK1/2-Snail-1-dependent epithelial-mesenchymal transition and fibrosis during peritoneal dialysis. EMBO Molecular Medicine. 2015 Jan 5;7(1):102–23.

Strutz F, Okada H, Lo CW, Danoff T, Carone RL, Tomaszewski JE, et al. Identification and characterization of a fibroblast marker: FSP1. J Cell Biol. 1995 ed. 1995 Jul;130(2):393–405.

Taddei ML, Giannoni E, Comito G, Chiarugi P. Microenvironment and tumor cell plasticity: an easy way out. Cancer Lett. 2013 ed. 2013 Nov 28;341(1):80–96.

Takatsuki H, Komatsu S, Sano R, Takada Y, Tsuji T. Adhesion of gastric carcinoma cells to peritoneum mediated by alpha3beta1 integrin (VLA-3). Cancer Res. 2004 Sep 1;64(17):6065–70.

Tan DS, Agarwal R, Kaye SB. Mechanisms of transcoelomic metastasis in ovarian cancer. Lancet Oncol. 2006 ed. 2006 Nov;7(11):925–34.

Théry C, Zitvogel L, Amigorena S. Exosomes: composition, biogenesis and function. Nature Reviews Immunology. 2002 Aug;2(8):569–79.

Thibault B, Castells M, Delord JP, Couderc B. Ovarian cancer microenvironment: implications for cancer dissemination and chemoresistance acquisition. Cancer Metastasis Rev. 2013 ed. 2014 Mar;33(1):17–39.

Tokuhisa M, Ichikawa Y, Kosaka N, Ochiya T, Yashiro M, Hirakawa K, et al. Exosomal miRNAs from Peritoneum Lavage Fluid as Potential Prognostic Biomarkers of Peritoneal Metastasis in Gastric Cancer. PLoS ONE. 2015;10(7):e0130472.

Tsujimoto H, Takhashi T, Hagiwara A, Shimotsuma M, Sakakura C, Osaki K, et al. Site-specific implantation in the milky spots of malignant cells in peritoneal dissemination: immunohistochemical observation in mice inoculated intraperitoneally with bromodeoxyuridine-labelled cells. Br J Cancer. 1995 Mar;71(3):468–72.

Tsukada T, Fushida S, Harada S, Yagi Y, Kinoshita J, Oyama K, et al. The role of human peritoneal mesothelial cells in the fibrosis and progression of gastric cancer. Int J Oncol. 2012 May 18;41(2):476–82.

Vaksman O, Trope C, Davidson B, Reich R. Exosome-derived miRNAs and ovarian carcinoma progression. Carcinogenesis. 2014 Aug 27;35(9):2113–20.

Valcourt U, Kowanetz M, Niimi H, Heldin C-H, Moustakas A. TGF-β and the Smad Signaling Pathway Support Transcriptomic Reprogramming During Epithelial-Mesenchymal Cell Transition. Mol Biol Cell. 2005 Apr;16(4):1987–2002.

Vargha R, Endemann M, Kratochwill K, Riesenhuber A, Wick N, Krachler A-M, et al. Ex vivo reversal of in vivo transdifferentiation in mesothelial cells grown from peritoneal dialysate effluents. Nephrol Dial Transplant. 2006 Oct;21(10):2943–7.

Vi L, de Lasa C, DiGuglielmo GM, Dagnino L. Integrin-Linked Kinase Is Required for TGF-β 1 Induction of Dermal Myofibroblast Differentiation. J Investig Dermatol. Nature Publishing Group; 2010 Dec 9;131(3):586–93.

Wagner BJ, Lob S, Lindau D, Horzer H, Guckel B, Klein G, et al. Simvastatin reduces tumor cell adhesion to human peritoneal mesothelial cells by decreased expression of VCAM-1 and beta1 integrin. Int J Oncol. 2011 ed. 2011 Dec;39(6):1593–600.

Wakefield LM, Roberts AB. TGF-beta signaling: positive and negative effects on tumorigenesis. Curr Opin Genet Dev. 2002 Feb;12(1):22–9.

Wang X, Nie J, Jia Z, Feng M, Zheng Z, Chen W, et al. Impaired TGF-β signalling enhances peritoneal inflammation induced by E. coli in rats. Nephrology Dialysis Transplantation. 2010 Feb;25(2):399–412.

Watanabe T, Hashimoto T, Sugino T, Soeda S, Nishiyama H, Morimura Y, et al. Production of IL1-beta by ovarian cancer cells induces mesothelial cell beta1-integrin expression facilitating peritoneal dissemination. J Ovarian Res. 2012 Feb;5(1):7.

Wels J, Kaplan RN, Rafii S, Lyden D. Migratory neighbors and distant invaders: tumor-associated niche cells. Genes & Development. 2008 ed. 2008 Mar 1;22(5):559–74.

Wikberg ML, Edin S, Lundberg IV, Van Guelpen B, Dahlin AM, Rutegard J, et al. High intratumoral expression of fibroblast activation protein (FAP) in colon cancer is associated with poorer patient prognosis. Tumour Biol. 2013 ed. 2013 Apr;34(2):1013–20.

Winiarski BK, Cope N, Alexander M, Pilling LC, Warren S, Acheson N, et al. Clinical Relevance of Increased Endothelial and Mesothelial Expression of Proangiogenic Proteases and VEGFA in the Omentum of Patients with Metastatic Ovarian High-Grade Serous Carcinoma. Transl Oncol. 2014 Apr;7(2):267–276.e4.

Wu QJ, Gong CY, Luo ST, Zhang DM, Zhang S, Shi HS, et al. AAV-mediated human PEDF inhibits tumor growth and metastasis in murine colorectal peritoneal carcinomatosis model. BMC Cancer. 2012 ed. 2012 Mar;12:129.

Yamamura S, Matsumura N, Mandai M, Huang Z, Oura T, Baba T, et al. The activated transforming growth factor-beta signaling pathway in peritoneal metastases is a potential therapeutic target in ovarian cancer. Int J Cancer. 2011 Apr 18;130(1):20–8.

Yanez-Mo M, Lara-Pezzi E, Selgas R, Ramirez-Huesca M, Dominguez-Jimenez C, Jimenez-Heffernan JA, et al. Peritoneal dialysis and epithelial-to-mesenchymal transition of mesothelial cells. N Engl J Med. 2003rd ed. 2003 Jan 30;348(5):403–13.

Yeh Y-C, Wei W-C, Wang Y-K, Lin S-C, Sung J-M, Tang M-J. Transforming growth factor-β 1 induces Smad3-dependent β 1 integrin gene expression in epithelial-to-mesenchymal transition during chronic tubulointerstitial fibrosis. Am J Pathol. 2010 Oct;177(4):1743–54.

Yokoyama Y, Sedgewick G, Ramakrishnan S. Endostatin binding to ovarian cancer cells inhibits peritoneal attachment and dissemination. Cancer Res. 2007 Nov 15;67(22):10813–

22.

Yoshimura A, Wakabayashi Y, Mori T. Cellular and molecular basis for the regulation of inflammation by TGF-beta. J Biochem. 2010 ed. 2010 Jun;147(6):781–92.

Yu G, Tang B, Yu PW, Peng ZH, Qian F, Sun G. Systemic and peritoneal inflammatory response after laparoscopic-assisted gastrectomy and the effect of inflammatory cytokines on adhesion of gastric cancer cells to peritoneal mesothelial cells. Surg Endosc. 2010 ed. 2010 Nov;24(11):2860–70.

Yu Q, Stamenkovic I. Cell surface-localized matrix metalloproteinase-9 proteolytically activates TGF-β and promotes tumor invasion and angiogenesis. Genes & Development. 2000 Jan 15;14(2):163–76.

Zeisberg EM, Potenta SE, Sugimoto H, Zeisberg M, Kalluri R. Fibroblasts in kidney fibrosis emerge via endothelial-to-mesenchymal transition. Journal of the American Society of Nephrology. 2008 ed. 2008 Dec;19(12):2282–7.

Zhong Y-C, Zhang T, Di W, Li W-P. Thrombin promotes epithelial ovarian cancer cell invasion by inducing epithelial-mesenchymal transition. J Gynecol Oncol. 2013 Jul;24(3):265–72.

Zhu Z, Yao J, Wang F, Xu Q. TNF-alpha and the phenotypic transformation of human peritoneal mesothelial cell. Chin Med J. 2002 Apr;115(4):513–7.

Ziprin P, Ridgway PF, Pfistermuller KL, Peck DH, Darzi AW. ICAM-1 mediated tumor-mesothelial cell adhesion is modulated by IL-6 and TNF-alpha: a potential mechanism by which surgical trauma increases peritoneal metastases. Cell Commun Adhes. 2003rd ed. 2003 May-Jun;10(3):141–54.

ANNEX I

Table 1. Top 100 downregulated genes in AFMCs compared to HPMCs.

Symbol	Gene name	Log Ratio	p-value
CYP17A1	Cytochrome P450, family 17, subfamily A, polypeptide 1	-11.305	1.65E-02
SEL1L2	Sel-1 suppressor of lin-12-like 2 (C. Elegans)	-8.976	5.00E-05
SLC30A2	Solute carrier family 30 (zinc transporter), member 2	-8.666	2.02E-02
LRP2	Low density lipoprotein receptor-related protein 2	-7.847	1.50E-04
OVCH2	Ovochymase 2 (gene/pseudogene)	-7.681	5.00E-05
SMTNL2	Smoothelin-like 2	-7.581	9.50E-04
NPHS1	Nephrosis 1, congenital, Finnish type (nephrin)	-7.570	5.00E-05
SPANXN1	SPANX family, member N1	-7.432	1.00E-03
MT1G	Metallothionein 1G	-7.298	5.00E-05
CAPN6	Calpain 6	-7.162	1.00E-04
ITM2A	Integral membrane protein 2A	-7.072	5.00E-05
KCNB1	Potassium channel, voltage gated Shab related subfamily B, member 1	-6.979	5.00E-05
RGS7BP	Regulator of G-protein signalling 7 binding protein	-6.924	5.00E-05
UPK3B	Uroplakin 3B	-6.760	5.00E-05
ITLN1	Intelectin 1 (galactofuranose binding)	-6.675	3.50E-04
SPANXC	SPANX family, member C	-6.644	3.17E-02
VIPR2	Vasoactive intestinal peptide receptor 2	-6.546	5.00E-05
CPB1	Carboxypeptidase B1 (tissue)	-6.525	5.00E-05
SEPP1	Selenoprotein P, plasma, 1	-6.443	5.00E-05
KLK5	Kallikrein-related peptidase 5	-6.367	2.00E-04
MYCN	V-myc avian myelocytomatosis viral oncogene neuroblastoma derived homolog	-6.338	1.00E00
ITIH3	Inter-alpha-trypsin inhibitor heavy chain 3	-6.329	7.50E-04

HBE1	Hemoglobin, epsilon 1	-6.295	5.00E-05
MT1H	Metallothionein 1H	-6.096	3.75E-03
OR51B4	Olfactory receptor, family 51, subfamily B, member 4	-6.077	2.60E-02
MYOZ2	Myozenin 2	-5.648	5.00E-05
KLK7	Kallikrein-related peptidase 7	-5.594	2.00E-04
KLHL31	Kelch-like family member 31	-5.564	5.00E-05
MTUS2	Microtubule associated tumor suppressor candidate 2	-5.505	5.00E-05
CLIC5	Chloride intracellular channel 5	-5.498	5.00E-05
MYL7	Myosin, light chain 7, regulatory	-5.478	1.15E-03
SYNPO2L	Synaptopodin 2-like	-5.403	5.00E-05
SLC27A2	Solute carrier family 27 (fatty acid transporter), member 2	-5.337	5.00E-05
RGS5	Regulator of G-protein signalling 5	-5.321	5.00E-05
KCNA4	Potassium channel, voltage gated shaker related subfamily A, member 4	-5.314	5.00E-05
IGFL2	IGF-like family member 2	-5.235	5.00E-05
FGF9	Fibroblast growth factor 9	-5.220	1.90E-03
NPR3	Natriuretic peptide receptor 3	-5.202	5.00E-05
FLT3	Fms-related tyrosine kinase 3	-5.178	1.00E00
ILDR2	Immunoglobulin-like domain containing receptor 2	-5.172	5.00E-05
SFTPD	Surfactant protein D	-5.172	5.00E-05
SERTM1	Serine-rich and transmembrane domain containing 1	-5.155	5.00E-05
SERPINE3	Serpin peptidase inhibitor, clade E (nexin, plasminogen activator inhibitor type 1), member 3	-5.116	5.00E-05
HPD	4-hydroxyphenylpyruvate dioxygenase	-5.061	5.00E-05
MRVI1	Murine retrovirus integration site 1 homolog	-5.050	5.00E-05

CLSTN2	Calsyntenin 2	-5.047	5.00E-05
THBD	Thrombomodulin	-5.038	5.00E-05
TUBB4A	Tubulin, beta 4A class iva	-5.010	5.00E-05
PRG4	Proteoglycan 4	-4.970	4.50E-04
IGFL3	IGF-like family member 3	-4.958	1.20E-03
SBK2	SH3 domain binding kinase family, member 2	-4.917	9.70E-03
CGN	Cingulin	-4.891	5.00E-05
WNT2B	Wingless-type MMTV integration site family, member 2B	-4.889	5.00E-05
HBD	Hemoglobin, delta	-4.884	2.99E-02
SMPD3	Sphingomyelin phosphodiesterase 3, neutral membrane (neutral sphingomyelinase II)	-4.841	5.00E-05
HSD3B1	Hydroxy-delta-5-steroid dehydrogenase, 3 beta- and steroid delta-isomerase 1	-4.840	6.50E-03
CNGB1	Cyclic nucleotide gated channel beta 1	-4.838	5.00E-05
ERICH5	Glutamate-rich 5	-4.832	5.00E-05
KLK11	Kallikrein-related peptidase 11	-4.809	5.00E-05
ALOX15	Arachidonate 15-lipoxygenase	-4.798	1.35E-01
NOX1	NADPH oxidase 1	-4.792	5.00E-05
PTPRZ1	Protein tyrosine phosphatase, receptor-type, Z polypeptide 1	-4.787	5.00E-05
ZFP42	ZFP42 zinc finger protein	-4.783	5.00E-04
RSPO1	R-spondin 1	-4.770	5.00E-04
GKN1	Gastrokine 1	-4.754	9.50E-04
PODXL	Podocalyxin-like	-4.752	5.00E-05
LAMB4	Laminin, beta 4	-4.743	5.50E-04
ANKRD2	Ankyrin repeat domain 2 (stretch responsive muscle)	-4.704	5.00E-05

MYOZ1	Myozenin 1	-4.692	2.15E-03
MGAT4C	MGAT4 family, member C	-4.606	5.00E-05
PIP5K1B	Phosphatidylinositol-4-phosphate 5-kinase, type I, beta	-4.593	5.00E-05
NRK	Nik related kinase	-4.578	5.00E-05
MAOB	Monoamine oxidase B	-4.569	5.00E-05
ENPP1	Ectonucleotide pyrophosphatase/phosphodiesterase 1	-4.565	5.00E-05
CST6	Cystatin E/M	-4.536	5.00E-05
CNTN5	Contactin 5	-4.515	5.00E-05
MUC19	Mucin 19, oligomeric	-4.461	6.75E-03
CD244	CD244 molecule, natural killer cell receptor 2B4	-4.455	4.50E-04
CTNNA2	Catenin (cadherin-associated protein), alpha 2	-4.453	5.00E-05
CPA4	Carboxypeptidase A4	-4.410	5.00E-05
HOGA1	4-hydroxy-2-oxoglutarate aldolase 1	-4.407	5.00E-05
CLDN15	Claudin 15	-4.386	5.00E-05
ITGA7	Integrin, alpha 7	-4.386	5.00E-05
KCNK2	Potassium channel, two pore domain subfamily K, member 2	-4.379	5.00E-05
SBSPON	Somatomedin B and thrombospondin, type 1 domain containing	-4.350	5.00E-05
PKHD1L1	Polycystic kidney and hepatic disease 1 (autosomal recessive)-like 1	-4.317	5.00E-05
MT1F	Metallothionein 1F	-4.300	5.00E-05
VTN	Vitronectin	-4.268	5.00E-05
CALB2	Calbindin 2	-4.266	5.00E-05
CYP24A1	Cytochrome P450, family 24, subfamily A, polypeptide 1	-4.263	8.50E-04
PSG9	Pregnancy specific beta-1-glycoprotein 9	-4.223	5.00E-05

SLPI	Secretory leukocyte peptidase inhibitor	-4.212	5.00E-05
REEP1	Receptor accessory protein 1	-4.200	5.00E-05
ISM2	Isthmin 2	-4.175	5.00E-05
HHIP	Hedgehog interacting protein	-4.124	5.00E-05
RAB17	RAB17, member RAS oncogene family	-4.120	5.00E-05
RAET1E	Retinoic acid early transcript 1E	-4.110	5.00E-05
EXTL1	Exostosin-like glycosyltransferase 1	-4.092	1.05E-03
FRY	Furry homolog (Drosophila)	-4.069	5.00E-05
DLGAP2	Discs, large (Drosophila) homolog-associated protein 2	-4.055	5.00E-05

Table 2. Top 100 upregulated genes in AFMCs compared to HPMCs.

Symbol	Gene name	Log Ratio	p-value
MMP1	Matrix metallopeptidase 1	12.37	1.03E-01
SIGLEC1	Sialic acid binding Ig-like lectin 1, sialoadhesin	11.12	2.51E-01
MMP3	Matrix metallopeptidase 3	10.30	7.00E-03
HAMP	Hepcidin antimicrobial peptide	10.20	2.45E-01
HK3	Hexokinase 3 (white cell)	9.67	5.00E-05
KLHDC7B	Kelch domain containing 7B	9.63	2.75E-03
EHF	Ets homologous factor	9.60	2.29E-01
CSF3	Colony stimulating factor 3 (granulocyte)	9.41	3.40E-02
ESM1	Endothelial cell-specific molecule 1	9.30	1.65E-03
FPR3	Formyl peptide receptor 3	9.27	7.50E-04
CCL4L1/CCL4L2	Chemokine (C-C motif) ligand 4-like 1	8.97	5.00E-05
EGR3	Early growth response 3	8.94	1.00E-04
STAB1	Stabilin 1	8.90	5.00E-05
TREM1	Triggering receptor expressed on myeloid cells 1	8.89	1.34E-02
NGEF	Neuronal guanine nucleotide exchange factor	8.77	5.00E-05
NDUFA4L2	NADH dehydrogenase (ubiquinone) 1 alpha subcomplex, 4-like 2	8.74	5.00E-05
SERPINA3	Serpin peptidase inhibitor, clade A (alpha-1 antiproteinase, antitrypsin), member 3	8.70	4.11E-02
SPP1	Secreted phosphoprotein 1	8.64	9.50E-04
CXCL8	Chemokine (C-X-C motif) ligand 8	8.57	5.00E-05
TNFAIP6	Tumor necrosis factor, alpha-induced protein 6	8.56	8.00E-04
IL33	Interleukin 33	8.51	5.00E-05
PTPN22	Protein tyrosine phosphatase, non-receptor type 22 (lymphoid)	8.46	5.00E-05

MME	Membrane metallo-endopeptidase	8.45	5.00E-05
IFI44L	Interferon-induced protein 44-like	8.25	5.00E-05
G0S2	G0/G1 switch 2	8.20	5.10E-03
CXCL3	Chemokine (C-X-C motif) ligand 3	8.10	1.10E-03
IL1B	Interleukin 1, beta	8.09	5.00E-05
NTM	Neurotrimin	8.08	5.45E-03
WNT7A	Wingless-type MMTV integration site family, member 7A	8.06	1.00E+00
SPI1	Spi-1 proto-oncogene	8.04	8.82E-02
SLC11A1	Solute carrier family 11 (proton-coupled divalent metal ion transporter), member 1	8.02	9.50E-04
HSD11B1	Hydroxysteroid (11-beta) dehydrogenase 1	8.01	5.00E-05
TNF	Tumor necrosis factor	7.97	4.50E-04
LILRB2	Leukocyte immunoglobulin-like receptor, subfamily B (with TM and ITIM domains), member 2	7.92	5.00E-05
TSLP	Thymic stromal lymphopoietin	7.92	2.00E-04
MMP9	Matrix metallopeptidase 9	7.91	1.80E-03
CSF2	Colony stimulating factor 2 (granulocyte-macrophage)	7.90	1.18E-02
PTX3	Pentraxin 3, long	7.82	5.00E-05
MSR1	Macrophage scavenger receptor 1	7.78	9.59E-02
TREM2	Triggering receptor expressed on myeloid cells 2	7.71	2.42E-01
HSPA7	Heat shock 70kda protein 7 (HSP70B)	7.61	1.37E-02
KMO	Kynurenine 3-monooxygenase (kynurenine 3-hydroxylase)	7.61	5.00E-05
LILRA6	Leukocyte immunoglobulin-like receptor, subfamily A (with TM domain), member 6	7.59	5.40E-03
LYZ	Lysozyme	7.59	5.00E-05
CLEC7A	C-type lectin domain family 7, member A	7.56	5.60E-03

CXCL1	Chemokine (C-X-C motif) ligand 1 (melanoma growth stimulating activity, alpha)	7.39	5.00E-05
LILRB4	Leukocyte immunoglobulin-like receptor, subfamily B (with TM and ITIM domains), member 4	7.33	2.31E-01
GPR183	G protein-coupled receptor 183	7.31	4.84E-02
GNA15	Guanine nucleotide binding protein (G protein), alpha 15 (Gq class)	7.27	1.00E+00
KYNU	Kynureninase	7.26	5.00E-05
LILRB5	Leukocyte immunoglobulin-like receptor, subfamily B (with TM and ITIM domains), member 5	7.25	8.40E-03
FOLR1	Folate receptor 1 (adult)	7.21	2.39E-01
MMP7	Matrix metallopeptidase 7	7.20	1.40E-01
PTGER2	Prostaglandin E receptor 2 (subtype EP2), 53kda	7.20	1.00E+00
PTPRC	Protein tyrosine phosphatase, receptor type, C	7.19	6.45E-03
COL6A3	Collagen, type VI, alpha 3	7.09	5.00E-05
CCL3L3	Chemokine (C-C motif) ligand 3-like 3	7.05	5.00E-05
TNFRSF6B	Tumor necrosis factor receptor superfamily, member 6b, decoy	7.03	1.00E+00
RSAD2	Radical S-adenosyl methionine domain containing 2	7.01	5.00E-05
SYK	Spleen tyrosine kinase	6.95	6.09E-02
GLI1	GLI family zinc finger 1	6.90	6.00E-04
CXCL2	Chemokine (C-X-C motif) ligand 2	6.86	5.00E-05
FCGR3A/FCGR3B	Fc fragment of igg, low affinity iiia, receptor (CD16a)	6.82	1.00E+00
CXCR4	Chemokine (C-X-C motif) receptor 4	6.75	2.19E-01
ABCB4	ATP-binding cassette, sub-family B (MDR/TAP), member 4	6.74	1.00E+00
HAS2	Hyaluronan synthase 2	6.74	2.09E-01
SOX17	SRY (sex determining region Y)-box 17	6.71	5.80E-03
NCF4	Neutrophil cytosolic factor 4, 40kda	6.70	1.88E-01

CXCL5	Chemokine (C-X-C motif) ligand 5	6.63	5.00E-05
SLC44A4	Solute carrier family 44, member 4	6.60	1.12E-02
GBP5	Guanylate binding protein 5	6.58	6.80E-03
ANXA10	Annexin A10	6.58	5.00E-05
INHBE	Inhibin, beta E	6.56	5.00E-05
FCER1G	Fc fragment of ige, high affinity I, receptor for; gamma polypeptide	6.56	5.16E-02
SLA	Src-like-adaptor	6.51	5.00E-05
SLC7A11	Solute carrier family 7 (anionic amino acid transporter light chain, xc- system), member 11	6.51	5.00E-05
EGR1	Early growth response 1	6.46	5.00E-05
FIBIN	Fin bud initiation factor homolog (zebrafish)	6.37	9.80E-03
IL13RA2	Interleukin 13 receptor, alpha 2	6.37	5.00E-05
CTHRC1	Collagen triple helix repeat containing 1	6.36	5.00E-05
ADM2	Adrenomedullin 2	6.36	5.00E-05
UCN2	Urocortin 2	6.35	1.00E+00
IRF8	Interferon regulatory factor 8	6.34	1.01E-01
PHLDA1	Pleckstrin homology-like domain, family A, member 1	6.30	5.00E-05
PTGS2	Prostaglandin-endoperoxide synthase 2 (prostaglandin G/H synthase and cyclooxygenase)	6.30	5.00E-05
XDH	Xanthine dehydrogenase	6.29	1.00E+00
HIF3A	Hypoxia inducible factor 3, alpha subunit	6.24	1.00E+00
FOSB	FBJ murine osteosarcoma viral oncogene homolog B	6.22	5.00E-05
KLRC4-KLRK1/KLRK1	Killer cell lectin-like receptor subfamily K, member 1	6.19	1.00E+00
CD52	CD52 molecule	6.18	1.56E-02
RGCC	Regulator of cell cycle	6.18	2.41E-01

CD69	CD69 molecule	6.17	1.00E+00
SLAMF8	SLAM family member 8	6.17	5.00E-05
FOXC2	Forkhead box C2	6.17	1.00E+00
ITGA11	Integrin, alpha 11	6.12	5.00E-05
RPLP0P2	Ribosomal protein, large, P0 pseudogene 2	6.12	5.00E-05
EPCAM	Epithelial cell adhesion molecule	6.04	5.00E-05
C15orf48	Chromosome 15 open reading frame 48	6.00	5.00E-05
KLF2	Kruppel-like factor 2	5.99	5.00E-05
C5AR1	Complement component 5a receptor 1	5.97	3.35E-03